PV BASED LED STREETLIGHT & WATER PUMPING SYSTEM

DISSERTATION

SUBMITTED IN PARTIAL FULFILLMENT OF THE REQUIREMENTS

FOR THE AWARD OF THE DEGREE

OF

MASTER OF TECHNOLOGY

IN

POWER SYSTEM

Submitted by:

JASPREET SINGH

Roll No. 2K16/PSY/06

Under the supervision of

Prof. PRIYA MAHAJAN

DEPARTMENT OF ELECTRICAL ENGINEERING

DELHI TECHNOLOGICAL UNIVERSITY

(Formerly Delhi College of Engineering)

Bawana Road, Delhi-110042

2018

DEPARTMENT OF ELECTRICAL ENGINEERING

DELHI TECHNOLOGICAL UNIVERSITY

(Formerly Delhi College of Engineering)

Bawana Road, Delhi-110042

CERTIFICATE

I, Jaspreet Singh, Roll No. 2K16/PSY/06 student of M.Tech. Power System (PSY), hereby declare that the dissertation/project titled **"PV based LED streetlight & water pumping system"** is a bonafide record of work carried out by me under the supervision of Prof. Priya Mahajan of Electrical Engineering Department, Delhi Technological University, Delhi in partial fulfillment of the requirement for the award of the degree of Master of Technology has not been submitted elsewhere for the award of any Degree.

Place: Delhi **JASPREET SINGH**

Date: 11/07/2018

Dr. PRIYA MAHAJAN

(SUPERVISOR)

Professor

Department of Electrical Engineering

Delhi Technological University

ACKNOWLEDGEMENT

I am highly grateful to the Department of Electrical Engineering, Delhi Technological University (DTU) for providing this opportunity to carry out the project work.

The constant guidance and encouragement received from my supervisor Prof. Priya Mahajan of Department of Electrical Engineering, DTU, has been of great help in carrying my present work and is acknowledged with reverential thanks.

My sincere thanks to my M.Tech Coordinator, Prof. Rachana Garg, for her guidance and her continuous support throughout this course work.

I would like to express a deep sense of gratitude and thanks to Prof. Madhushudan Singh for providing the laboratory and other facilities to carry out the project work. Again, the help rendered by Prof. Priya Mahajan, for the literature, and for experimentation is greatly acknowledged.

Finally, I would like to expresses gratitude to other faculty members of Electrical Engineering Department, DTU for their intellectual support throughout the course of this work.

JASPREET SINGH

2K16/PSY/06

M. Tech. (POWER SYSTEM)

Delhi Technological University

ABSTRACT

In this work two Application of standalone PV system i.e. Solar LED Street light and water pumping system are carried out. These applications help in reducing the electric energy consumption and also enhance the rural electrification where grid is not present. In this thesis the techno economic analysis of different lighting schemes is carried out by using DIALux Software, which results in LED as an efficient light and then modeling of LED is discussed. The PFC buck converter based LED driver circuit is designed and implemented in this work.

Solar Fed LED Street lighting system has different components i.e. SPV array, MPPT, dc-dc converter and battery unit. In this system MPPT plays a main role in battery charging so, the comparison of different MPPTs is carried out. In Solar Fed street lighting system which is modeled in Matlab-Simulink, the intensity of Street light is controlled from traffic hours to non traffic hours which results in saving the electricity consumption to half as compared to the non intensity controlled system. The PV hybrid street light is also implemented in this work.

Solar oriented energy is an outstanding solution for rural regions where the grid isn't accessible. Most supported use of the SOLAR-PV System (SPV) is in water pumping system driven by DC/AC motors. Solar Powered DTC controlled Induction motor drive is superior to DC motor based system. The system includes MPPT (INC) with dc-dc boost converter, Voltage source inverter and a 3-phase induction motor drive. The DTC controlled techniques estimate the torque and flux, based on the instantaneous error of flux and torque the switching of VSI is generated. The reference speed is estimated by pump affinity law and DC link voltage regulation. The modeling of water pumping system is carried out using Matlab-Simulink.

TABLE OF CONTENTS

LIST OF FIGURES

LIST OF TABLES

ABBREVIATIONS

CCM	Continuous Conduction Mode
CFL	Compact Fluorescent Lamp
CRI	Color Rendering Index
DBR	Diode Bridge Rectifier
DTC	Direct Torque Control
IN	Incandescent
INC	Incremental Conductance
LED	Light Emitting Diode
LENI	Lighting Energy Numerical Indicator
MF	Maintenance Factor
MPPT	Maximum Power Point Tracking
P&O	Perturbation And Observation
PFC	Power Factor Correction
PWM	Pulse Width Modulation
RI	Room Index
SPV	Solar Photovoltaic
STC	Standard Test Conditions
UF	Utilization Factor

LIST OF SYMBOLS

E_Y	Electric energy consumption
N_t	Number of luminaries required
lm	Luminous flux
I_{LED}	Forward Current of LED
R_{LED}	Series resistance of LED
V_{LED}	Forward Voltage of LED
D	Duty Cycle of converter
SOC	State Of Charge
DoD	Depth Of Discharge
E_b	Back EMF of motor
T_d	Developed Torque
T_l	Load Torque
ω_m	Angular frequency of Induction Motor
ω_{slip}	Slip angular frequency
I_a	Armature Current
I_{abc}	Three phase current vector
$I_{\alpha\beta\gamma}$	Two phase stationary reference frame current vector
R_s	Stator Resistance of Induction Motor
R_r	Rotor Resistance of Induction Motor
L_{sr}	Rotor self Inductance of Induction Motor
L_{ss}	Stator self Inductance of Induction Motor
L_m	Mutual Inductance of Induction Motor
I_α	α axis current(Stationary frame of reference)
I_β	β axis current(Stationary frame of reference)
V_α	α axis voltage(Stationary frame of reference)
V_β	β axis voltage(Stationary frame of reference)
Ψ_{sr}	Total stator flux
K_l	proportionality pump constant
C_{dc}	DC link capacitor

CHAPTER 1
INTRODUCTION

Concerns over worldwide climate change, air pollution & reserve shortage make the alternative and renewable source of energy more fascinating over the worldwide. The sources of energy that are never-ending because they can be provided by nature and can be replenished in short time period are recognized as renewable energy assets. Sunlight, tides, wind and waves which can be harnessed constantly, are term as renewable energy sources. The earth is blessed with infinite amount of solar energy. The Sun is a reliable, never-ending & eco-friendly source of electrical energy. Solar energy experienced by us as heat and light, can be used as follows:

(i) The thermal energy uses the heat for cooking i.e. solar cookers, water heating etc and power generation.

(ii) The solar energy can be converted into electricity using P-V cells. This energy can be utilized for road lighting, water pumping, and independent power supply in provincial zones.

The government of India, on 05-June-2017, has passed a proposal for retrofitting over 10 Lakh traditional street light by solar-powered LED-based streetlight in Andhra Pradesh. This was the India's first launched rural LED based street light scheme under GOI's Street Lighting National Project (SLNP). This retrofitting of streetlight will help the city to save approximately 147 million units of electricity yearly and this also led to reduce 12 crore tones of CO_2 emission. This will be advantageous in many aspects beside economic concerns like environmental, lessening in road accidents & lighting performance.

This thesis highlights about the study of LED Light, and the application of Standalone SPV System in LED street light and Water pumps. Techno economic comparison of LED lighting source with other lighting sources such as incandescent (IN Lamp) and fluorescent (CFL) lamp with respect to different parameters such as electricity consumption, no. of luminaries etc has been done. Further an efficient arrangement of luminaries of taken room is designed in DIALux software. And then the working PFC buck converter based LED driver is discussed.

Solar street lights are Pole-mounted light sources which are powered by batteries and solar panels. The Solar Photovoltaic (SPV) panels charge a rechargeable battery, which supply LED light during the night. Solar streetlights are planned to work all through the night. Solar streetlight can work for couple of days by the batteries if sun light is not available as in cloudy & rainy season. For safety purpose solar streetlight can also be integrated with grid so as to have continuous supply.

Still today many of the street lights are switched ON & OFF manually and thus due to manual error they are not switched at proper time, sometimes it can be observed streetlights are remains ON during daytime also .So there is need to develop Automatic working streetlight that can turn ON & turn OFF itself by sensing solar Irradiance.

This work highlights the energy efficient SPV street lighting using LEDs through intelligent algorithm interface for energy management between SPV panel, Battery and Load. Also the amount of energy used by LED load is controlled by controlling its intensity during Traffic hours and low traffic hours. So, the proposed SPV based LED streetlight can be operated for nothing cost with adequate solar charging. And a PV Hybrid LED street Lighting system is also discussed in thesis.

Water pumps have a direct use in irrigation purposes. As in some rural areas there is lack of grid connectivity, so, solar powered water pump will be the best alternative in the field of agriculture and in India solar Irradiance of 1000W/m^2 is available for 6-8 hrs daily. In this work Solar powered Induction motor drive water pump is developed in Matlab-Simulink and its performance under different states have been analyzed.

1.1 SOLAR ENERGY POTENTIAL & VARIOUS SCHEMES IN INDIA [1]

In India Solar energy is growing at a very fast speed. The govt. has installed a capacity 20GW of solar power plant across the whole country, this capacity was initially targeted to be achieved by govt. of India till 2022 but it was achieved four year early of the schedule period i.e. 20GW was achieved by Feb 2018. The 20GW achieved capacity was achieved as 3GW was added in 2015-16, 5GW was added in 2016-17 and approx 10GW was added in 2017-18.So by achieving this goal there is a phenomenon dip in solar tariff to USD 0.04 per unit.

India have set a target of 100GW of solar power by 2022. The improvement in solar power technology in recent year has made the task achievable .India is developing

standalone PV system for local energy needs. Standalone PV system is working positively for rural areas where there is limited grid connectivity.

International Solar Alliance (ISA) is also formed which focus on promoting and helping in building solar energy in an efficient manner. India is building several solar parks like Andhra Pradesh Solar Park of 1000MW capacity and many more parks are in developing position.

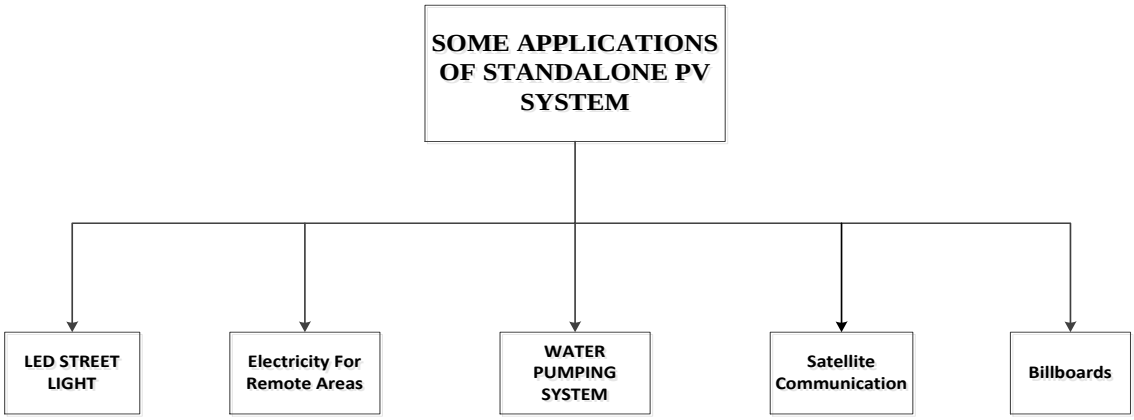

Fig.1.1 Applications of standalone PV system

GoI have also launches various schemes to replace conventional streetlight with Solar fed LED streetlights as discuss in above section. Some of the replacement drives are in progress in some states like Gujarat, Andhra Pradesh and Rajasthan. Rajasthan is the leading state in replacement of streetlight with an installation of 7.85 lakh lights.

GoI have also launches capital subsidiary scheme in 2014 for building up solar Photovoltaic water pumping system meant for irrigation purposes. Tentative target for 2014-15 was to install 30000 units water pumping system across the country major states were focus are Uttar Pradesh, Punjab, Rajasthan, Andhra Pradesh.Gov. is providing 25 Years of warranty for this system, this is very much attractive for Farmers, Fig.1.1 show some applications of Standalone PV system

NABARD is playing role of subsidy channelizing agency. Government has setup test labs in 2018 to certify the solar powered water pumping system with respect to their standards. In 2018 GoI has announced a Financial assistance of ₹48,000 crore for the SPV powered water pumps. This initiative will help in reducing harmful effect on climate i.e. air pollution, energy shortage issues etc.

1.2 MOTIVATION

The technology based on solar energy is increasing day by day and government also have a keen focus on making innovative ideas to make it use effectively in various sectors like rural development, highway's conventional lights replacement etc. So, by implementing these ideas we can directly promoting in making eco-friendly environment. The big issue in streetlight is how to use it efficiently; this can be done by making an automatic working light, controlling the intensity in peak hours and non peak hours and making it connected with utility to work without any interruption where there is overcast weather for more than 3 days. For rural areas, the irrigation is the backbone of the agriculture. As there is problem of uncertainty of electricity in rural areas so solar powered Water pumping system is very much vital for the progress in that areas. The main problem of solar water pumping system is the variation of performance under varying environmental conditions like irradiation changes etc. The DTC scheme is implemented with induction motor and performances under different stages have been analyzed.

1.3 DISSECTION OF THESIS

This thesis consists of Seven Chapters. Chapter 1 is an Introduction and Chapter 2 deals with the Literature reviews. Chapter 3 describes Solar PV system, Batteries and comparison of MPPTs techniques. Chapter 4 describes the Techno Economic comparison of Different Lighting schemes, LED modelling and their Driver circuit. Chapter 5 describes the modelling and design of SPV based street Light and Hybrid LED Street light. Chapter 6 describes the pump affinity law and modeling of Solar powered DTC controlled Induction Motor for water pumping. The conclusion and future work of the present work discussed in Chapter 7. All the work is implemented in Matlab-Simulink.

1.4 CONCLUSION

In this chapter a brief about solar energy potential in India, application Standalone PV system and some Government ongoing projects based on solar have been discussed here. This chapter also provide a quick look of the topics discussed in the thesis/dissertation.

CHAPTER 2
LITERATURE REVIEW

Based on the organization of thesis, the literature reviews of a portion of the significant research work done under these regions are examined underneath:

2.1 MODELING OF SOLAR PV ARRAY [2-4]

Villalva et al. (2009) [2] has proposed modelling of PV arrays. The authors has realised the parameters of the I-V equation of solar by modifying the curve with respect to the open circuit voltage, short circuit current and maximum power. These three has been useful for providing datasheets for all industrial array, the authors has proposed the best I-V equation for the single diode PV model taking the effect of parallel and series resistance. With the three parameters of the modified I-V equation one can build a PV module with any simulator by using different math blocks. The authors initially presented the basic tutorials of PV and different parameters that can compose single diode PV model.

Sinha et al. (2014) [3] has demonstrated that PV array exhibits the non linear characteristics of voltage and current this characteristic directly depend on the solar irradiation and some environmental factors. The author discussed the equivalent configuration of PV cells with respect to environmental conditions and from the observations the I-V characteristics has been plotted. The author has analyzed the performance for accomplishing the maximum power.

Solanki (2016) [4] explained the terms associated with batteries e.g. battery limit, DoD, battery cycle, C-rating etc and the types of batteries used for standalone system and which of battery is most preferable as per their properties.

2.2 CONTROL ALGORITHM FOR TRACKING OF MAXIMUM POWER UNDER SOME CONDITIONS [5-8]

Sharma & Katti (2017) [5] explained the advantages of solar energy and compared it with the traditional energy sources. The authors also discussed the drawback of solar energy as it depend upon irradiation and temperature conditions due to these conditions efficiency of the system decreases. The author has also discussed maximum power point

tracking to improve the efficiency of the system. The author has discussed P&O algorithm with dc-dc converter and comparison has been made with solar without MPPT, results has been analyzed in simulation.

Femia et at. (2005) [6] demonstrate the positive and negative aspects of P&O algorithm, the positive aspect as the low cost of implementation, easy to use method for maximum power tracking and the negative aspects as at the steady state condition the oscillations at the operating point around the MPP is large, P&O algorithm also sometime get confused the rapidly changed atmospheric conditions.

Islam et al. (2016) [7] proposed the hybrid algorithm for maximum power tracking with the combination of perturb and observation (P&O) and incremental conductance (INC). The authors has compare the P&O, INC algorithm with the hybrid algorithm and the model has been proposed gave the observation in regarding transients at MPP in various algorithms. Theoretical and the design principle of the proposed model have been discussed by the authors.

R.Chafle & B Vadiya (2013) [8] explained the importance of solar energy and problem facing in using solar energy and the authors has also explained the INC algorithm used for Maximum power point tracking. This paper proposed the advantage of Incremental conductance algorithm as its high steady-state accuracy and adaptability in different environmental conditions. The authors has proposed INC algorithm as most important technique used in SPV system.

2.3 TECHNO ECONOMIC ANALYSIS OF DIFFERENT LIGHTING SCHEMES [9-17]

Zalitis & Berzina (2016) [9] developed the effective lighting design for the old buildings that has been used to decrease the power consumption and increase the efficiency. The authors achieved a lower power consumption model without effecting the light intensity and quality. The proposed model used the low consumption lighting fixtures and the integration with daylight decreased the maintenance cost. The authors had examined the computer aided logical models which then compared with physical model.

Sathya & Natranjan (2014) [12] described the solution for energy and power demand management by using white LED for domestic purpose as energy management has become very complex. Authors explained the benefits of LED lamp as it consumed less

power and have high lumens. Authors had use laboratory as case study, lighting model of laboratory by using LED luminaries has been developed in DIALux 4.11 using the CAD window. The calculated results described the LED lighting system as the efficient lighting system for domestic uses and photometric values of LED lighting also analyzed.

Godinho et al. (2016) [13] described the demand of electricity consumption over worldwide and the challenges facing in 21st century to control it. The main objective of the paper to decrease the electricity consumption for exterior lighting and this was done by using selected lighting solutions; model was developed in DIALux software.

Dixit et al. (2015) [17] explained the biggest problem that was facing by developed countries i.e. energy crises; the illumination account almost 40% of the total electricity consumption. The paper presented the comparison of different luminaries with respect to different parameters like burning hours, electricity consumption and authors analyzed burning hours of lamp as the major consideration in life cycle cost of different luminaries.

2.4 LED MODELING AND DRIVERS CIRCUITS [18-26]

Ray-Lee Lin & Jhong-Yan Tsai (2015) [18] presented four-parameter Taylor series for LED model to describe the I-V characteristics of LED at different junction temperature, the four parameters has been taken as rated operating point, knee point, maximum knee point and temperature coefficient. The authors also achieved the small signal simulation, analyses for LED drivers and DC simulation by using the proposed LED model and I-V characteristics under different simulation model have compared.

Ray-Lee Lin, Yi Fan Chen (2009) [19] presented the approximate equivalent model of LED including small signal and DC model, piece-wise linear model. The authors has built a linear piece wise model by selecting the superposition theory for the multi-branch equivalent model and the small signal and DC model is performed on piece wise linear model.

Hwu et al. (2011) [20] demonstrated the synchronously rectified flyback converter with a multifunction circuit which has been playing a role of LC snubber circuit and also observing the zero crossing of the current to reduce the switching losses of the switch,

for all over operating range these converters has high efficiency. The authors uses power factor corrected ac dc converter for feeding LED streetlight.

Gacio et al. (2009) [21] presented that as luminous efficiency requirement is increasing day by day so HB-LED has been in this paper. The author has use an integrated buck – fly back converter for LED streetlight which performs a PFC operation and AC source was taken as an input. Firstly the author modeled the LED and developed the closed loop system by sensing the current and also developed the controller.

Ramanjaneya & Narasimharaju (2015) [24] has designed buck-boost LED driver for wide AC input voltage applications. The proposed driver circuit uses uncontrolled DBR followed by buck-boost converter and the work has been given the input supply from 85-265V. The driver accomplished the low total harmonic distortion (THD) and the power factor near to unity. The authors implemented the controlled scheme that consists of voltage controller, reference current generation and a PWM generator.

Bryant & Kazimierczuk (2005) [25] has developed transfer functions which represent the quasi digital behavior of the closed loop current model for giving duty to the dc-dc converter which is working in continuous conduction mode by using current loop gain, PCM control. This transfer function has a pole that can be in either in right half and left half plane and catches the example and-hold impact precisely, empowering the portrayal of the present circle pick up and shut current circle for PWM dc– dc converters with PCM.

2.5 SOLAR FED LED STREETLIGHT [27- 29]

Vijay M. et al. (2015) [27] has concerned about global warming and weather changes, as they are increasing day by day so researchers are giving more consideration on renewable energy. The authors used solar PV as it's is exceptional source of energy and also available in DC form so, it has been utilized for LED streetlight by the authors. In past decades LED has been tremendously popular due its benefit over all other luminaries and also works on DC. Authors also had taken traffic scenario in consideration and control the intensity of the street light by controlling the switching of the switch that was used in buck-boost converter. The model analyzed by the authors consists of SPV system, Li-ion battery, MPPT, buck converter and buck –boost converter, LED load.

Ling et al. (2016) [29] presented the use of photovoltaic power connected in LED road lighting and an intelligent road lighting framework is created. The authors proposed a model that consists of solar PV array, Li-Ion Phosphate battery, an AC/DC circuit, LED driver, LED array, Power switching circuit, a 16-bit microcontroller and a wireless communication. The authors used a MCV control for selection between battery output, battery charging and AC/DC output to supply the LED array. Potential of LED Street light has been monitored in the paper by using communication. The authors used MPPT for the Solar PV panel that has been achieved by CN3722 so, the battery charging efficiency reaches to 85%.

2.6 DIFFERENT CONTROL TECHNIQUES FOR WATER PUMPING SYSTEM [30-37]

Vongmanee et al. (2002) [30] presented the vector control technique for driving water pump by Solar PV system that was implemented by current control voltage source inverter. In this technique the torque (T) and flux (Ψ) of a motor was related with the solar array voltage (V_{pv}) and current (I_{pv}) at MPP that varies with different irradiation levels. The authors performed the control process by using a digital signal processing chip (DSP) i.e. ADMC331. The results proved that the motor speed changes with the variations of maximum power at different irradiation.

Shukla & Singh (2018) [31] developed a single stage solar PV Feed sensor less vector control of IM drive which has been superior than conventional IM drives. The authors estimated the speed of motor by stator flux i.e sensor less approach of speed calculation, uses INC based MPPT algorithm for MP from Solar PV array. The authors obtained a smooth starting of the IM which is controlled by Field oriented control and authors developed results both in simulink and by experiment implementation.

Sharma et al. (2018) [32] presented a scalar control of IM drive for Water Pumping system fed by solar PV system. The system is comprises of two stage comparison of power i.e first stage is DC-DC conversion by using the boost converter and second one is the DC to AC conversion by Voltage source inverter that is controlled by scalar control of IM drive. The authors uses INC algorithm for extracting maximum power as an MPPT technique. The authors reduced the speed sensor and estimate the sensed speed by current of the motor and control the motor speed by pump affinity law and PWM frequency.

Takahashi et al. (1986) [34] proposed the high efficiency vector control of Induction motor which is somewhat different from Field oriented control. The differences that authors presented based on limit cycle control of torque and flux using best PWM voltage (output) and a lookup table is developed for selecting best inverter switching for fast response and low harmonics losses; efficiency also optimized under steady state condition.

Patel N. Disha (2017) [36] demonstrated that V/F drives and Field oriented control are widely used in many industries and in recent improvement in the controlling has made the advancement in high controlling drives. The author has presented the direct torque control method which has been a rapid control of flux and torque and also discussed the response of control technique under the variation in sector region in DTC techniques.

2.7 PERFORMANCE OPTIMIZATION OF WATER PUMPING SYSTEM [38-42]

Zhang et al. (2012) [38] explained that step size in MPPT methods play an adverse role in stability and dynamics of the solar PV fed water pumping system. The author has given a solution for determining the step size of MPPT based on controller capabilities and system parameters. The authors performed an experiment which gives the optimized size of MPPT together with an smoothing capacitor.

Singh & Singh (2015) [39] explained the pump affinity law i.e. the power of the motor is directly proportional to the cube of the speed of the pump has been running, the affinity law estimate the reference speed component and other reference speed component is estimated by the difference between DC link voltage and the reference voltage, this signal is passed through PI controller. The developed modeled by the authors demonstrated the adequate performance of the controller under different conditions.

Bhat et al. (1987) [41] developed that PV water pump optimization techniques which suggested the relationship between v-f for a given pump head which can optimize the motor inputs; under varying different head condition there has been a possibility to extract maximum power from solar PV array.

2.8 CONCLUSION

This chapter presents the literature survey of Solar based LED streetlight and water pumping system. This helps in gaining the fundamental knowledge of the system and also present the overview of the research work done so far.

CHAPTER 3
STANDALONE PV SYSTEM

The PV system is fabricated to supply electric power to the loads that can be DC or AC, depending upon the type of application. The system can work for day-time, night-time or even for whole day. Since, PV generate power only in day-time so, some energy storage elements i.e. battery are required for standalone system

3.1 SOLAR PHOTOVOLTAIC'S

The most copious fuel source in the area of renewable energy is the sun. Solar panels generate electricity through single photovoltaic cells linked in series and parallel. This type of energy is possible in areas of the world where the sun is copious, and can be used in remote areas or on houses to decrease the increasing cost of electricity. To change the sun power into electricity, cell captures photons to create flowing electrons that flow across the cells to generate current [2]. The competence of the panel is dependent upon the semiconductor matter that the cells are prepared from as well as the method used to assemble the cells. Solar panel is of three type i.e. amorphous, polycrystalline and mono crystalline. To gets the best results, there are many methods that can be used to manage the output of the PV panels. Components used to generate the desired current and voltage is solar trackers, converters. The PV output power is affected by many variables like Irradiance, temperature, dust etc. all through the day. These variables have adverse effects like variations in current & voltage that make the panel unproductive if the outputs are not regularly attuned to maximize the output power. Since solar energy is only present during the day, the system requires energy storage equipment like battery or linking to the grid to supply power through the night.

3.1.1 Effect of atmospheric conditions on Solar Energy

Many factors that contribute for the variation of the PV power include solar irradiation, temperature, cloud cover and angle of the sun. Most of the factors are dependent on season and change with the change in season. During the whole year, the sun moves between its maximum peak in the sky during summer season and its lowest during the winter season, this result in variation of Irradiation so it have effect on PV Power. The

angles at which the panels are positioned determine how much sun rays are collected and how much is reflected off the surface. Most structures use fixed-angle mounts that are positioned fixed for a specific season. Solar trackers are used for increasing the no. of hours a system generate energy this lead to have efficient solar energy generation. When the panel tracker is added with solar panel it will increase the generation of current in morning and evening hours also. Temperature fluctuations have an evident effect on PV cells. As shown in fig.3.1 the PV output current, voltage and power decreases as the temperature increases so, due to this efficiency also decreases[2].

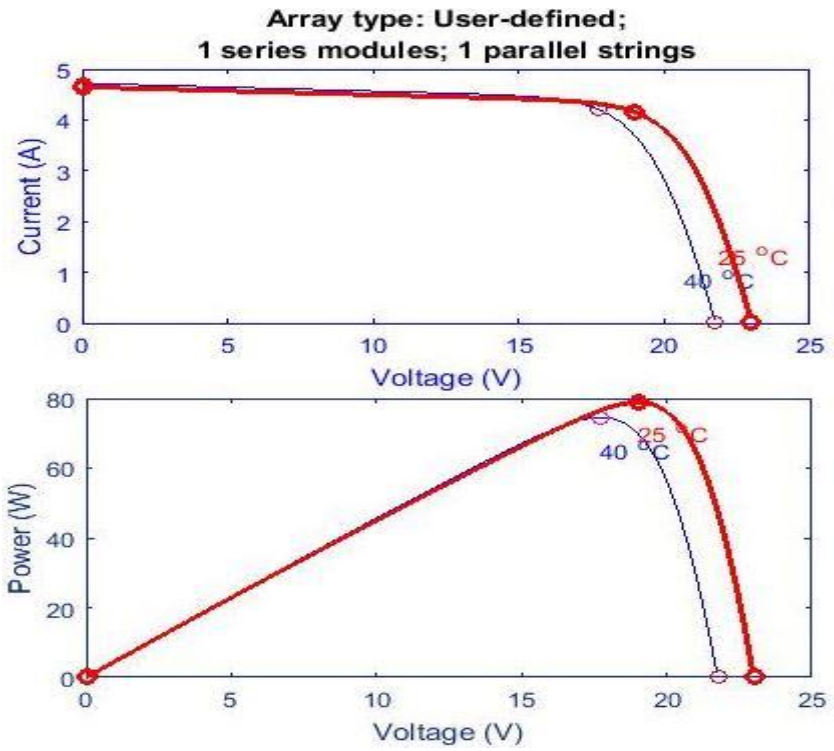

Fig.3.1 Current, Voltage, Power and Temperature Variations of a Photovoltaic Cell

It is observed that amount of power generated is inversely proportional to the increase in temperature.

3.1.2 PV Modeling

PV system can be modelled using various diode models such as single, double or three diode models. This work uses single diode model of PV cell. Single diode equivalent circuit of photovoltaic cell is shown in fig.3.2 [3].

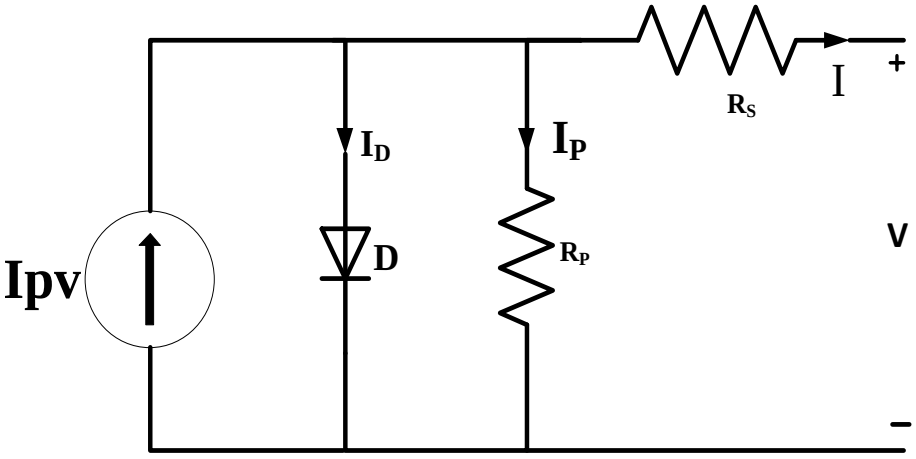

Fig.3.2 Single diode model of PV cell

Applying the Kirchhoff current law current I of photovoltaic cell is given by

$$I = Ipv - Io\left[e^{\left(\frac{V+IRs}{aVt}\right)} - 1\right] - \left[\frac{V+IRs}{Rp}\right] \quad (3.1)$$

Where I and V are output current and voltage of photovoltaic array respectively, I_0 is Saturation Current as in equation (3.2)

$$Io = \frac{I_{sc,n}+KiΔT}{\exp\left(\frac{Voc,n+KvΔT}{aVt}\right)-1} \quad (3.2)$$

$$I_{pv} = (I_{pv,n} + K_iΔT)\frac{G}{G_n} \quad (3.3)$$

Where $I_{sc,n}$ is nominal short circuit current $V_{oc,n}$ is nominal open circuit voltage, K_i is short circuit current/temperature coefficient, K_v is open circuit voltage/temperature coefficient, V_t is the thermal voltage, a is ideality factor, I_o is saturation current, G is Irradiance (W/m^2), G_n is Irradiance at STC = 1000 W/m^2 ,$I_{pv,n}$ is the current of ideal current source at STC,R_s & R_p are the series and parallel resistance of single diode model of SPV. In practical systems R_p is generally larger than R_s.

3.2 STANDALONE SPV SYSTEM

Standalone SPV systems are designed to fulfil the load necessities in the best feasible way. Standalone SPV system is shown in fig.3.3 the various components of standalone system are PV array, converters, controllers, battery unit and load (AC or DC) and are explained below.

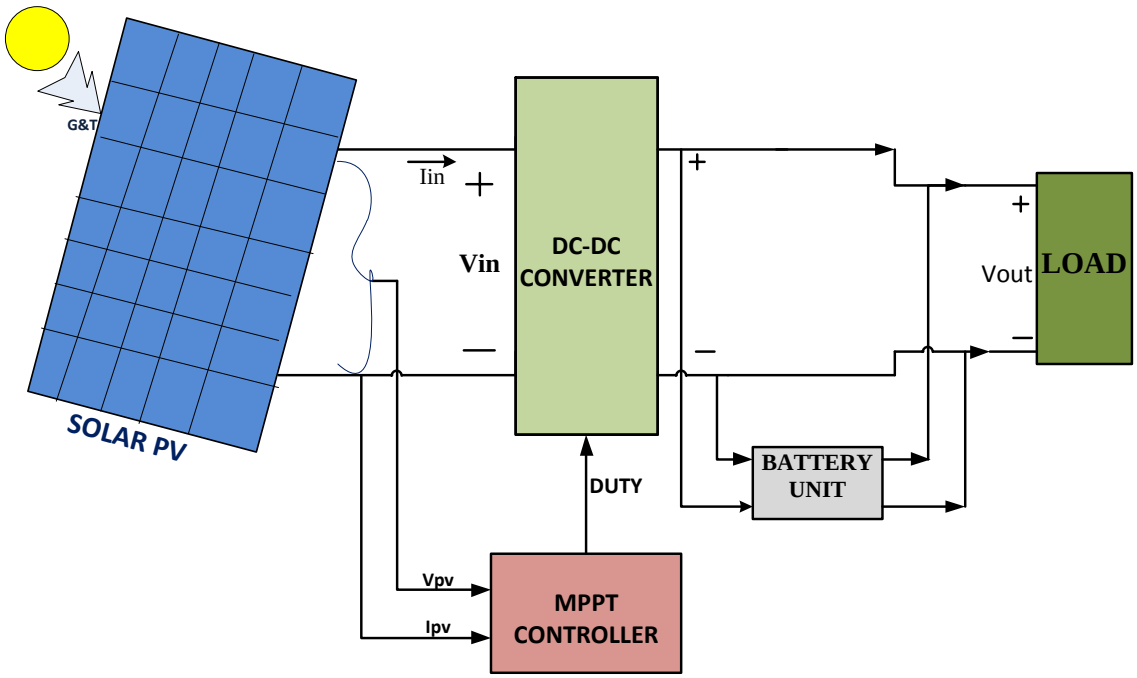

Fig.3.3 Standalone PV System

3.2.1 PV Array

Solar Array is the system made up by the combination of solar modules in series and parallel. In order to increase a current PV modules are connected in parallel and to increase voltage the modules are connected in series.

3.2.2 DC-DC Converter

DC to DC converter is used to convert one level of unregulated DC voltage into regulated or controlled DC voltage of same or different levels. These converter also plays a important role in battery charging, MPP and help in interfacing the PV source with different type of loads. The input and output of converter is DC only. In this work buck converter is used to step down 19V to 12V.

3.2.3 Battery [4]

Solar panel generated energy is stored in battery. When the demand of the load is not fulfilled by the solar panel, then in this conditions battery will play an important role for meeting up the required energy demand, in streetlight the battery play a major role because street light works when there is no solar energy available.

3.2.3.1 Performance Indicators of battery

There are a few terms related for a given type of battery which are useful indicators of the battery performance.

a. *Battery limit (Ah):* It is the greatest storage charge limit of a battery, measured in terms of ampere-hour. Ah, limit additionally speaks the max amount of energy that can be supplied from battery under certain conditions. The rechargeable batteries are accessible in an extensive variety of Ah limits, for example, 3 Ah, 7.5Ah, 20Ah, 50Ah, 110Ah, 150Ah, 250Ah etc.

b. *Battery voltage (V):* The battery is made up of no. of cells that add up and form the battery voltage level. The working voltage is generally indicated by the makes. The rechargeable batteries are accessible with the different voltage rating of 3V, 6V, 12V, 24V, 30V and so forth

c. *Depth Of Discharge (DoD):* Complement of state of charge (SOC) is DoD i.e. 100% charged battery subtract by SOC give DoD. The DoD represent percentage that is remaining to be charged. The relation between battery life and DoD is logarithmic.

d. *Battery life cycle:* It is characterized as the quantity of a total charge-release cycle that the battery can perform before its accessible limit falls beneath 80% of its underlying appraised limit. The average life cycle of the batteries is 500 to 1500 cycles.

e. *Charge rate or C-Rating:* The discharge and charge current or rate is given in terms of C-rating. The C-rating is defined as charge or discharge rate given in terms of capacity of the battery divided by the number of hours for full charge or discharge. Thus, it is represented as C/X rating, where X is the hours of time for full charge or discharge.

3.2.3.2 Types of Batteries used in SPV System

There are a couple of sorts of rechargeable batteries, which are:

a. Lead-Acid (LA) Battery

These batteries are the most generally utilized as a part of sun based fuelled frameworks because of its development in innovation and low evaluating. They must be utilized with low Depth of Discharge (DOD) keeping in mind the end goal to expand its life expectancy. There are two kinds of LeadAcid batteries, i.e. overwhelmed and Valve - Regulated Lead- Acid (VRLA) batteries.

b. *Nickel-Cadmium (Ni-Cad) Battery*

Though Ni-Cad battries have resistance forhigher release and longer life expectancy, they are not generally used as a part of solar based controlled system because of its high expense and constrained ease of access. Further, cadmium is also unsafe.

c. Lithium-Ion (LI) or Lithium-Polymer (LP) Battery

Lithium based batteries are viewed as the future of batteries utilized and many researches are going regarding this battery. This is because of various factors, for example, high energy density, high D.o.D rate, zero maintenance, low self discharge rate and a higher number of charging cycles.

3.2.4 MPPT Algorithms

Various MPPT algorithms have been developed for controlling the duty cycle of converters. This section discusses about two algorithms as follows:

1). Perturbation & Observe based MPPT algorithm.

2). Incremental conductance algorithm

3.2.4.1 Perturb and Observe algorithm

In this method duty (D) is perturbed and resulting array current & voltage values are sensed, then power is calculated. Once the power is identified, the operating region of the P-V curve is checked constantly & duty ratio is perturbed. If power increases by increasing duty, then duty is increased further and if power decreases by increasing duty, then duty ratio is decreased. Similarly, if power increases by decreasing duty, then duty is decreased further and if power decreases by decreasing duty, then duty ratio is increased. The P&O algorithm is described by the flowchart as shown in Fig.3.4. and the algorithm oscillates around MPP when stable condition is arrived, the MPP maximum power is obtained. The step size of perturbation is optimized to keep the power and the oscillation variation small, [5,6].

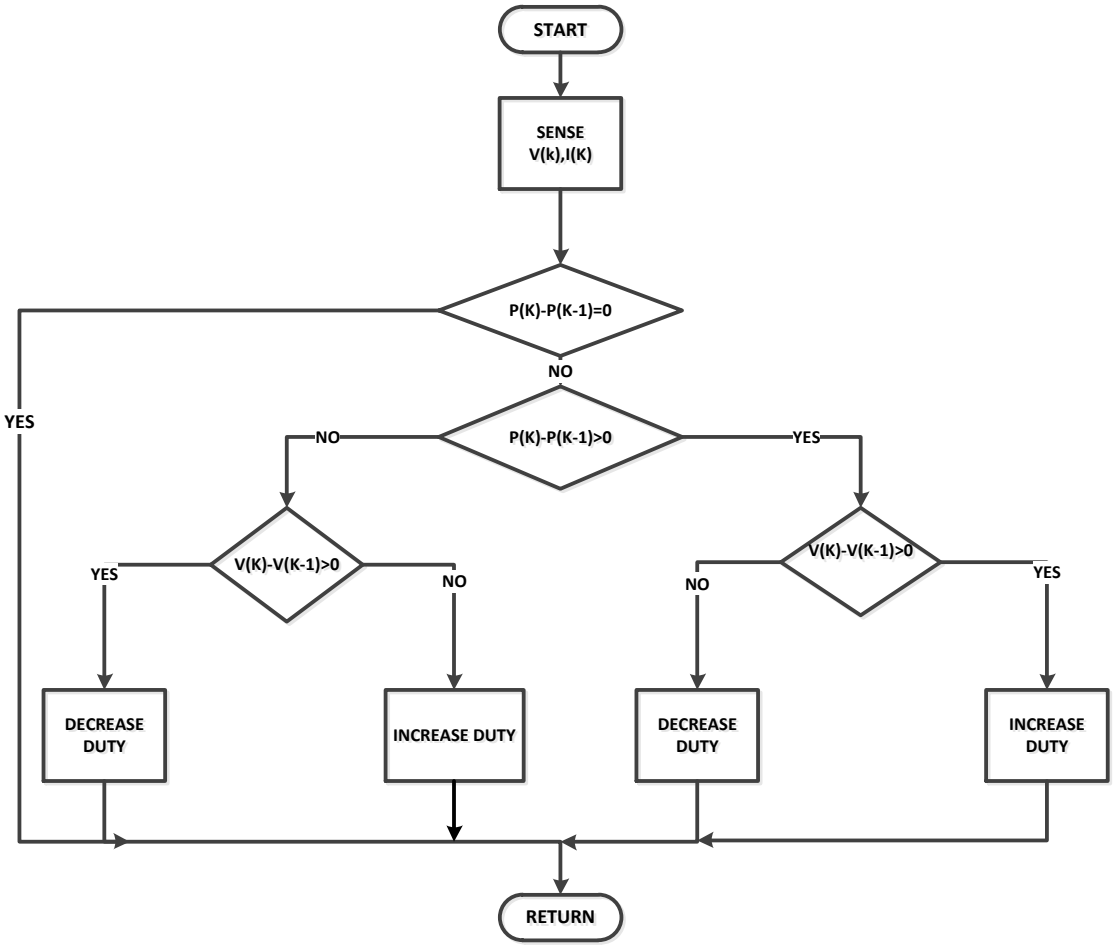

Fig.3.4 Perturbation & Observe MPPT Algorithm

3.2.4.2 Incremental-Conductance Algorithm

There is a nonlinear connection between P_{spv} and V_{spv} in solar PV characteristic. However, because of its inbuilt disadvantage of oscillation at Maximum power point (MPP) and losses linked with P&O algorithm as discussed in previous section, an INC control algorithm as shown in Fig.3.6 has been used. The principle equations for analysing the working principle of INC algorithm are given below,

At maximum power point (MPP) the slope of the PV graph is zero so,

$$\frac{dP_{spv}}{dV_{spv}} = 0 \tag{3.4}$$

$$P_{spv} = V_{spv} * I_{spv} \tag{3.5}$$

Differentiating the above equation wrt to V_{spv}, we get

$$\frac{dP_{spv}}{dV_{spv}} = I_{spv} * \frac{dV_{spv}}{dV_{spv}} + \frac{dI_{spv}}{dV_{spv}} * V_{spv} \tag{3.6}$$

From equation (3.4)

$$0 = \mathrm{I_{spv}} + \frac{\mathrm{dI_{spv}}}{\mathrm{dV_{spv}}} * \mathrm{V_{spv}} \tag{3.7}$$

$$\frac{\mathrm{dI_{spv}}}{\mathrm{dV_{spv}}} = -\frac{\mathrm{I_{spv}}}{\mathrm{V_{spv}}} \tag{3.8}$$

Where V_{spv}, I_{spv} &P_{spv} is instantaneous solar PV voltage, current and power respectively, $\frac{I_{spv}}{V_{spv}}$ is the instantaneous conductance and $\frac{dI_{spv}}{dV_{spv}}$ is the incremental conductance. [7, 8]

From the above equations, it is clear that on the left-hand side of MPP the slope of the curve is increasing in nature which means $\frac{dI_{spv}}{dV_{spv}} > -\frac{I_{spv}}{V_{spv}}$ and on the right-hand side of MPP the slope of the curve is decreasing in nature which means $\frac{dI_{spv}}{dV_{spv}} < -\frac{I_{spv}}{V_{spv}}$ and at MPP slope the curve is zero as shown in Fig.3.7.

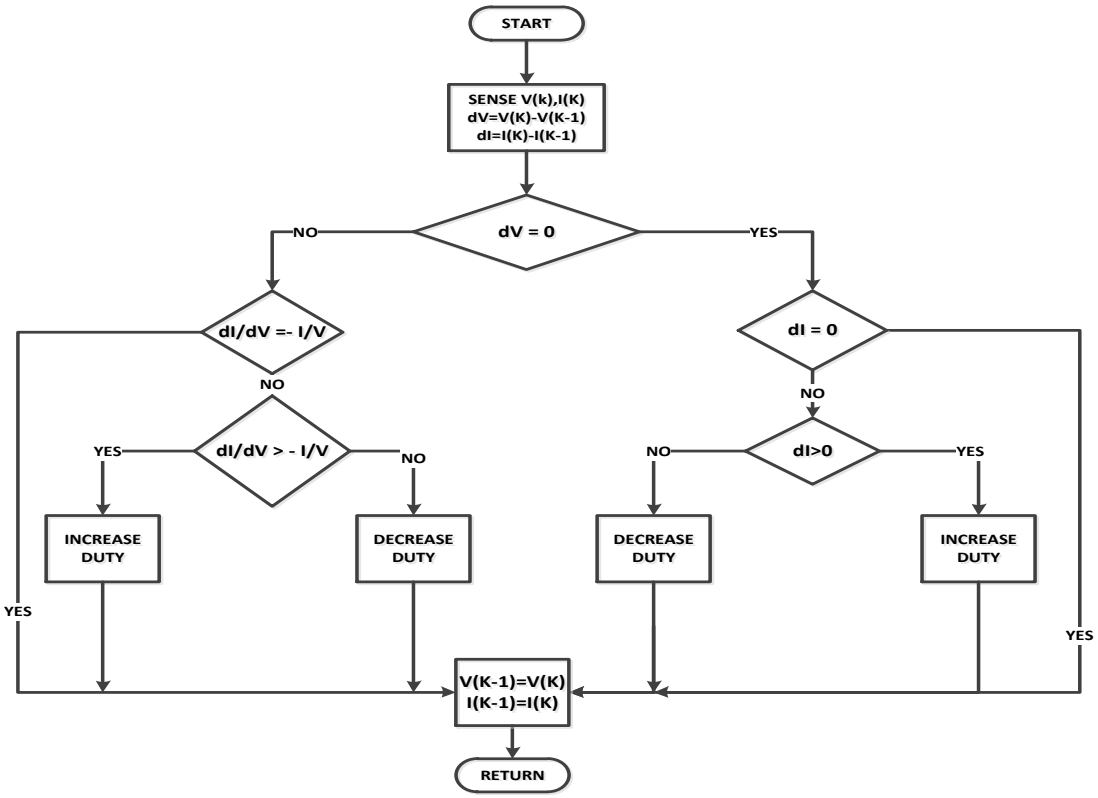

Fig.3.5 Incremental Conductance Algorithm

3.3 COMPARISON OF MPPT ALGORITHM IN BATTERY CHARGING

A standalone SPV system is designed for battery charging purpose & the model components used are Solar PV array of 75W specification as given in Table I, dc-dc buck converter with MPPT, a generic Li battery of 12V. The model in fig.3.6 has been implemented in Matlab-Simulink and the simulink models are given Appendix 1. The comparison of P&O and INC has been done with respect to three parameters i.e. output power, battery charging voltage and State Of charge (SOC) of battery.

TABLE I SOLAR PANEL SPECIFICATIONS

SOLAR PANEL SPECIFICATIONS	
Open circuit voltage (V_{oc})	23V
Short Circuit Current (I_{sc})	4.65A
Max power (P_{max})	75W
Voltage at P_{max} (V_{mp})	19 V
Current at P_{max} (I_{mp})	4.15A
Tolerance (At STC)	5%

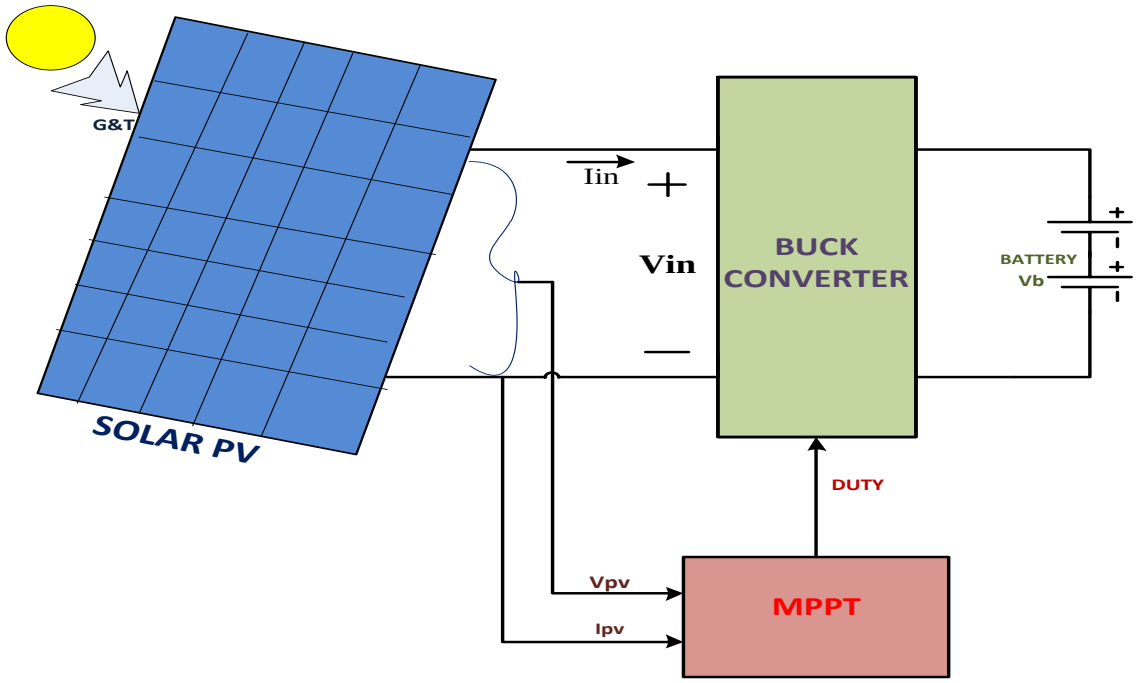

Fig.3.6 Simulation model of Comparison of MPPT for Battery Charging

Table II shows how the MPPT algorithm works when the irradiance changes, at point '3' as in fig.3.7, the irradiation is 1KW/m^2suddenley irradiation changes to 0.6 KW/m^2, so now position tracked by MPPT is '6' for tracking the maximum power if position changes to '7' so, at that position power decreases and voltage increases so the duty should be increases, so like this MPPT will track maximum power.

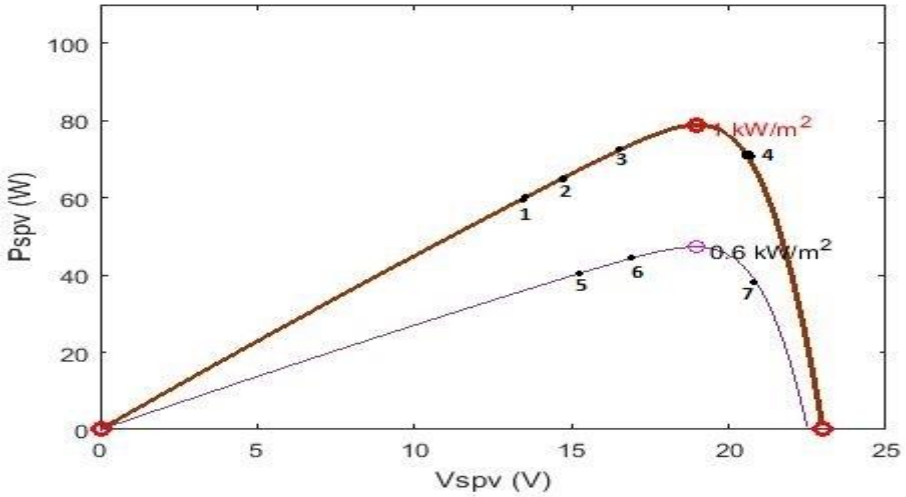

Fig.3.7 Power v/s voltage graph of PV array

TABLE II MPPT ALGORITHMS DURING IRRADIANCE CHANGED

Solar irradiance	Current position → Next position	Power & voltage	Duty (D)
1KW/m^2	1 → 2	P_{spv} ↑& V_{spv} ↑	D ↑
	2 → 3	P_{spv} ↑& V_{spv} ↑	D ↑
	3 → 4	P_{spv} ↓& V_{spv} ↑	D ↑
	4 → 3	P_{spv} ↑& V_{spv} ↓	D ↓
At point '3',Solar irradiance changes suddenly, new operating point is '6'			
0.6KW/m^2	6 → 7	P_{spv} ↓& V_{spv} ↑	D ↑
	7 → 6	P_{spv} ↑& V_{spv} ↓	D ↓
	6 → 5	P_{spv} ↓ & V_{spv} ↓	D ↓
	5 → 6	P_{spv} ↑& V_{spv} ↑	D ↑

When P&O is used as MPPT in the proposed model for solar irradiance of 1000W/m^2, the Oscillation in Output power is about 30W and when the irradiance is changed to 600W/m^2 there are some transients in the output power across battery as shown in Fig.3.8 but in INC based model have almost constant power output for 1000 & 600 W/m^2.

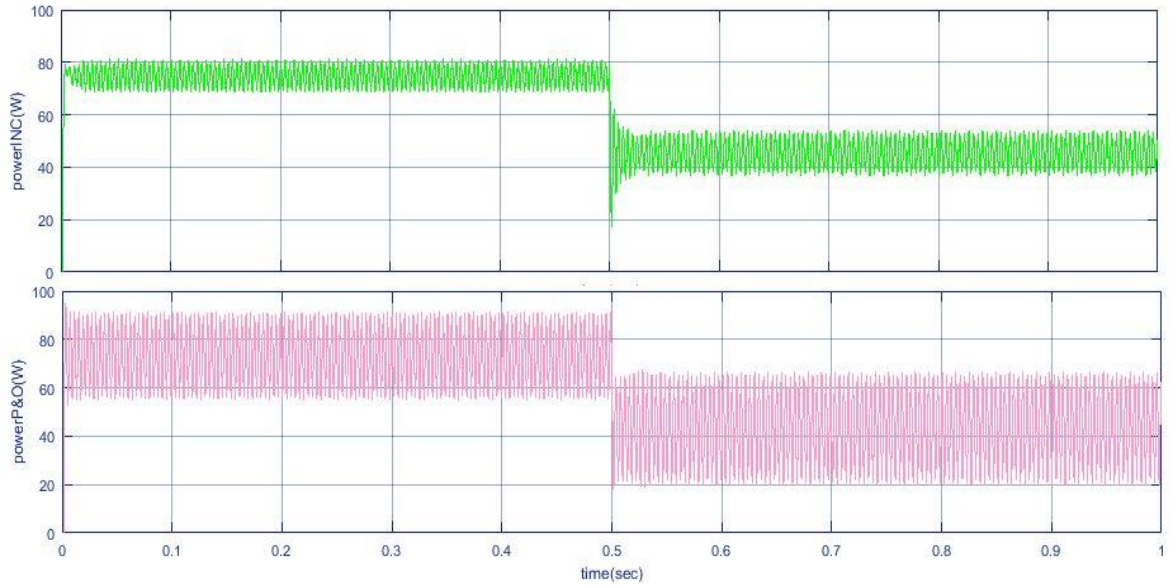

Fig.3.8 Output Power (W) across Battery

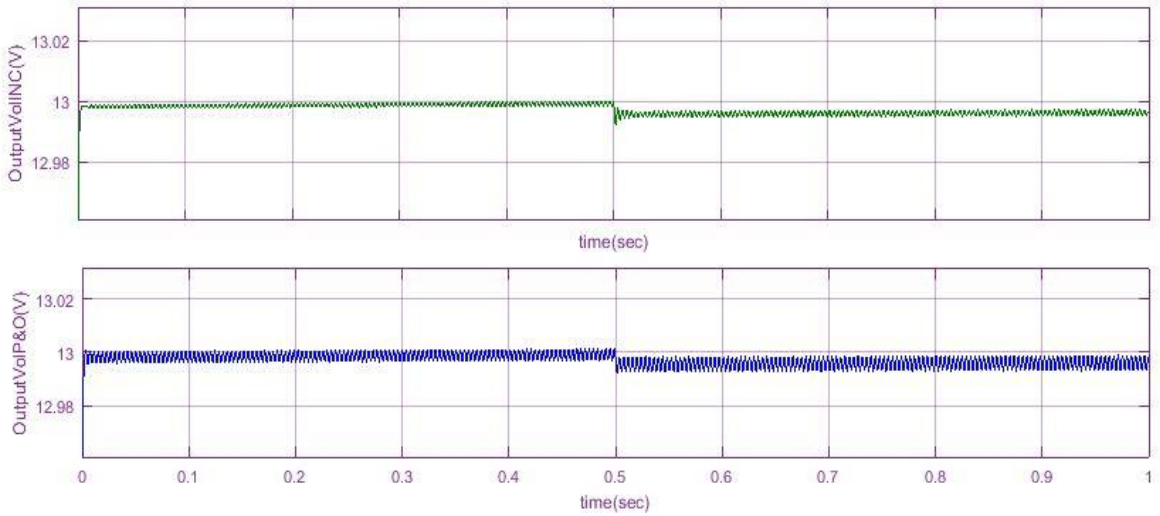

Fig.3.9 Voltage (V) across Battery

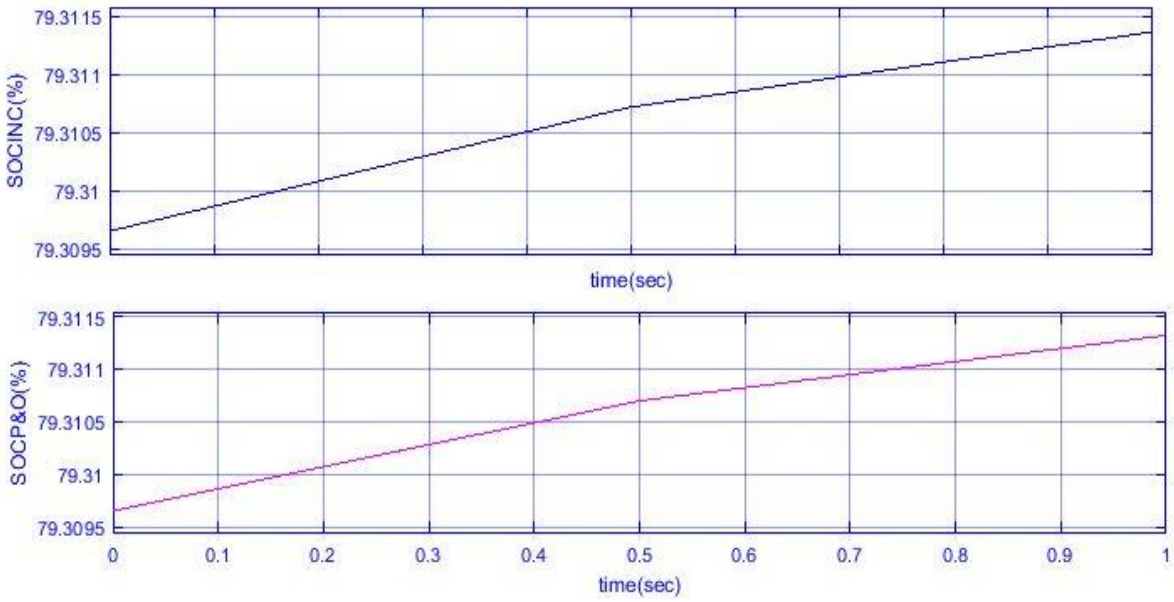

Fig.3.10 SOC (%) of Battery

Similarly in battery voltage at the time of charging the variation in voltage for P&O based model is more as compare to INC based model and SOC in INC based model is increasing at fast rate as shown in Fig.3.9 & 3.10. So, INC algorithm is preferred over P&O algorithm for battery charging and also for any standalone SPV system.

3.4 CONCLUSION

This chapter presents the basic of solar photovoltaic construction, effect of atmospheric conditions on solar and modelling equations of solar module. This chapter also presents an idea of standalone SPV system components i.e. battery, MPPT etc. The comparison of two MPPT algorithm i.e. P&O and INC for battery charging also performed, this comparison shows that INC algorithm has better performance & also fast battery charging than P&O.

CHAPTER 4

DESIGN & ANALYSIS OF LED LIGHTING

In the past decade, LED lighting has become popular because of many advantages such as high luminous efficiency, long life span, compact size, durability, quick start, low electricity consumption. Moreover, high brightness LEDs are solid state devices which allows their utility in automotive lighting, streetlight lightings, railway display board, indoor and outdoor lightings applications. LEDs are semiconductor devices which emit visible light from a small square block of semiconductor material, thus LED lighting is also known as solid state lighting.

4.1 TECHNO ECONOMIC ANALYSIS OF DIFFERENT LIGHTING SCHEMES

Illuminance plays a major role in human life. The illuminance produced by electrical sources is more regulated reliable and elegant in operation than other sources. Poor Illumination results in dangerous effects like eyestrain, headaches, accident due to insufficient lighting. The main objective of lighting designs is to facilitate quick and accurate work, and to create a comfortable visual environment.

Lighting is one of the major consumption of electrical energy. It consumes around 20% of the world's total electricity generation [9]. The energy efficiency, reduction of CO_2 emissions are the major significant issues that concern people and professionals working in the field of electrical energy [10]. Relative to the conventional low energy efficient lamps, current LED lamps convert 95% of the energy into light and only 5% is wasted as heat. It acts as an environmentally friendly light source from production to disposal. LEDs have a better quality of light distribution as other types of lighting sources waste energy by emitting light in all directions. The above mentioned features and decrease in the cost of LED driver circuit, is resulting in increased usage of LED source in domestic applications.

In this work techno economic comparison of LED lighting source with other lighting sources such as incandescent (IN Lamp) and fluorescent (CFL) lamp with respect to different parameters such as electricity consumption, no. of luminaries etc has been

done. Further an efficient arrangement of luminaries is designed in DIALux software. A Room is taken as a case study for the comparison of different lighting sources and to implement the lighting layout for the room.

4.1.1 Lighting System Design

Electrical lighting installations provide constant illuminance on a horizontal working plane by distributing luminaries evenly over the ceiling [11]. For each type of working environment, there is a range of brightness that cause minimum fatigue and give optimum output in terms of quality and quantity. So, for better lighting conditions the illumination of the working area is required.

The data required for luminaries distribution are dimension of a room, illuminance level required, maintenance and utilization factor, luminous flux produced per lamp etc.

The steps required to design an effective lighting system are:

a. Choice of Perfect luminary

Color rendering index (CRI) is the major factor while deciding the choice of luminary. Higher the CRI, better will be the color rendering capability so, for a room luminary of a color rendering index from 80-90 is considered as a good light source. It indicates how correct a luminary exhibits colors as compared to daylight.

b. Determination of the Utilization factor

Utilization factor (UF) is the ratio of total number of lumens reaching the working plane to the total no. of lumens emitting from source. It depends upon room index (RI) and room reflectances. Corresponding to the calculated RI and given room reflection coefficient of ceiling (C), walls (W) and floor (F), UF can be determine as given in Table III.

TABLE II TYPICAL UTILIZATION FACTOR DATA [11]

Room index(RI)	1.0	1.25	1.5	2.0	2.5	3.0
Room reflectance's C W F						
70 - 50 - 20	0.42	0.47	0.51	0.56	0.60	0.63
30	0.36	0.42	0.46	0.52	0.56	0.59
10	0.32	0.37	0.41	0.47	0.52	0.55
50 - 50 - 20	0.38	0.43	0.46	0.51	0.54	0.57
30	0.34	0.38	0.42	0.51	0.51	0.53
10	0.30	0.35	0.38	0.44	0.48	0.50
30 - 50 - 20	0.35	0.39	0.42	0.46	0.49	0.51
30	0.31	0.35	0.38	0.43	0.46	0.48
10	0.28	0.32	0.35	0.40	0.44	0.46
0 - 0 - 0	0.24	0.28	0.30	0.34	0.37	0.39

Here room index is defined by equation (4.1)

$$\text{Room index (RI)} = \frac{L*W}{H*(L+W)} \tag{4.1}$$

where L = length of the working room, W = width of the working room [11] and H is Mounting height of the working room and is given by equation (4.2)

$$H = h - x \tag{4.2}$$

Here, h = height of the working room, x = working plane height

c. Determination of the maintenance factor

Maintenance factor is the ratio of illumination of a light source under normal working conditions to the illumination when everything is clean. Its value is always less than 1, and it varies from 0.7 - 0.9. This is due to the accumulation of dust, dirt and smoke on the lamps that emit less light than they emit when they are very clean. Frequent cleaning of lamps will improve the maintenance factor. Table IV indicates the typical MF corresponding to different environmental conditions.

TABLE IV TYPICAL MAINTENANCE FACTOR DATA [11]

Environmental condition	MF
Very clean room, low yearly maintenance	0.90
Clean room, 3 yr maintenance cycle	0.80
Exterior installation, 3 yr maintenance cycle	0.70

d. Calculation of number of luminaries required

Knowing the dimension of a room, the particular luminary UF, luminous flux produced per lamp, the maintenance factor, the number of luminaires required can be deduced using equation (4.3)

$$N_t = \frac{E_x * A_{lw}}{lm * UF * MF} \tag{4.3}$$

where:

N_t = the number of luminaries required

E_x = the illumination required in LUX

A_{lw} = working area in square meter

lm = luminous flux produced per lamp in lumen

UF = Utilization factor

MF = Maintenance factor

e. Calculation of Power utilized and Lighting energy numerical indicator

Power utilized by the complete lighting system is given by =

$$N_t * \text{Wattage of each lamp} \tag{4.4}$$

Lighting energy numerical indicator (LENI) is the ratio of energy consumed (E_Y) by the total numbers of luminaries per unit area (A) of the considered workspace. Once, No. of luminaries required are known, LENI is as given by (5)

$$LENI = \frac{E_Y}{A_{lw}} \tag{4.5}$$

Low the value of LENI more efficient the lighting system.

f. *Layout of luminaries in the room*

From the above step the number of luminaries has been calculated. This number of luminaries will fulfill the illuminance needed for the task. The next step is to design the layout of the luminaries in the room. It can be done by rounding off the number found to a whole number that can be easily divided into a regular grid.

The permissible layout depends upon the space to height ratio limit. For luminaries fixed on the ceiling, the mounting height (H) will be given by equation (4.2) but for luminaries suspended below the ceiling, mounting height will be given by the difference between luminary suspended height and the working plane height. Fig.4.1 & 4.2 shows the luminaries layout and spacing between lamps in section and plan view. In the plan and section view, the S is centre to centre spacing between the two luminaries and S/2 is spacing between the wall and the luminary.

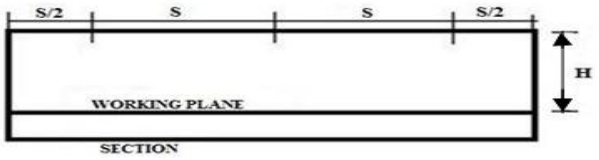

Fig.4.1 Section view of a room & luminaries

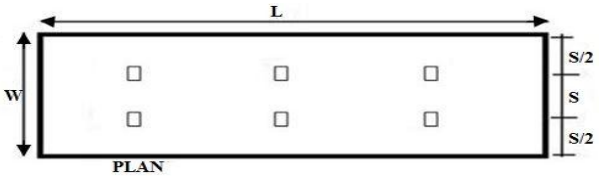

Fig.4.2 Plan view of a room & luminaries

Various softwares are available for studying the lighting layout. These softwares create genuine graphical models of the physical system under various light conditions and the models created can be analyzed effectively. DIALux is one of these popular softwares for design of lighting layout [12-15]. Lighting design using this software is simple yet precise. It creates realistic virtual lighting models of the physical system giving accurate and reliable representations of under different lighting conditions. It also calculates the power utilized by the lighting devices based on national and international regulations.

4.1.2 Case Study Analysis

A Room is selected for the case study for the comparison of different lighting schemes. The Room is rectangular in shape of width 5.94m, length 11.89m. The height of the room is 3m. The room reflectance of the ceiling, wall and floor are taken as $\rho_{ceiling}$ =70%, ρ_{walls} =50% and ρ_{floor} =20% respectively. The measurement of required illumination has been performed on a working plane and the height of the working plane is 0.98m. The required illuminance level used are 300 and 400 Lux. The tariff of Non – Domestic Low Tension (NDLT) load consumption in Delhi for 1kWh of electricity at the time of work was ₹ 8.5/kWhr [16].

a. Energy consumption by different lighting sources

In this work three different types of lamps as IN, CFL and LED lamps are compared in terms of no. of luminaries (N_t), total power utilized (P), power density (Pd), electric energy consumed (E_Y), cost of electricity (C_Y) and lighting energy numerical indicator (LENI) [17]. The Room is a clean room and it is also ensured that the failed lamp will be replaced promptly; So MF is taken as 0.8. The value of room index and corresponding UF are calculated using equation (4.1) and (4.2) and numbers of luminaries are calculated using equation (4.3). In the case study, the room working hours are supposed to be 8 hours a day, five days a week.

Electric energy consumption of Room in a year can be calculated as,

Electric energy consumption in a yr in KWh (E_Y) =

$$\frac{(room\ working\ hours * power\ utilized)}{1000} \tag{4.6}$$

Taking the local tariff, cost of electricity can be calculated as:

$$\text{Cost of electricity in a yr } (C_Y) = E_Y * \text{Tariff} \tag{4.7}$$

Table.V and Table.VI shows the comparison of different sources with respect to different factors for illuminance level of 300 & 400 Lux respectively.

TABLE III THE COMPARISON OF SOURCES AT 300 LUX

Lamp	N_t	P (W)	Pd (W/m^2)	E_Y (kWh)	C_Y (₹)	LENI (kWh/m^2)
IN 100W	30	3000	42.476	6000	51000	84.95
CFL 25 W	30	750	10.619	1500	12750	21.23
LED 25W	20	500	7.079	1000	8500	14.15

TABLE IVI THE COMPARISON OF SOURCES AT 400 LUX

Lamp	N_t	P (W)	Pd (W/m^2)	E_Y (kWh)	C_Y (₹)	LENI (kWh/m^2)
IN 100W	40	4000	56.635	8000	68000	113.2
CFL 25 W	40	1000	14.158	2000	17000	28.31
LED 25W	24	600	8.495	1200	10200	16.99

Fig.4.3 shows the comparison graphs for 300 and 400 Lux in terms of no. of luminaries, LENI. Fig.4.4 shows the comparison of LENI for IN, CFL with respect to LED

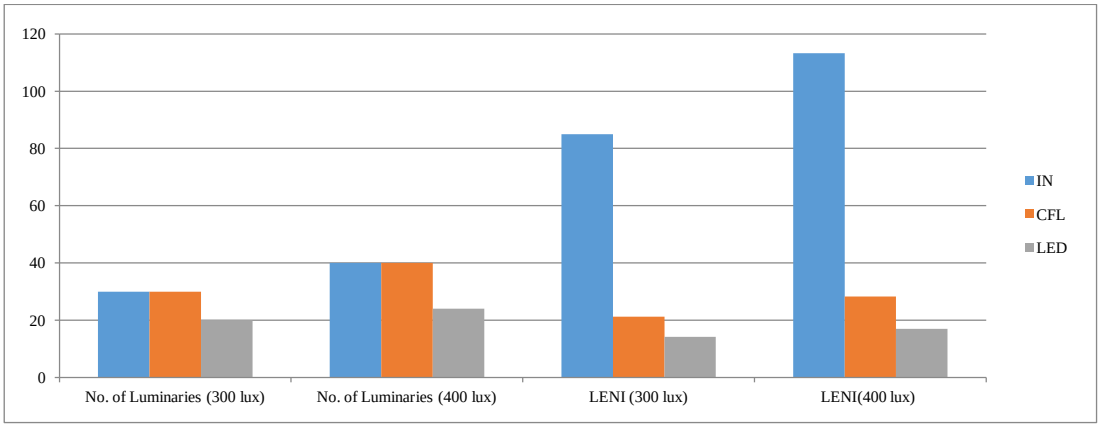

Fig.4.3 Comparison of No. of Luminaries & LENI between different luminaries for 300 & 400Lux

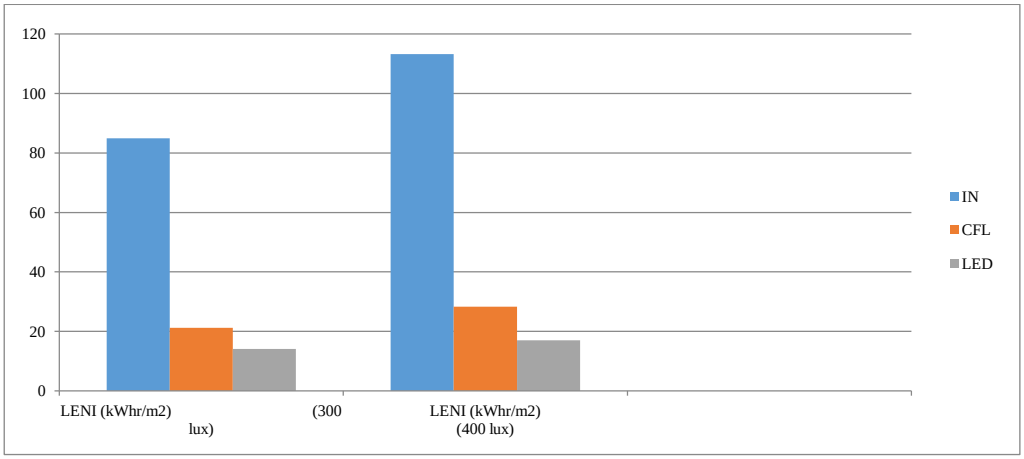

Fig.4.4 Comparison of LENI for IN, CFL with respect to LED

It has been observed that the LED luminary is 84.16 % more efficient than IN LAMP and 37.0 % more efficient than fluorescent luminary in terms of LENI as shown in fig.4.4. The power per unit area required for LED is less as compare to other luminaries.

4.1.3 DIALux Simulation

As is clear from the above graphs, LED is very much efficient than all other luminaries. So, LED source is used as lighting source to study the design of room using DIALux simulation software for LED luminary. The various lux values and electrical load are acquired in simulation.

The room is illuminated through the use of Philips RS341B1 X LED 26S/FMT MB is used as LED light source. The rating of source is 25W, 2500lm. Fig.4.5 shows the photometric diagram of the lamp. The photometric diagram represents the distribution of luminous intensity, in candela (cd), for the transverse and axial planes of the luminary

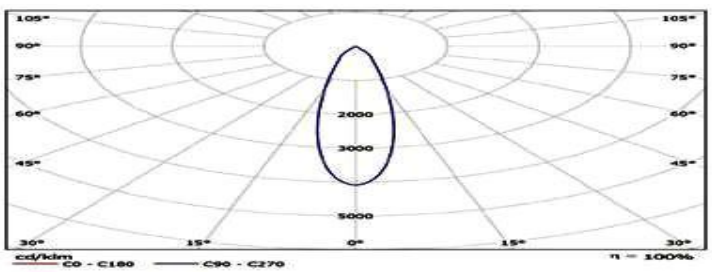

Fig.4.5 Photometric diagram of lamp LED - 25W, by Philips

Simulation result

The simulation results using DIALux as given in fig.4.6 show the room layout, distribution of luminaries and luminous flux, total lumen required for 300 Lux

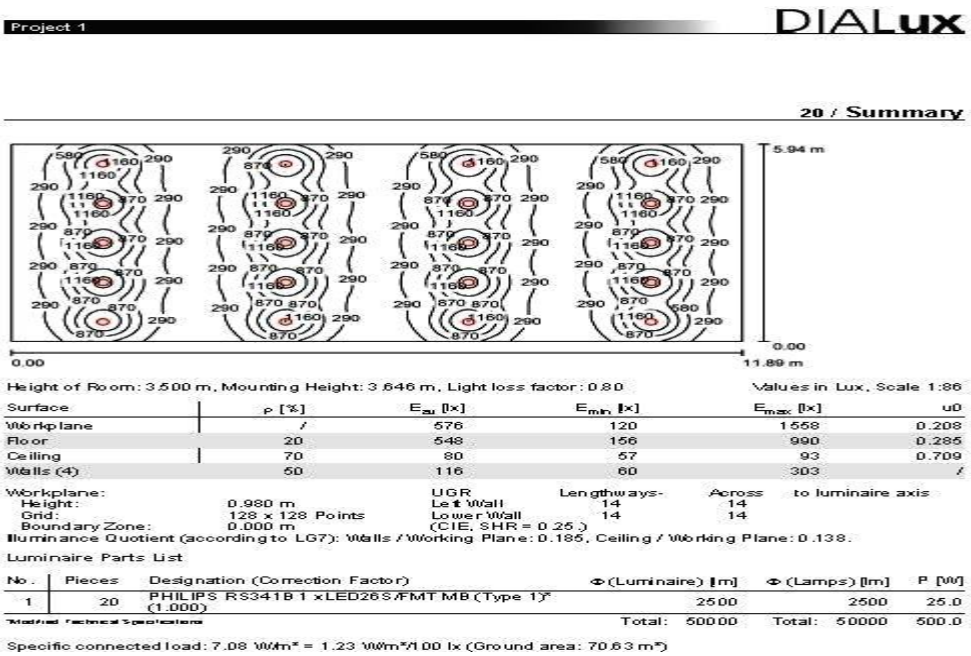

Fig.4.6 Simulated result from DIALux for 300Lux

It can be observed that for illumination level of 300 Lux no. of LEDs required are 20 as shown in Fig.4.6. It has been observed that no. of LED luminaries calculated using Dialux software matches with the calculated value as given in Table.V.

4.2 LED MODELLING

LED is a unique type of diode & they have analogous characteristics as the P-N junction diode (i.e. the P-N junction remittance light, when electrical energy is associated to it). This process is called as electroluminescence which can be defined as the ejection of light from a semiconductor affected by an electric field. The charge transporters recombine in a forward-one-sided P-N junction as the electrons cross from the N-region and recombine with the holes existing in the P-region. Free electrons are in the conduction band of energy levels, while holes are in the valence energy band. In this manner the energy level of the holes is not as much as the energy levels of the electrons. Some segment of the energy must be disseminated to recombine the electrons and the gaps. This energy is produced as warmth and light.

4.2.1 LED Characteristics and Model

In order to precisely describe the LEDs nonlinear characteristics, the exponential functions in equation (4.8) for the LED can be used to describe the relationship between forward voltage and forward current. Fig.4.7 shows the LED characteristics at different temperature i.e. 10^0C, 15^0C & 25^0C that are exponential in nature [18]. Data are taken from Cree® XLamp® XPE2 LED data sheet for plotting the graph [28]. So, from V_{LED} v/s I_{LED} graph it can be seen that LED can be modeled as an ideal diode D, the forward diode voltage drop V_f, and the series resistance R_{LED} as shown in Fig.4.8

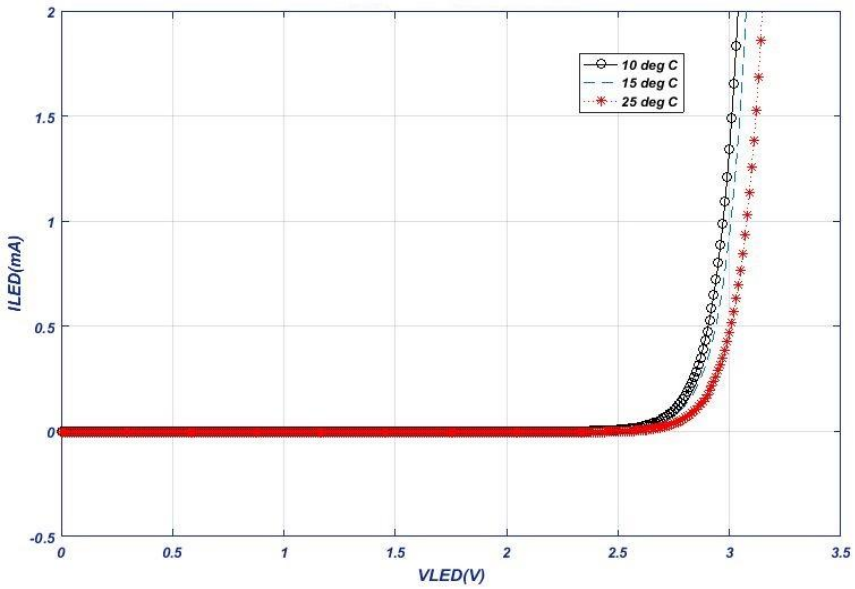

Fig.4.7 LED characteristics at different temperature

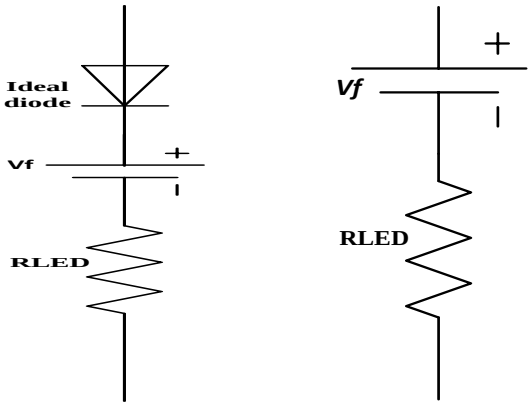

Fig.4.8 Equivalent circuit and Approximated linear cicuit of LED

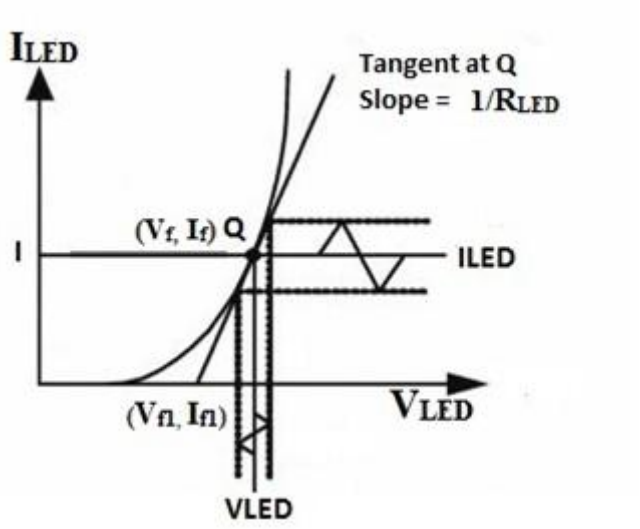

Fig.4.9 Approximate Linear Model

The non-linear V-I characteristics of the LED in exponential function to describe the measured V-I curve is shown [18], as below.

$$I_{LED} = I_{Sat} * \left(\exp^{\frac{V_{LED} * q}{K * T}} - 1\right) \quad (4.8)$$

Where,

V_{LED} = Forward Voltage of LED

I_{LED} = Forward Current of LED

I_{sat} = Saturation Current of the LED

q = electron charge ($1.602*10^{-19}$)

K = Boltzman's constant ($1.38*10^{-23}$)

T = temperature

The approximate linear model can be built to fit the exponential V-I curve of the LED, which are tangent to the exponential V-I curve at the operating point Q(V_f, I_f), as shown in Fig.4.9. The time-varying LED forward current I_{LED} depends on time-varying LED forward voltage V_{LED} and the slop of the tangent line [19]. Therefore, the approximate linear model only matches the exponential V-I curve of the LED at the operating point Q..

From the approximated linear model LED can be modeled as simple series resistance, R_{LED} and forward voltage drop, V_F is represented by a battery as shown in Fig.4.8.

As shown in fig.4.9, the Resistance of the LED can be calculated from the slope of the tangent is given as,

$$\frac{1}{R_{LED}} = \frac{I_f - I_{f1}}{V_f - V_{f1}} \tag{4.9}$$

Here, I_f is 0.35 A, I_{f1} is 0 A, V_f is 2.9V & V_{f1} is 2.6V from fig. 4.7.

Putting all values of I_f, I_{f1}, V_f and V_{f1} in above equations, the value of R_{LED} is,

$$\frac{1}{R_{LED}} = \frac{1}{1.16}$$

That result as $R_{LED} = 0.823\Omega$

4.3 BUCK CONVERTER BASED PFC LED DRIVER

In common purpose LED lighting, non-isolated and isolated PFC (power factor corrected) LED drivers are used. From a safety point of view, isolated converter topologies are preferred. Many researchers are working to develop single-stage PFC converter-based topologies with improved power quality. The double-stage PFC-based LED drivers have many drawbacks such as large number of components, high cost, less efficient but single-stage single switch PFC ac–dc converters have less number of components so cost is low and more efficient. In low-power applications, single-stage buck and flyback PFC converter topologies are most suitable because of low component count and cost. In flyback converter, because of high voltage stress across active switch owing to ringing phenomenon between the leakage inductance and transition capacitance of the MOSFET, a high rating snubber circuit is required [20–22].So because of the large power loss in the snubber circuit and extra cost required for snubber in flyback converter, buck PFC converter is preferred. As buck converter have low component count i.e. it have only one transistor and minimum cost.

In this model, power quality improvement (PQI) is done using a PFC buck converter operating in CCM. The proposed buck converter is the simple and has well regulated switching for low power LED lamp loads. The LED drivers should show almost unity power factor with total harmonic distortion (THD) of input AC current less than 17.27% for the universal ac mains voltage, which is as per the IEC-61000-3-2 class D requirements [23].

4.3.1 Working of the Buck PFC LED driver

The PFC buck ac–dc converter topology consists of a DBR, an output ripple filter at DBR output side, a buck converter and a LED output current control scheme as shown in fig.4.10 buck converter work in two mode i.e. switch is ON and switch is OFF.

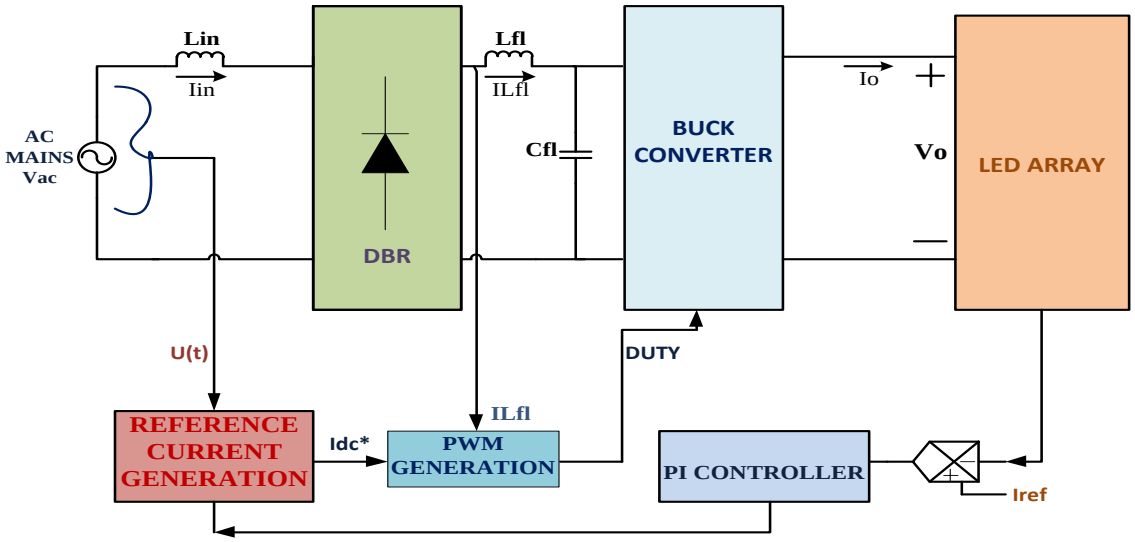

Fig.4.10 LED Driver Block Diagram

Mode 1 (Switch is ON):

When MOSFET 'S' is ON i.e. for DT time period as shown in fig.4.11 the diode will became reverse biased and the current will flow through Inductor L_f and the current will increases proportionally and store the energy and in this mode capacitor C_f will get charged up so, voltage will appear across R_l i.e. load resistance.

Mode 2 (Switch is open):

When MOSFET 'S' is OFF i.e. for (1-D) T time period, the diode became forward biased and the stored energy of inductor will flow from load to diode, diode will work as in freewheeling condition and the inductor current will decreased in proportional manner. In this mode capacitor will also charge up.

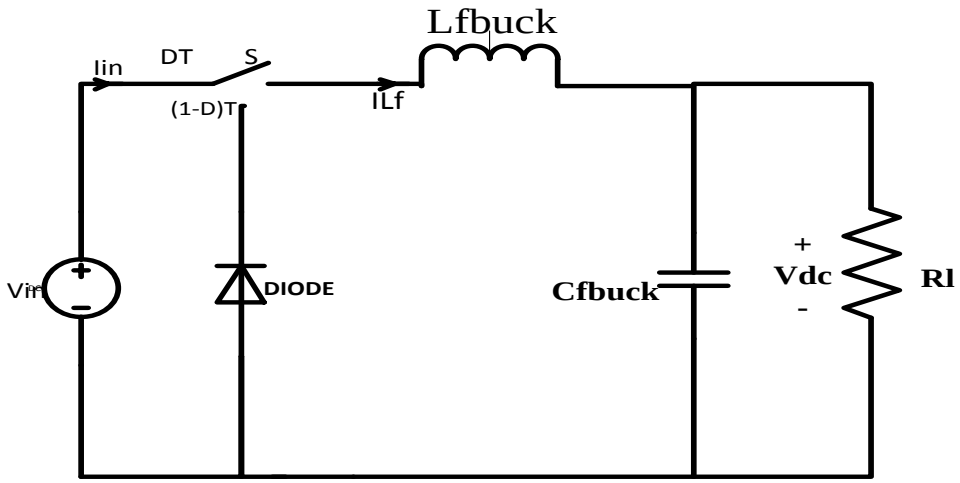

Fig.4.11 Buck Converter

4.3.1.1 Control Scheme Design

The buck converter with control scheme is shown in fig.4.10. The control scheme consist of LED current controller, reference current generator and current controller with PWM generator. The outer loop is to adjust the LED output current to desire output value by doing this the constant voltage across LED load is achieved [24]. Reference current generator is to produce the reference current by doing the product of two quantity i.e. LED PI current controller output and unit voltage template (u(t)) and this reference current is compare with sensed output current from DBR (I_{Lfl}) and this error is minimized by PI controller. The output is compared with 66KHz reference saw tooth signal and the MOSFET (Switch) is triggered. By performing such inner loop control the input AC current will be in phase with the input AC voltage (V_{ac}) i.e. power factor will be close to unity and THD will be under standard defined value.

Unity template is defined as magnitude of input AC voltage (absVac) with respect to the peak value of V_{peak}

$$U(t) = \frac{abs\, V_{ac}}{V_{peak}} \tag{4.10}$$

Where, $V_{a\,c}$ = Input AC voltage

V_{peak} = peak value of V_{ac}

Design calculation of Buck converter

The design of a PFC buck converter is carried out in CCM for improving the power quality at the universal ac mains.

Equations for calculating values of Inductor & Capacitor [25,26] are given by equations (4.12) & (4.13)

$$\text{Duty (D)} = \frac{Vout}{Vin} = 0.40 \tag{4.11}$$

$$\text{Inductance } (L_{fbuck}) = \frac{D(1-D)*V_{in}}{f_s.\Delta I_{Lf}} = 9.1\text{mH} \tag{4.12}$$

$$\text{Capacitance } (C_{fbuck}) = \frac{D(1-D).Vs}{8.f_s^2 L\Delta V_{Cf}} = 121.3\mu\text{F} \tag{4.13}$$

Where,

V_{in} = Input Voltage Of A Converter

V_{out} =Output Voltage across Load

f_s = Switching Frequency, 66 kHz

ΔI_{Lf} is the Inductor ripple current. Its value by 10% of $I_{out(max)}$

ΔV_{Cf} is Capacitor ripple voltage. Its value is given by 3% of V_{in}

The filter components L_{fl} and C_{fl} are taken as 1mH and 10^{-4}F respectively.

4.3.2 Result and discussion

The proposed PFC buck converter has been simulated using MATLAB-SIMULINK. Buck converter components have been designed using the above calculated inductance and capacitance values.AC supply has been used as input for the converter. In respect to Power quality of the model the THD has been calculated.

Simulation model

The simulink model as shown in Appendix 2 is consists of AC supply of 100V, Full wave Diode bridge rectifier (DBR),PFC buck converter with PI current controller, Reference current generation and PWM generation and LED lamp load. In simulation

array of 13 LED are connected in series. Each LED is having the forward voltage of 2.9V and forward current of 350mA.

The LED lamp current is maintained constant at 0.36A and thus the LED lamp voltage is maintained at 35.6V, the low harmonics at input current side and high power factor is observed. This is verified by observing input AC current, input AC voltage, LED Lamp output current and voltage waveforms as shown in fig.4.12, 4.13, 4.14 respectively for 100V AC supply.

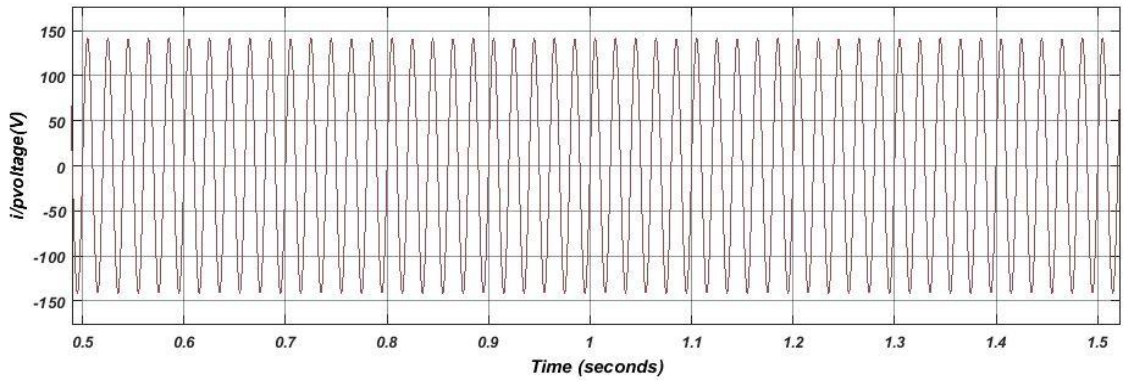

Fig.4.12 Supply Voltage, V_{ac}

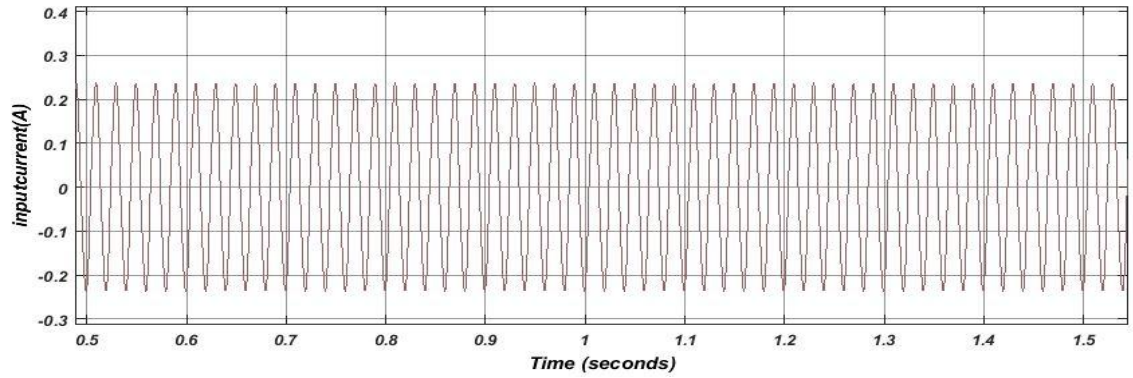

Fig.4.13 Supply Current, I_{in}

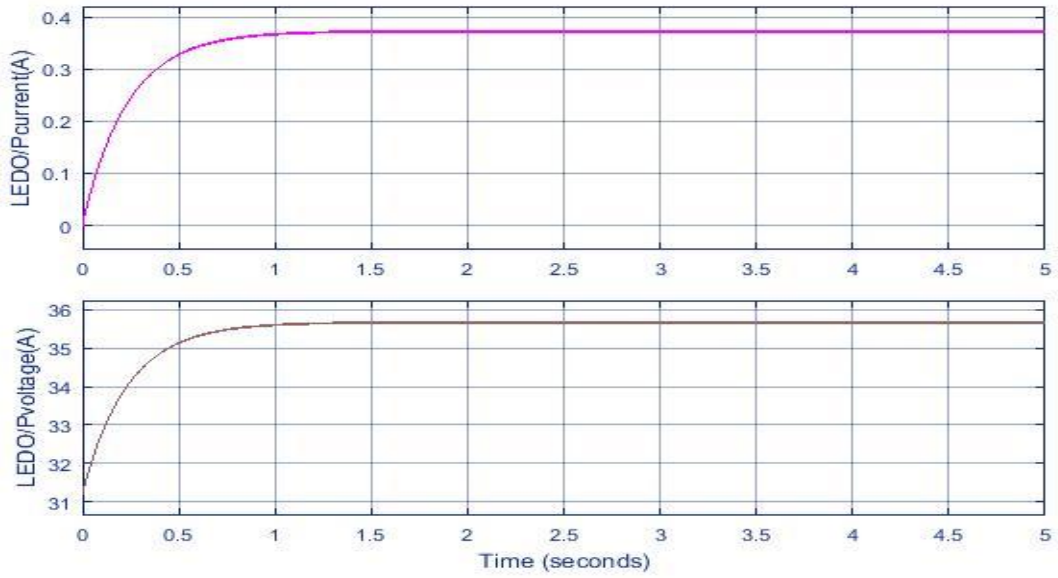

Fig.4.14 Output Current & Voltage across LED

It is observed from result that the THD is 4.68% which is fulfilling the limit of IEC 61000-3-2 (Class D) at ac mains and power factor is 0.989

4.4 CONCLUSION

This chapter deals with the techno economic comparison of various luminaries', LED modelling and their driver circuit. Techno economic comparison shows that LED luminary is more efficient and require low energy than other luminaries. The LED can be modelled as simple resistor in series with forward voltage drop which represents by a battery. PFC Buck converter based LED driver circuit is presented in this chapter which shows almost unity power factor with Total Harmonic distortion of 4.68 % which is fulfilling the limit of IEC standards.

CHAPTER 5

SMART SOLAR STREET LIGHT

Solar PV is an outstanding source of energy accessible all over the world but in Direct Current (DC) form. Light emitting diodes (LEDs) become more popular with respect to lighting applications because of their good intensity or high luminous with low power consumption as discussed in previous chapter and also, they work on DC very effectively. So, SPV and LED is a perfect combination for outdoor lights.

With rising concern about global warming and climate change, renewable energy systems are getting great attention. Rather than generating electricity in power plants and transmitting it to distant remote location, stand-alone SPV system generation is beneficial in many applications because it reduces transmission losses and avoid conversion from DC to AC, which consequence on increase in efficiency of the system. One of the typical examples of stand-alone SPV generation is to supply local load i.e. solar PV supplying electricity to a street light. The street-lighting has been equipped by LEDs now a days.

Normally, a LED driver circuit as discussed earlier. utilizes AC supply as an input to change it into a suitable DC voltage level by using PFC converters as described previously .As Solar PV generates power in unidirectional form i.e. DC which can be straightforwardly used by a LED lamp, so it is a very valuable combination for reducing harmful effect that are produced by conventional system [27].

5.1 PV LED LIGHTING SYSTEM

The quantity of power developed by a SPV system is dependent on the solar irradiance so by sensing irradiance energy management between SPV, Battery and load can be controlled. This work propose the battery charging, energy management between load and sources algorithm, also the automatic intensity control of the LEDs lamp by controlling the duty of the DC-DC converter i.e. boost converter. Depending on the traffic situations, the intensity of the street lamp can be adjusted from 0% to 100% automatically by making use of a DC-DC converter. A SPV system of a suitable capacity is being utilized throughout the day time to charge a Li-ion battery through the

DC-DC buck converter with MPPT. At night, the stored energy of battery is utilized by the Boost converter to power up the Load i.e.; LEDs lamp

5.1.1 System Description

The description of the proposed system is shown in Fig.5.1.The main purpose is to build up a standalone low power solar PV Street lighting system with the help of power LED arrays.

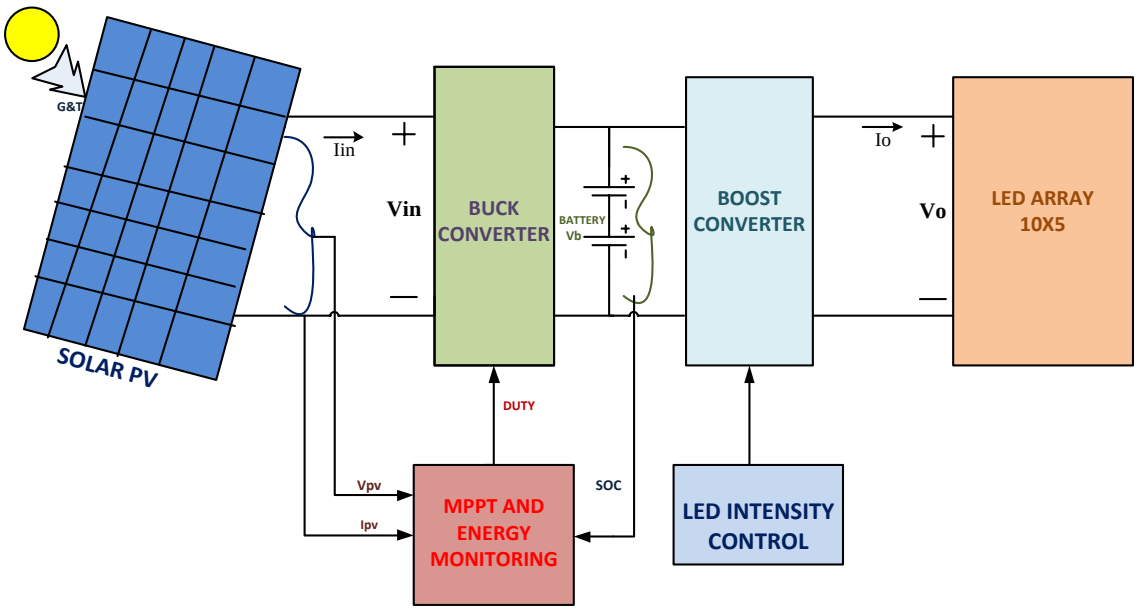

Fig.5.1 Solar Street Light Block Diagram

A SPV system of a capacity of a 200W peak with an output voltage and current of 39V and 5.20A (peak) is acting as the supply for the whole system. 10x5 LED array is used in LED light, Each LED is of 1W rating and each have forward voltage of 2.9V. An array of 10x5 LEDs is modelled to represent the LED load. Hence the overall voltage of 10 LEDs in series is 29V.

A Li-ion battery of 24V capacity is used to store the energy from the SPV system during the daytime; as the battery is charged in daytime and discharged during night through the LED array. During high traffic hours i.e. from dusk to 12:00 AM in the midnight, the LED lamp is planned to glow with its 100% intensity and during non-traffic hours i.e. next 6 hours the LED lamp intensity will be reduced down to 50%. A boost converter is utilized to control the intensity of the LED lamp. When LED lamp is

glowing at the full intensity, the dc-dc boost converter will boost the battery output voltage of 24 V to 29V.During wee hours (12:00AM to 6AM) the intensity is reduced to 50%, this done by boosting the battery voltage of 24 V to 27.8V.

Solar PV is designed to produce the output voltage of 39V; a dc-dc buck converter with MPPT is used to step down the SPV voltage to 24V for charging a battery. The battery capacity is selected such that even if there is cloudy and rainy climate for consecutive three days, the battery will able to supply electricity to LED light with any interruptions.

a. PV Array

A SPV system of a capacity of 200W peak is used in simulation and all the SPV specifications is described in Table.VII

TABLE VI SOLAR PANEL SPECIFICATIONS

SOLAR PANEL SPECIFICATIONS	
Open circuit voltage (V_{oc})	23V
Short Circuit Current (I_{sc})	5.8A
Max power (P_{max})	105W
Voltage at P_{max} (V_{mp})	19.5 V
Current at P_{max} (I_{mp})	5.20A
Tolerance (At STC)	5%

The maximum power is produced at 39V i.e. 200W at solar irradiance of 1000W/m^2 and 25^0C, 100W at Solar Irradiance of 500W/m^2 as shown in fig.5.2

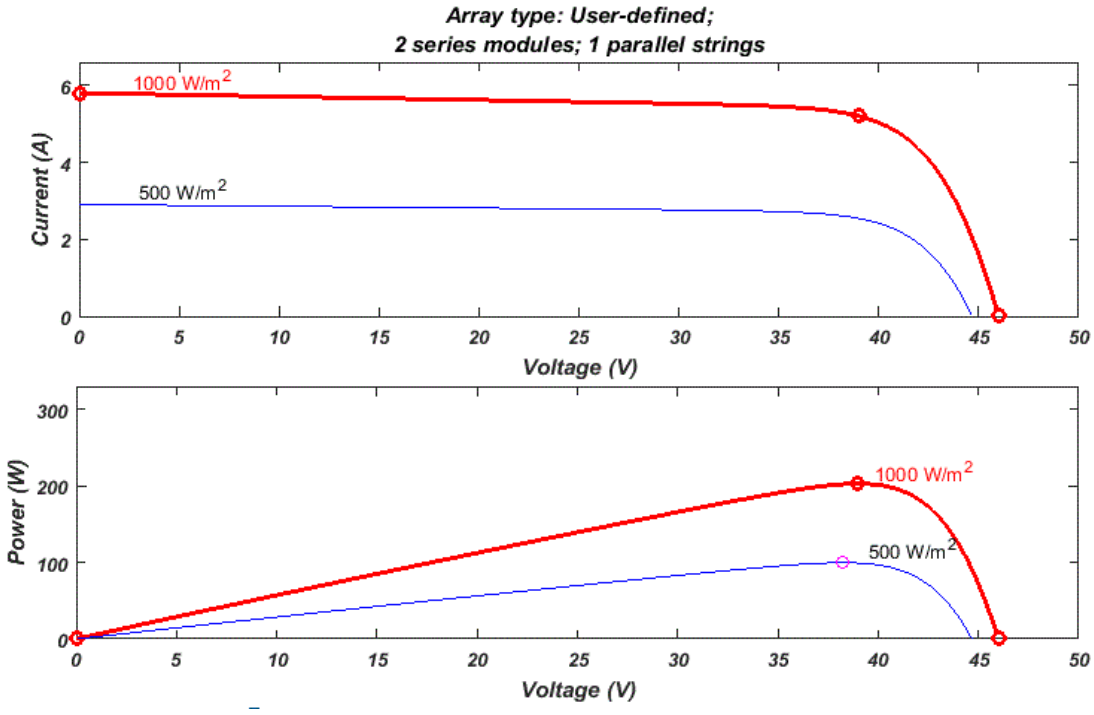

Fig.5.2 SPV current and Power V/S voltage Characteristics

b. DC-DC converter with MPPT

The duty cycle in DC to DC buck converter is varied by MPPT controller. The MPPT algorithm used for extracting the maximum power for charging the battery is Incremental conductance (INC).INC algorithm has been discussed refers 3.3.2. The INC is used with buck converter for switching the MOSFET at 125KHz. Buck converter is used for stepping down the PV output voltage of 39V to 24V i.e. is required by battery.

The buck converter can be designed by using following equations

$$\text{Inductance } (L_f) = \frac{D(1-D)Vs}{f_s.\Delta I_L} = 0.8488\ \mu H \qquad (5.1)$$

Where D is Duty cycle of the converter, V_s is input voltage, f_s is switching frequency, 125KHz, ΔI_L is Inductor ripple current

$$\text{Capacitance } (C_f) = \frac{D(1-D).Vs}{8.f_s^2 L\Delta V_C} = 0.73\ \mu F \qquad (5.2)$$

Where L is Inductance value, ΔV_c is Capacitor ripple voltage.

c. Solar Battery Storage

A battery of 24V is used to accumulate the energy provided by the PV array in daytime, and when there is not enough sunlight the will supply energy to the LED load. For this purpose Li-ion generic parameterized battery model is used which can be accessible in Matlab-Simulink. The battery capacity is selected such that even if there is cloudy and rainy climate i.e. overcastting for consecutive three days, battery will give supply with any interruption.

d. *DC-DC boost converter*

A boost converter is used for intensity control of LED and stepping the battery voltage i.e. 24V to the desired output voltage. So boost converter is used as a LED driver. The converter is working in continuous conduction mode (CCM) and value of Inductor and capacitor is calculated from the equation (5.5) & (5.6) respectively.

$$\Delta I = \left(\frac{(\text{currenttolerance})*(I)}{100}\right); \tag{5.3}$$

$$\Delta V = \left(\frac{(\text{voltagetolerance})*(V_s)}{100}\right); \tag{5.4}$$

$$L_{boost} = \left(\frac{\text{duty}*Vs}{(f_s*\Delta I)}\right); \ = 0.9 * 10^{-4}\ \text{H} \tag{5.5}$$

Where V_s is input voltage, f_s is switching frequency 13KHz,ΔI is Inductor ripple current

$$C_{boost} = \left(\frac{\text{duty}*I}{(f_s*\Delta v)}\right); \ = \ \ 3 * 10^{-5}\text{F} \tag{5.6}$$

Where L is Inductance value, ΔV is Capacitor ripple voltage

e. LED control and description

The LED lamp load is model as simple series resistance with battery. Each LED used have a forward voltage of 2.9V and a forward current of 350mA, I-V characteristics of LED is shown in fig.4.7 This data's are taken from Cree® XLamp® XPE2 LED data sheet [28].10X5 array of LED is modelled in Matlab-Simulink. The intensity of LED is controlled by changing the duty of the boost converter after 2.5sec in simulation.

5.1.2 System Designing

Battery Rating Calculation:

Normal power rating of LED =1W

The maximum energy required by the LEDs for 12 hours in a day ($6 * 50\text{W} + 25 * 6$) =450Wh

For 3 days, the required amount of energy ($450 * 3$) = 1350 Wh.

For 24V battery, Required Charge Capacity is 1350/24 = 56.25Ah.

Deep discharge batteries are used here with DoD in the range of 60% to 80%, Taking DoD of 70%, Required Charge Capacity $= 54/0.7$ = 80.35 Ah

PV Array rating calcultaion:

Consider the efficiency of the Battery, 90% and efficiency of SPV Array and Converter, 90%

Energy required at the battery = $\frac{1350}{0.9} = 1500Ah$

Energy that should be supplied by Buck Converter =$\frac{1500}{0.9} = 1666.67Ah$

Total Ah generated = $\frac{1666.67}{24} = 69.44Ah$

The SPV module's Power capacity is varied with respect to Solar Irradiation. In India average of 1000W/m^2 irradiation is for 6hrs & 500W/m^2 irradiation is for 4hrs, So total hrs for Solar irradiation of 1000W/m^2 is 8hrs a day. So, total current generate at buck converter output is 8.68A and correspondingly solar array should produce 5.5A short circuit current (Duty of converter = 0.65)

So, solar PV array rating will be 200W at STC.

5.1.3 Simulation Result & Discussion

The developed scheme has been modelled & simulated as shown in Appendix 3 using MATLAB/SIMULINK software. All the parameters have been designed using the above calculated values to obtain the good performance of the system. The LED lamp load is modelled as simple series resistance with battery as described in previous section.

As for whole day the solar irradiance is variable, so the battery charging is performed for two solar irradiations i.e. 1000W/m^2 and 500W/m^2. The Power-Voltage-Current graph of solar panel for both irradiance is shown in fig.5.3, 5.4 & 5.5 As is clear from fig that at 1000W/m^2 the maximum power is 200W and for decreased irradiance of 500W/m^2 i.e. after 2.5 sec of simulation time the maximum power is reduced to 100W. The battery parameters i.e. SOC, voltage and current are shown in fig.5.6, 5.7 & 5.8 respectively.

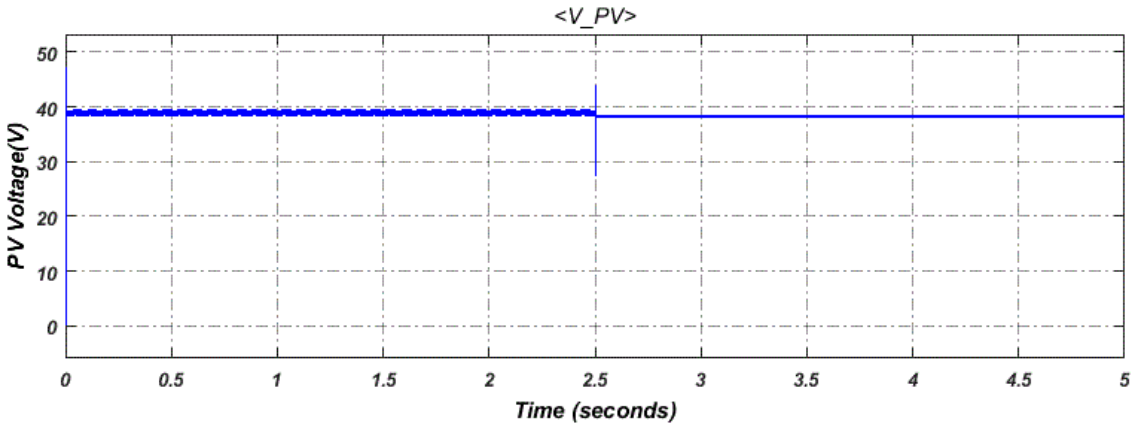

Fig.5.3 PV voltage at two Irradiation (1000W/m^2, 500W/m^2)

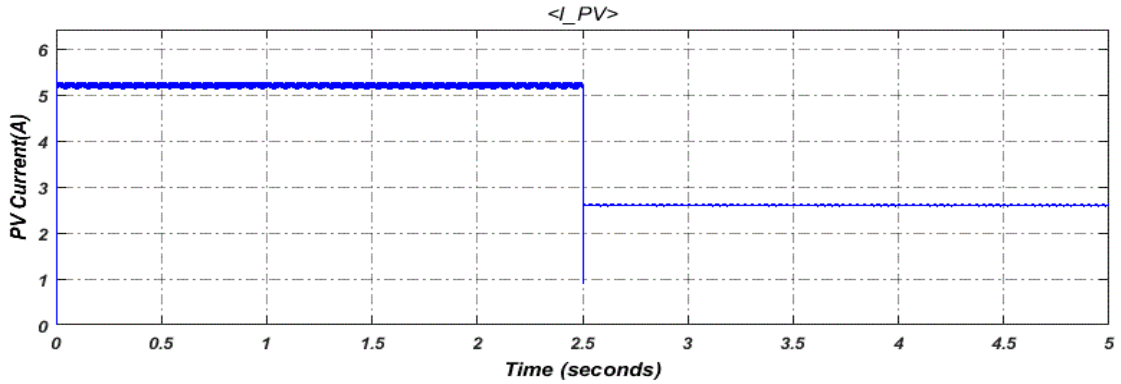

Fig.5.4 PV current at two Irradiation (1000W/m^2, 500W/m^2)

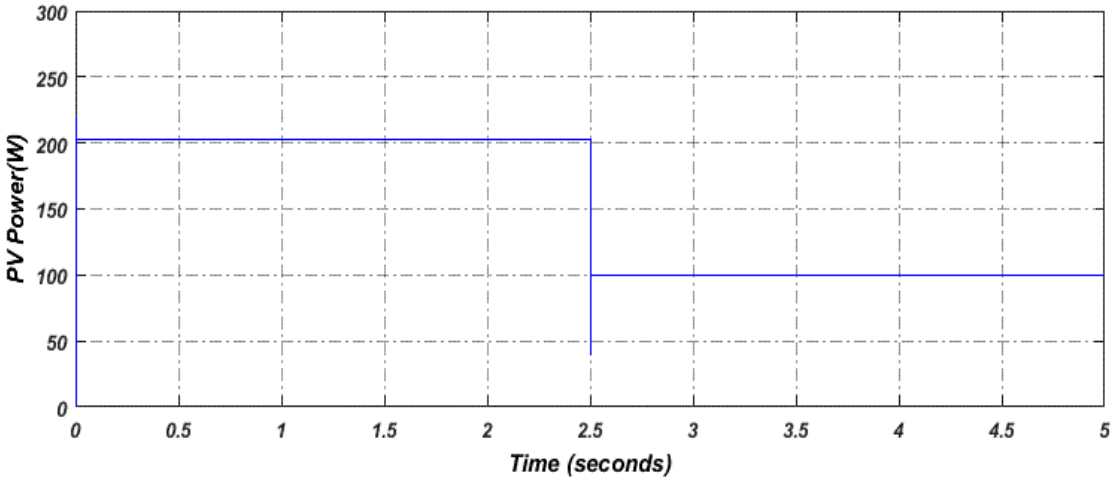

Fig.5.5 PV power at two Irradiation (1000W/m^2, 500W/m^2)

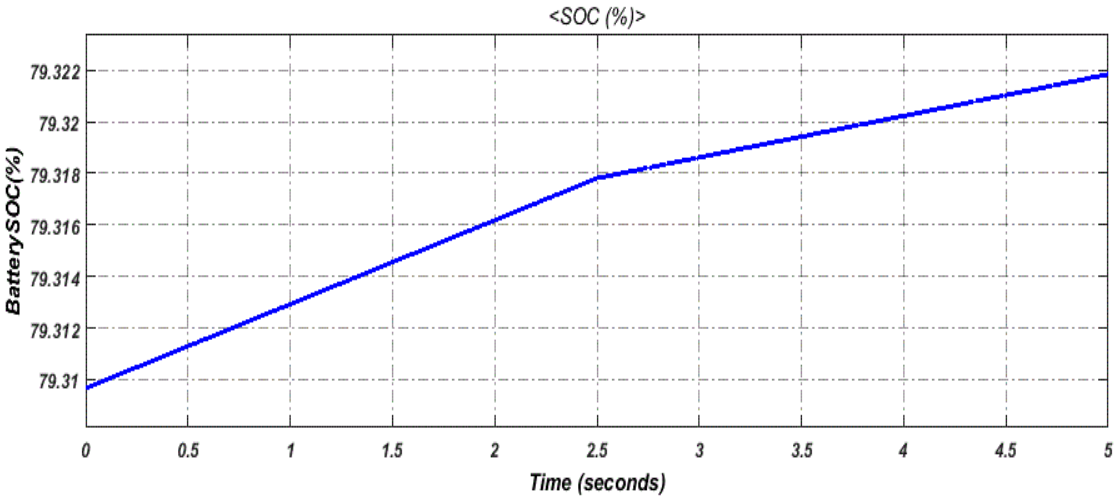

Fig.5.6 Battery SOC (%) at two Irradiation (1000W/m^2, 500W/m^2)

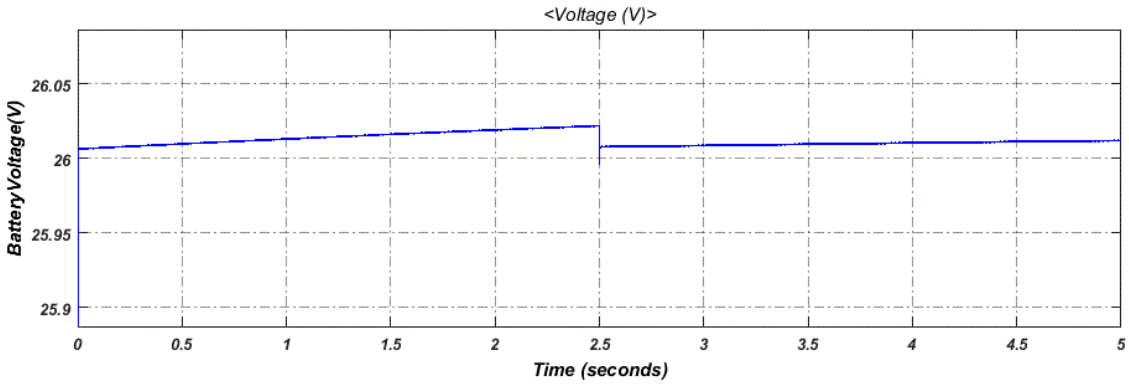

Fig.5.7 Battery Voltage (V) at two Irradiation (1000W/m^2, 500W/m^2)

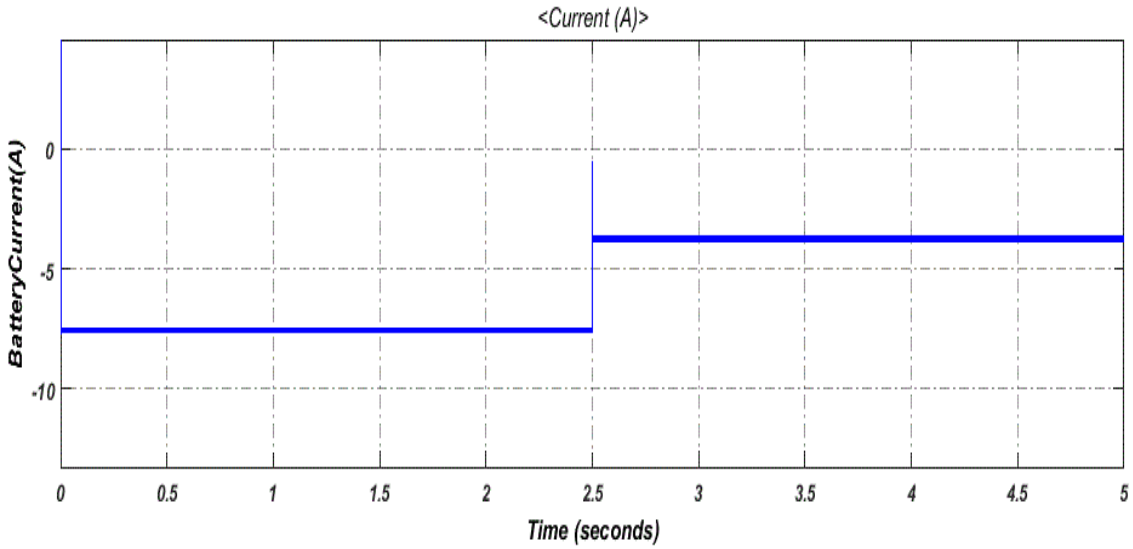

Fig.5.8 Battery Current (A) at two irradiation (1000W/m^2, 500W/m^2)

When solar is not available, the battery is supplying power to the LED lamps as shown in fig.5.9. From dusk to midnight the LED output current and voltage is 1.75A and 29 V respectively, so the power yield at the output is approx 50W. After midnight, as the traffic becomes very less so if intensity of luminary is controlled i.e. From midnight to 6:00AM i.e. after 2.5 sec in simulation the LED output current and voltage is 0.86A and 27.8 V respectively, so the power yield at the output is approx 24W. As it is clear from the results that the approximately 50 % of the energy is saved during the non traffic hours.

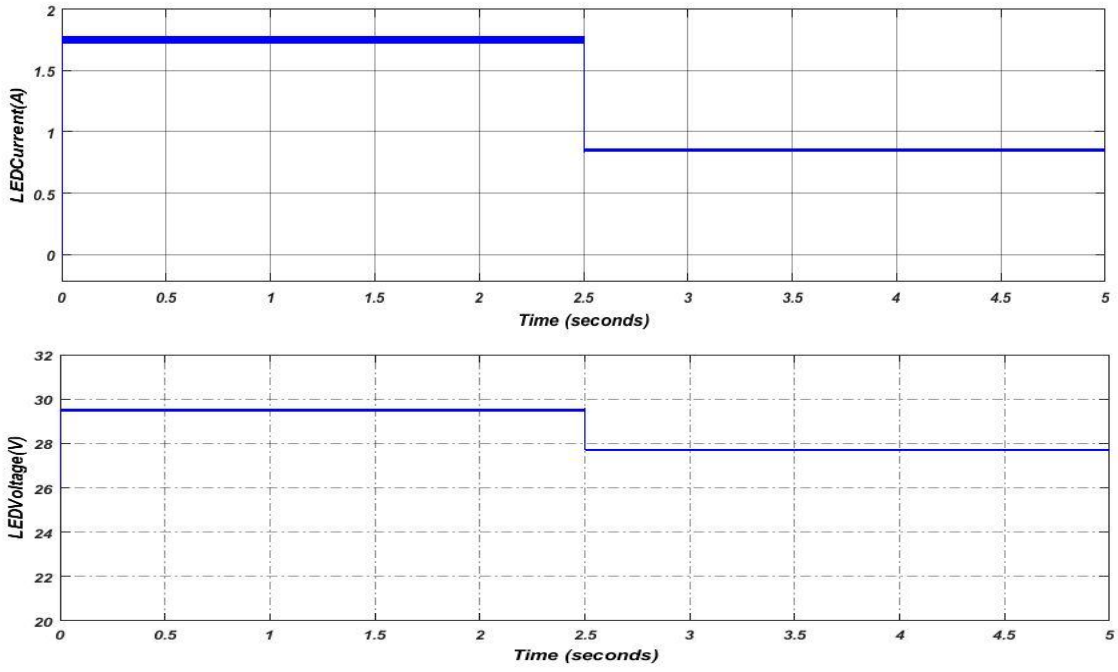

Fig.5.9 Output current (A), Output voltage (V) at different intensity

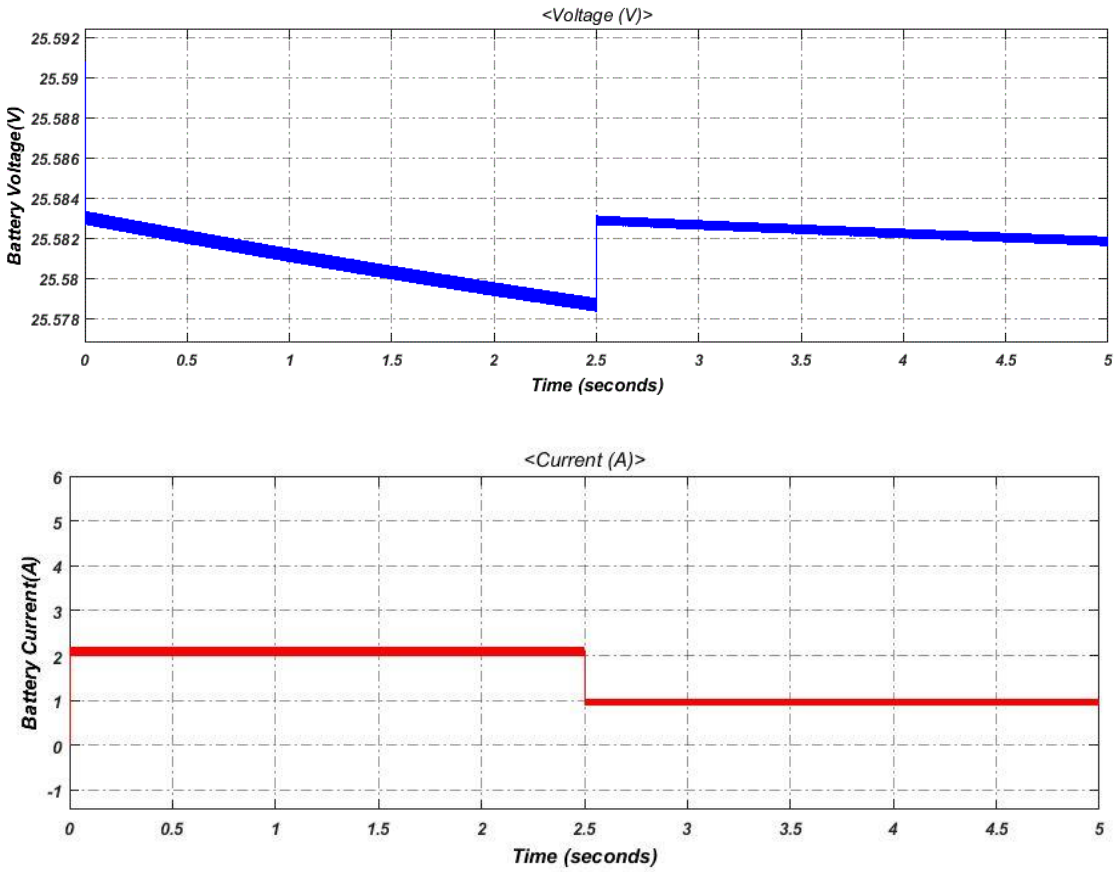

Fig.5.10 Battery Voltage (V), Current (A) at different intensity

All other parameters such as battery current, battery voltage at the time of load is consuming power is shown in fig.5.10. Fig clearly represent that the battery is discharging or supplying power.

5.2 PV HYBRID LED STREET LIGHTING SYSTEM

The output power of photovoltaic (PV) panels used in the street lighting system is usually limited to 200W because of the limited size of a mounting structure [29].So, because of Limitation for using SPV system greater than 200W in LED streetlight and overcast conditions, we cannot use the battery for more than 2 days if intensity of the LED load is not controlled. So, there is a need for another energy supplying element that can be Wind, Grid (Utility) etc.

The Structural block diagram of PV Hybrid is shown in Fig.5.11 and the working of the system can be explained with the help of vitality control algorithm as shown in fig.5.12. The framework comprises of SPV array of 200W, a lithium-ion battery of 24V/72Ah,

INC based MPPT, dc-dc Buck converter, a 230V AC/DC module and LED load of 50W.

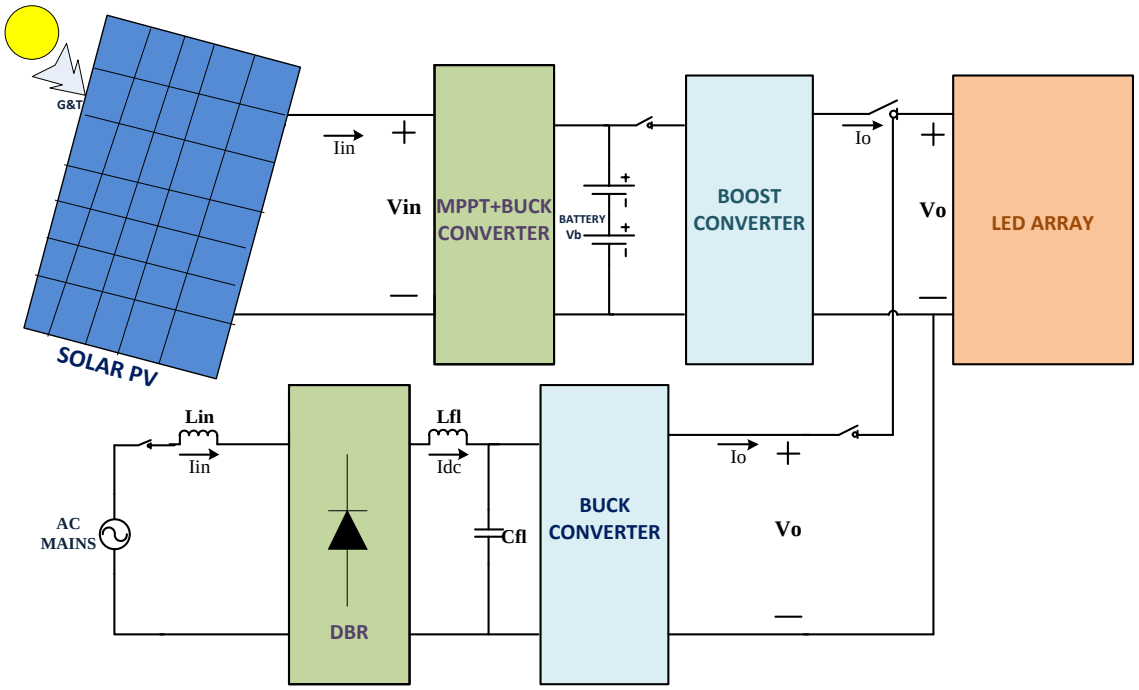

Fig.5.11 Block Diagram of PV Hybrid LED Street Lighting System

In the daytime, the battery is charged by PV array. During the night, the battery discharges to light up LED array. In the nonstop cloudy and rainy climate, there is no electric charge in the battery and here LED array will be lit up by the AC/DC (Grid) module. The power exchange switch circuit is utilized to choose either the battery or the AC/DC module to light up LED array from dusk to dawn, while in the daytime the power exchanging switches are in open mode because no power is needed by load as it is in OFF state.

5.2.1 System Designing

Battery Rating Calculation:

Normal power rating of LED =1W

The maximum energy required by the LEDs for 12 hours in a day $(50 * 12)$ =600Wh

For 2 days, the required amount of energy $(600 * 2)$ = 1200 Wh.

For 24V battery, Required Charge Capacity is 1200/24 = 50 Ah.

Deep discharge batteries are used here with DoD in the range of 60% to 80%, taking DoD of 70%, Required Charge Capacity $= 50/0.7$ = 71.42 Ah

PV Array rating calculation:

Consider the efficiency of the Battery, 90% and efficiency of SPV Array and Converter, 90%

Energy required at the battery = $\frac{1200}{0.90} = 1333.33Ah$

Energy that should be supplied by Buck Converter =$\frac{1333.33}{0.9} = 1481.47$

Total Ah generated = $\frac{1481.47}{24} = 61.72$Ah

The SPV module's Power capacity is varied with respect to Solar Irradiation. In India average of 1000W/m^2 irradiation is for 6hrs & 500W/m^2 irradiation is for 4hrs, So total hrs for Solar irradiation of 1000W/m^2 is 8hrs a day. So, total current generated at buck converter output is 7.71A and correspondingly solar array should produce 5.24A short circuit current (Duty of converter = 0.65)

So, solar PV array rating will be approx 200 W at STC and 2 Nos. of Module of 100W are connected in series, Its specification is given in Table VII.

Vitality Control Algorithm: This algorithm is used for maintaining the energy balance between PV Array, Battery, and Utility (AC/DC Module). The algorithm only sense voltage (V) & current (I) of PV and SOC of the battery, if Power (P = V*I) is less than 20W and battery SOC is between 30 to 80% the battery will supply the load. If SOC is not within the given limit the grid will be connected from dusk till dawn. If power of PV is greater than 20W then battery will be charged and other sources and load will be in OFF condition.

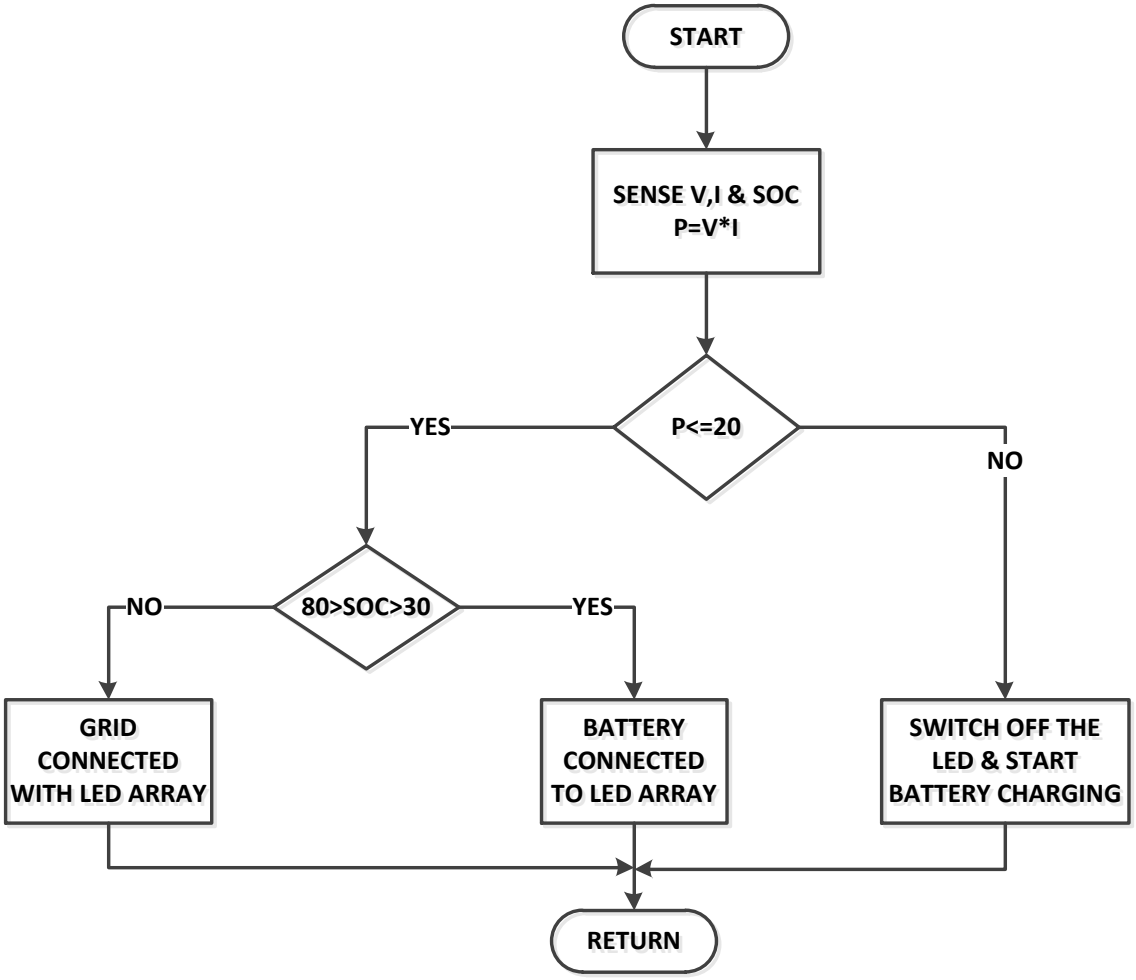

Fig.5.12 System Control Algorithm

5.2.2 Simulation Result & Discussion

The developed scheme has been modelled & simulated as shown in Appendix 4 using MATLAB/SIMULINK software. All the parameters have been designed using the above calculated values; The LED lamp load is modelled as simple series resistance with battery as described in previous section and 10x5 array of LED is used as a Load.

As for whole day the solar irradiance is variable, so the battery charging is performed for two solar irradiations i.e. 1000W/m^2 and 500W/m^2. The Power graph of solar panel for both irradiance is shown in fig.5.5 is clear from fig that at 1000W/m^2 the maximum power is 200W and for decreased irradiance of 500W/m^2 i.e. after 2.5 sec of simulation time the maximum power is reduced to 100W. Fig.5.6 & 5.7 show the battery charging i.e. SOC is increasing.

When solar is not available, the battery is supplying power to the LED lamp as shown in fig.5.13 & 5.14. From dusk to dawn the LED output current and voltage is 1.73A and 29.5V respectively and the current from utility is zero as shown in fig.5.15

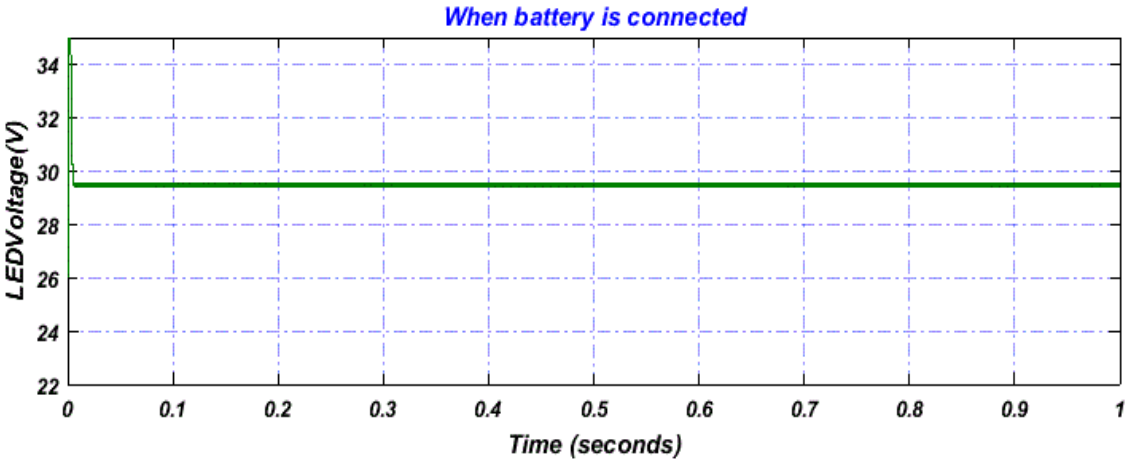

Fig.5.13 Output Voltage across LED

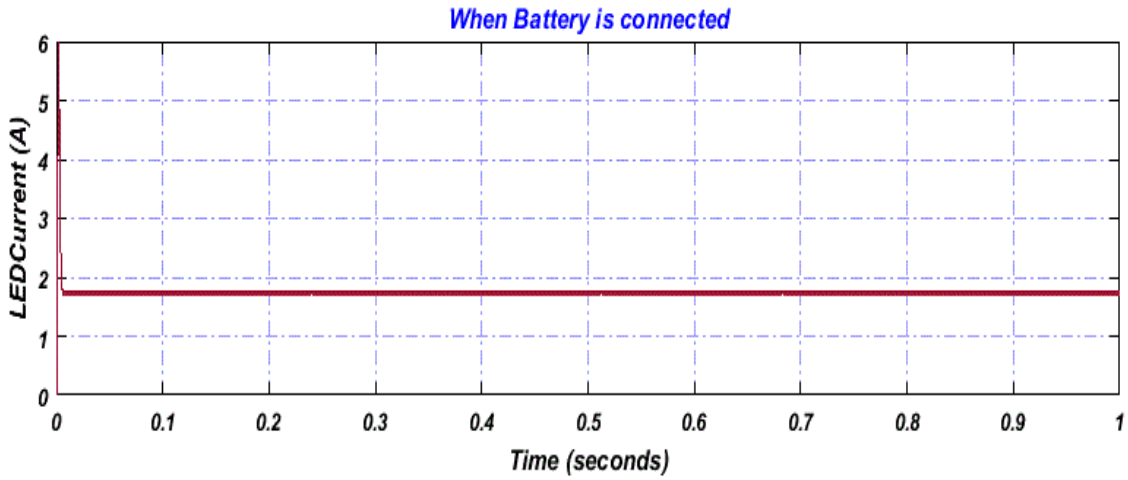

Fig.5.14 Output Current across LED

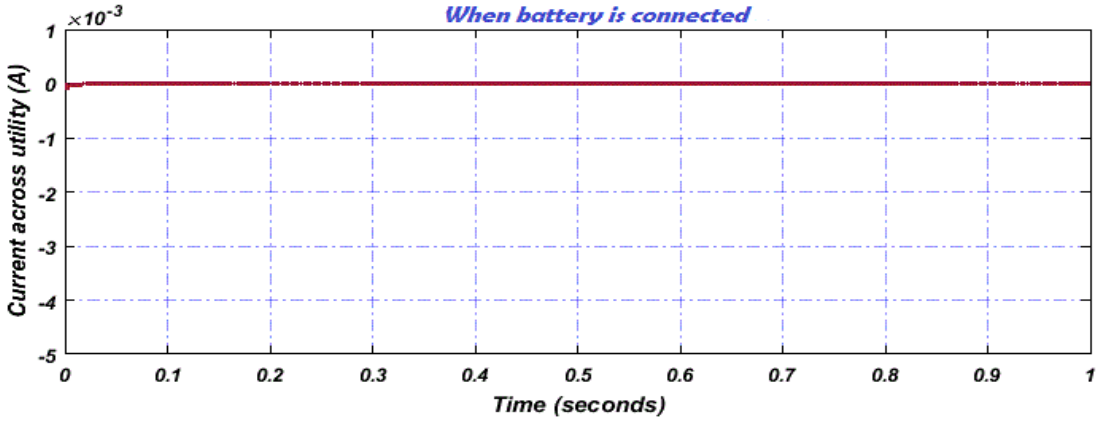

Fig.5.15 Output current from utility

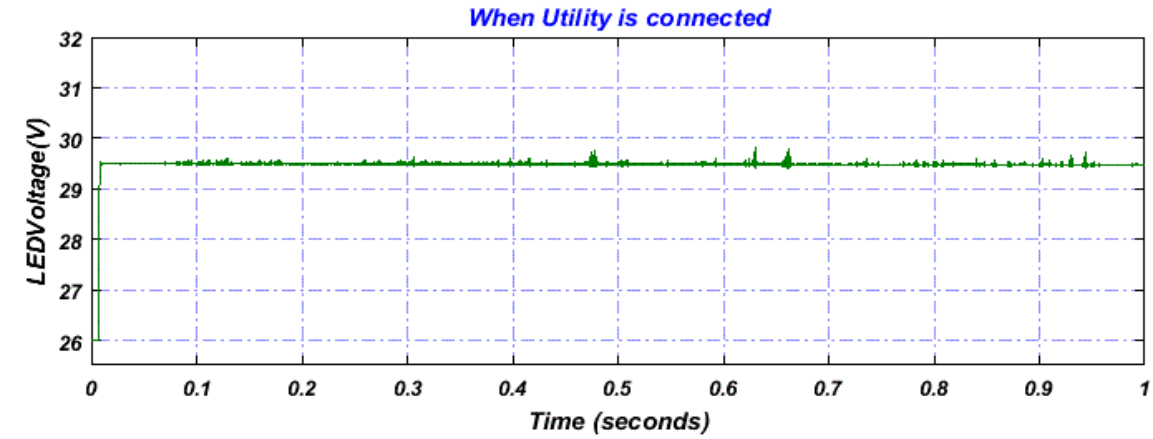

Fig.5.16 Output Voltage across LED

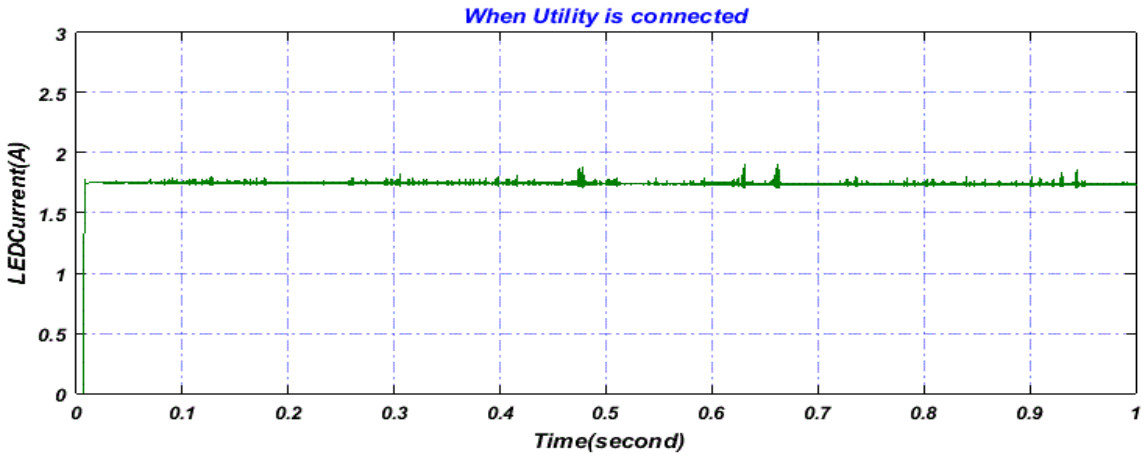

Fig.5.17 Output current across LED

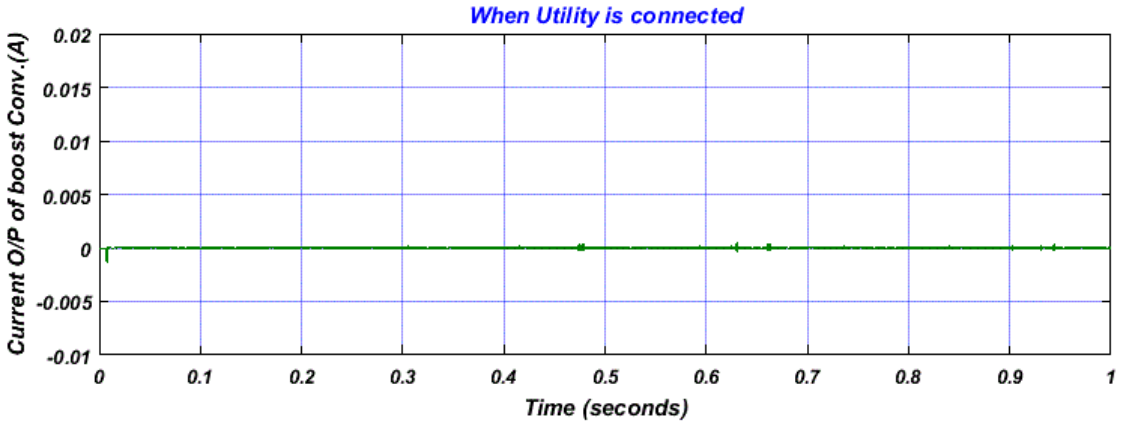

Fig.5.18 Output current of boost converter

If there is continuous overcast situation, the LED Street lamp is lit by the AC/DC System (Grid) and output current and voltage 1.75A and 29.5V respectively are shown in Fig.5.16 & 5.17. and O/P current from boost converter is zero as shown in fig.5.18. It has been observed that the voltage and current remain same, whether the LED load is lit up by battery or utility. So the system is working very efficiently and accurately.

5.3 CONCLUSION

The two models of smart solar LED street lighting are successfully designed and implemented. Based on the Model calculation and simulink results it has been observed that intensity control of LED has benefits such as less energy consumption and battery can work more efficiently giving higher duration of backup than compared to the streetlight which is working without any intensity control. Further a PV hybrid system is designed which can continuously under any weather conditions.

CHAPTER 6

SOLAR POWERED INDUCTION MOTOR DRIVE FOR WATER PUMPING

Sun oriented energy is an outstanding solution for rural regions where the grid isn't accessible or the grid is exceptionally unusual. Most supported use of the SOLAR-PV System (SPV) [30-32] is in water pumping system driven by DC/AC motors. In recent times, the SPV based water pumping system is accepting wide consideration in the domestic, industrial and agricultural purposes as roughly for 6 - 8 hours continuous supply can be obtained from this application without the requirement of any energy storage equipments. As India's most of the economy is depend on agriculture so for making it more efficient using SPV based pumping system is very much helpful, as many parts in India are blessed with high solar irradiance but the accessibility of the ground water is very tough and water pumps are specifically required to extract the water for the ground.

In pumping systems, though DC motors have been used since their inception, they are not as economical and efficient as 3 phase induction motor. It has the additional cost of maintenance of brushes, brush holders, commutators etc, and the initial cost of DC motor is also more. In pumping systems, high precision and soft transient performance are not required, so they can be operated in open loop. Most of the times, system operates in steady state only. Pumping systems based on induction motors appear attractive solution for reliable and maintenance free operation [33]. With the advent of outperforming solid state switches, high power controllers and efficient motor control algorithms, AC motors have taken a step ahead to DC motors.

6.1 SYSTEM DESCRIPTION

The description of the proposed system is shown in fig.6.1. The main purpose is to build up a standalone solar PV Water pumping system with the help of Induction Motor.

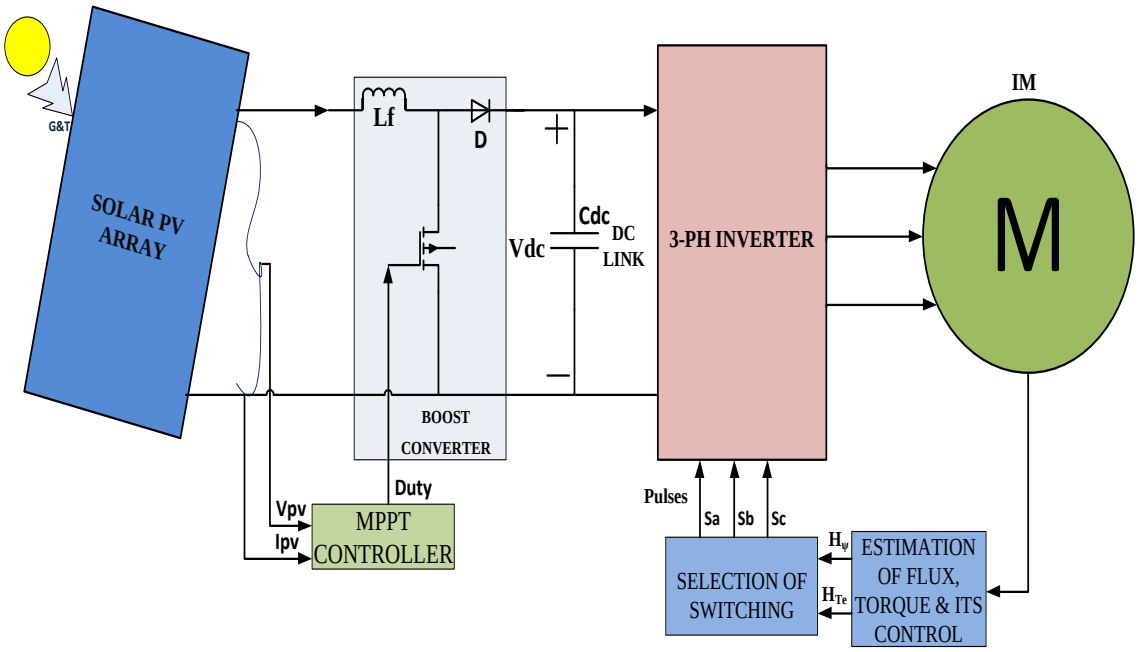

Fig.6.1 Proposed Solar Powered Induction motor drive for Water Pumping

Solar PV System consists of solar PV array with MPPT for tracking maximum power and a boost converter which supplies DC Power to the 3-phase voltage source inverter, which is feeding 3-phase supply to DTC based induction motor driving a water pump. By using INC based MPPT control algorithm, duty is given to the Switch of the boost converter and DTC based scheme is use to produce the switching sequence for the inverter feeding to an induction motor.

6.2 INDUCTION MOTOR DRIVE

Induction motor drives are used in almost all the industrial, domestic and in agricultural applications because of their rugged and robust performance, also the performance of induction motor is very promising in high speed applications. If we compare induction motor and DC motor, then the main advantage that DC motor have over Induction Motor is its continuously controlling of speed as torque and speed are decoupled from each other in DC motor. It can be observed from equations 6.1(a) and 6.1(b) that both the torque and speed are independent from each other.

$$E_b = \frac{P.\Psi.Z.\omega_m}{2.\pi.A} \qquad (6.1(a))$$

$$T_d = \frac{P.\Psi.Z.I_a}{2.\pi.A} \qquad (6.1(b))$$

Here P is number of poles, Z is total number of conductors, E_b is the back emf of motor, T_d is the developed torque, ω_m is the angular mechanical speed, I_a is the armature current, A is the number of parallel paths and Ψ is the flux per pole of motor [34,35].

In DC machines mmf axis is established at 90˚ electrical to the main field axis. The developed torque (T_d) is directly proportional to the field flux (Ψ) and armature current (I_a). Ψ is proportional to the field current (I_f) and is unaffected by the armature current (I_a) because of orthogonal relationship between field mmf & armature mmf. In a separately excited DC machine, as the field flux is constant so, the torque is directly proportional to the armature current. Hence only controlling of armature current gives controlled torque and quick response. In Induction motor the flux and torque components are mutually coupled, so the controlling of induction motor as compared to DC motor is not effective. But DC motor is not economical it has the additional cost of maintenance of brushes, brush holders, commutators etc, and the initial cost of DC motor is also more. So, a substitute is needed which is economical as well as have better controlling in steady state. As discussed induction motor are robust and rugged and have almost no maintenance cost, so it can be used in place of the DC motor if we can decouple the flux and torque component of induction motor.

Induction motor controlling is divided into two parts:

a. Scalar-control of Induction Motor
b. Vector-control of Induction Motor

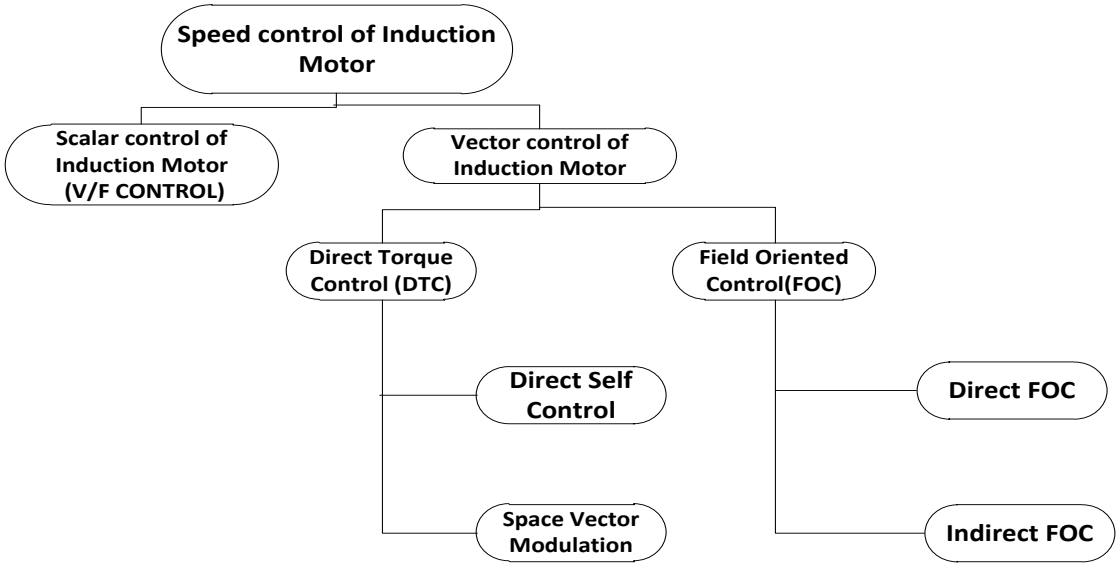

Fig.6.2 Classification of vector control methods used for speed control of Induction Motor

6.3 DIRECT TORQUE CONTROL (DTC) OF INDUCTION MOTOR

In vector control, three phase component are transformed into two quadrature components i.e. abc into αβ, one of which is responsible for flux component which in turn effect the speed and the second component is responsible for the torque[36].

The methods from which the 3-phase quantities are transformed into 2-phase quadrature quantities are:

a. Clarke-Transformation
b. Park-Transformation

6.3.1 Clarke Transform

Clarke-transformation as shown in fig.6.3. It is used to transform the three phase quantities into stationary two phase quantities which are orthogonal to each other. Clarke transformation is given by following equation 6.2.

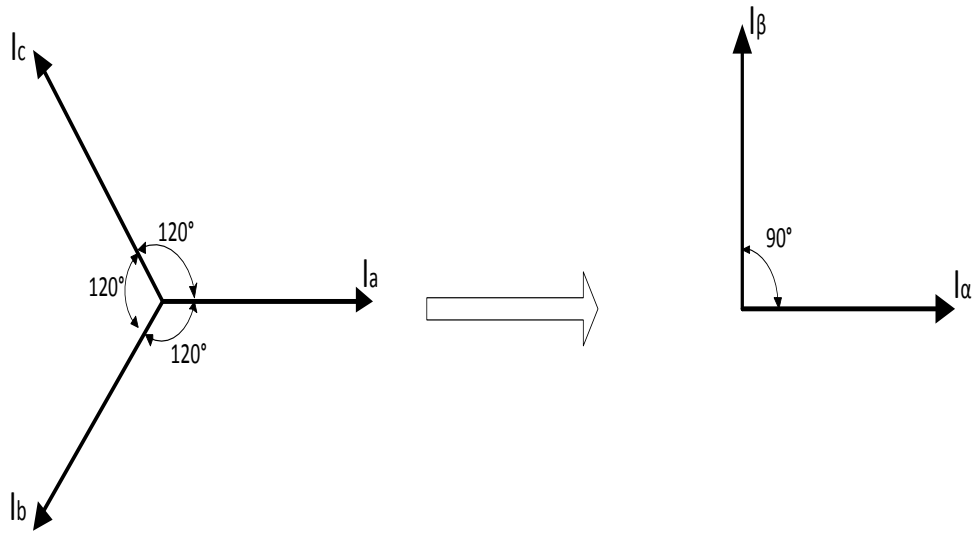

Fig.6.3 Clarke Transformation

$$I_{\alpha\beta\gamma} = \frac{2}{3}\begin{bmatrix} 1 & -\frac{1}{2} & -\frac{1}{2} \\ 0 & \frac{\sqrt{3}}{2} & -\frac{\sqrt{3}}{2} \\ \frac{1}{2} & \frac{1}{2} & \frac{1}{2} \end{bmatrix} . I_{abc} \qquad (6.2)$$

where I_a I_b I_c are three phase quantities and I_α I_β I_γ are transformed quantities and I_γ is zero as vector sum of three phase quantities displaced equally and of same magnitude is zero, so I_α and I_β are given by equation 6.3 and 6.4.

$$I_\alpha = \frac{2}{3}\left(I_a - \frac{1}{2}I_b - \frac{1}{2}I_c\right) \tag{6.3}$$

$$I_\beta = \frac{1}{\sqrt{3}}(I_b - I_c) \tag{6.4}$$

Also inverse Clarke transformation is used to transform the stationary two phase orthogonal components to three phase balanced components which is given by equation 6.5

$$I_{abc} = \begin{bmatrix} 1 & 0 & 1 \\ -\frac{1}{2} & \frac{\sqrt{3}}{2} & 1 \\ -\frac{1}{2} & -\frac{\sqrt{3}}{2} & 1 \end{bmatrix} . I_{\alpha\beta\gamma} \tag{6.5}$$

6.3.2 Direct Torque Control Scheme

Direct Torque Control scheme is implemented by using blocks that are Estimation of Flux and torque, speed regulator, torque and flux control, and selection of switching of inverter as shown in fig.6.4. The flux is estimated by integrating back emf and resultant flux is obtained by eq.(6.7),

$$\text{emf} = V - I.R_s \tag{6.6}$$

$$\Psi = \int \text{emf} = \int (V - I.R_s) \tag{6.7}$$

In squirrel cage IM it can be assumed that the rotor flux is constant because rotor time constant is much high [37] so, stator flux per pole in α β stationary coordinate is written as

$$\Psi_\alpha = \int (V_\alpha - I_\alpha . R_s) \tag{6.8}$$

$$\Psi_\beta = \int \left(V_\beta - I_\beta . R_s\right) \tag{6.9}$$

$$\Psi_{sr} = \sqrt{(\Psi_\alpha^2 + \Psi_\beta^2)} \tag{6.10}$$

And torque is then estimated by cross product of flux and stator currents in α β stationary coordinate as given in eq. (6.11)

$$T = \frac{3*P}{2*2}\left(\Psi_\alpha I_\beta - \Psi_\beta I_\alpha\right) \quad (6.11)$$

Where ψ_α, ψ_β are stator flux in α β stationary coordinate, ψ_{sr} is the resultant stator flux, T is the electromagnetic torque, P is no. of pole pair, I_α, I_β stator current in α β stationary coordinate, R_s is stator resistance.

In this scheme, one component of the reference speed is developed from the PV power using the pump-affinity laws. It determines the flow-rate of the water pump. The reference speed(ω_r^*) from SPV array is expressed as,

$$P_{pv} = K_l \, x \, \omega_m{}^3 \quad (6.12)$$

$$\omega_m = (P_{pv}/K_l)^{1/3} \quad (6.13)$$

Where K_l is constant for converting PV power into speed [38]

And another component (ω_{dc}) of reference speed is generated by comparison of reference dc voltage with dc link voltage and passing the error through P-I controller. So, the reference speed (ω_r^*) is the addition of ω_m and ω_{dc} [39].

The error between the sensed speed and reference speed is passed through P-I controller to produce reference torque (T^*) and the reference flux (ψ^*) is taken as 0.9 or can be calculated through flux table.

These estimated values are then compared to the preset reference values and if the deviation is high then the switching of power electronic device is done such that these values are brought back to their references. Fig.6.4 shows block diagram of Direct Torque Control (DTC) scheme [40-42].

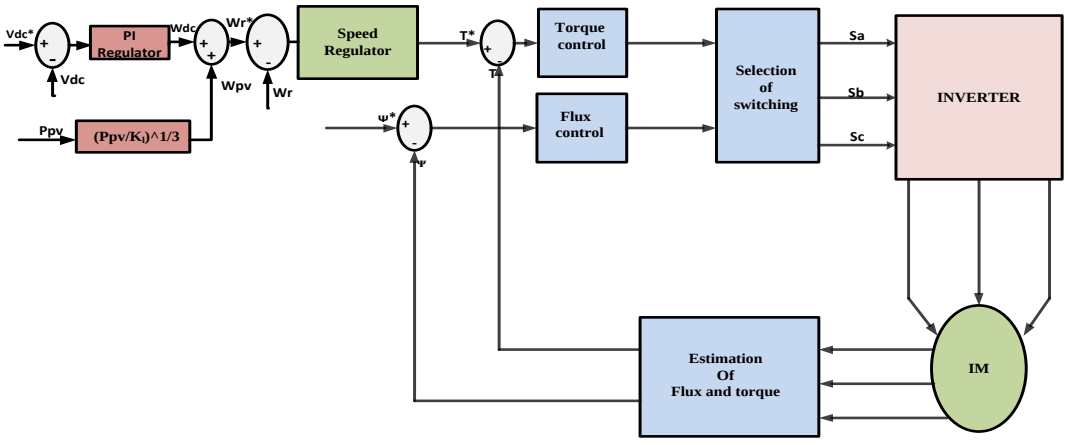

Fig.6.4 Block diagram for Direct Torque Control scheme

The stator flux Ψ* and the electromagnetic torque T^* are the reference signals which are compared with the estimated Ψ and T values respectively. The flux and torque errors are delivered to the hysteresis controllers. From the hysteresis controller output appropriate voltage vector is generated and corresponding switching table is formed. Thus, the selection table generates pulses S_A, S_B, S_C to control the power switches in the inverter.

For the flux is defined two-level hysteresis controller and for the torque three-level hysteresis controller as shown in fig.6.5.

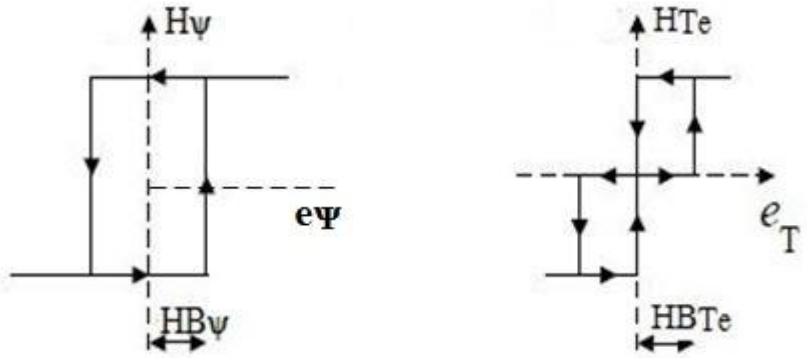

Fig.6.5 Hysteresis controller for flux and torque

The output signals Hψ and H_{Te} are defined as:

$H\psi = 1$ for $e\psi > HB_\psi$ (6.14)

$H\psi = 0$ for $e\psi > HB_\psi$ (6.15)

$H_{Te} = 1$ for $e_T > HB_{Te}$ (6.16)

$H_{Te} = 0$ for $e_T = 0$ (6.17)

$H_{Te} = -1$ for $e_T < HB_{Te}$ (6.18)

These error hysteresis controller output is used to generate the lookup table for switching the voltage source inverter (VSI) as shown in Table VIII. The Matlab code for lookup table to generate switching signal is shown in fig.6.6.

TABLE VI VOLTAGE VECTOR LOOKUP TABLE FOR DTC CONTROL

Hψ	H_{Te}	S(1)	S(2)	S(3)	S(4)	S(5)	S(6)
1	1	V_2	V_3	V_4	V_5	V_6	V_1
	0	V_0	V_7	V_0	V_7	V_0	V_7
	-1	V_6	V_1	V_2	V_3	V_4	V_5
-1	1	V_3	V_4	V_5	V_6	V_1	V_2
	0	V_7	V_0	V_7	V_0	V_7	V_0
	-1	V_5	V_6	V_1	V_2	V_3	V_4

```
Lookup table*   newdiode.m   polar.m
 1   function u = TABLE(HF,HT,n)
 2   u=0;
 3   %sector 1
 4   if(HF==1)&&(HT==1)&&(n==1)
 5       u=2;
 6   end;
 7   if(HF==1)&&(HT==0)&&(n==1)
 8       u=7;
 9   end;
10   if(HF==1)&&(HT==-1)&&(n==1)
11       u=6;
12   end;
13   if(HF==-1)&&(HT==1)&&(n==1)
14       u=3;
15   end;
16   if(HF==-1)&&(HT==0)&&(n==1)
17       u=0;
18   end;
19   if(HF==-1)&&(HT==-1)&&(n==1)
20       u=5;
21   end;
```

Fig.6.6 Lookup Table code to generate switching

In Direct torque control method plane is divided into six sectors as shown in fig.6.7. And the code for Sector detection is shown in fig.6.8.

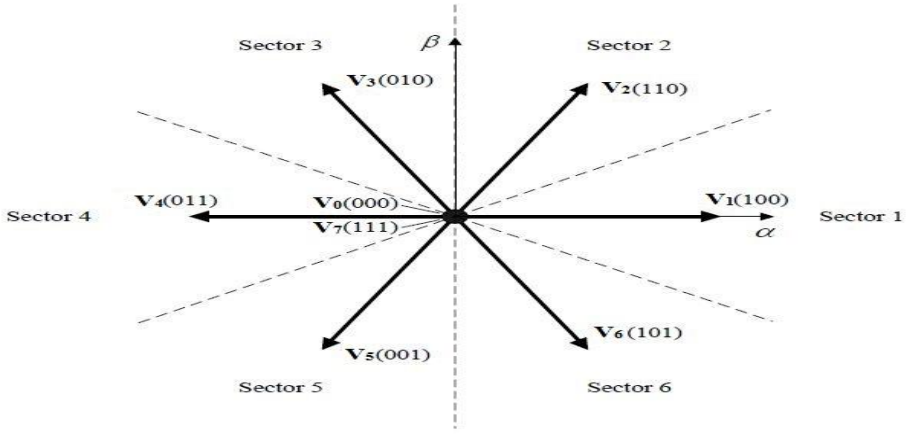

Fig.6.7 Different switching states and sectors for an inverter

```
Sector detection*   code.m   ledvolcur.m
function n = SECTOR(Falpha,Fbeta)
n=0;
Angle=atan2(Fbeta,Falpha);
if(Angle>=-pi/6)&&(Angle<pi/6)
    n=1;
end;
if(Angle>=pi/6)&&(Angle<pi/2)
    n=2;
end;
if(Angle>=pi/2)&&(Angle<5*pi/6)
    n=3;
end;
if(Angle>=5*pi/6)&&(Angle<pi)
    n=4;
end;
if(Angle>=-pi)&&(Angle<-5*pi/6)
    n=4;
end;
if(Angle>=-5*pi/6)&&(Angle<-pi/2)
    n=5;
end;
if(Angle>=-pi/2)&&(Angle<-pi/6)
    n=6;
end;
```

Fig.6.8 Code for sector detection

As we know that a 3 phase inverter has three arms and six switches. Now for controlling the speed of Induction Motors different switching patterns are obtained. Three switches from different arms get ON and the remaining three gets OFF as shown in fig.6.9, and according to switching a voltage vector appears on the terminals of the 3 phase Induction Motor, which affects the performance of Induction Motor.

Fig.6.7. shows the different switching states. Here the vectors showing 0 and 1 show the states of switching state Sa, Sb and Sc, which is explained by equation 6.20(a), 6.20(b) and 6.20(c).

$$\text{Sa} = \begin{Bmatrix} 1 \text{ if S1 is ON and S4 is OFF} \\ 0 \text{ if S1 is OFF and S4 is ON} \end{Bmatrix} \quad (6.20(a))$$

$$\text{Sb} = \begin{Bmatrix} 1 \text{ if S2 is ON and S5 is OFF} \\ 0 \text{ if S2 is OFF and S5 is ON} \end{Bmatrix} \quad (6.20(b))$$

$$\text{Sc} = \begin{Bmatrix} 1 \text{ if S3 is ON and S6 is OFF} \\ 0 \text{ if S3 is OFF and S6 is ON} \end{Bmatrix} \quad (6.20(c))$$

In above equations the S1, S2, S3, S4, S5, S6 represents the six switches in the arms of the inverter as shown in fig.6.9.

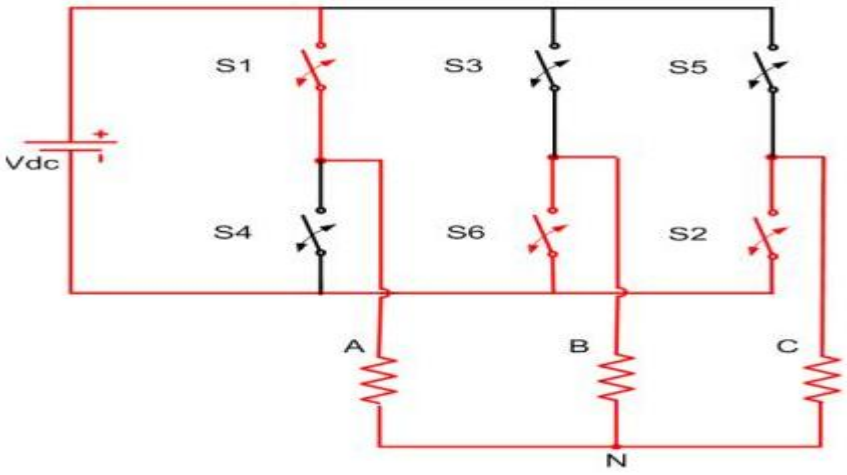

Fig.6.9 Simple circuit diagram of a 3 phase inverter

6.4 DESIGN OF A PROPOSED SYSTEM

A 2.4kW Solar PV system is used to drive a 3 phase Induction Motor of 3hp power capacity. The system uses an INC based maximum power point tracking (MPPT) as discussed in section (3.3.2), DC-DC boost converter and voltage source inverter.

a. Solar PV system design:

A SPV system of a capacity of 2400W peak is used in simulation and all the SPV specifications are described in Table IX

TABLE IX SOLAR PANEL SPECIFICATIONS

SOLAR PANEL SPECIFICATIONS	
Open circuit voltage (V_{oc})	32.9V
Short Circuit Current (I_{sc})	8.2A
Max power (P_{max})	198W
Voltage at P_{max} (V_{mp})	28.33 V
Current at P_{max} (I_{mp})	6.97A
Tolerance (At STC)	5%

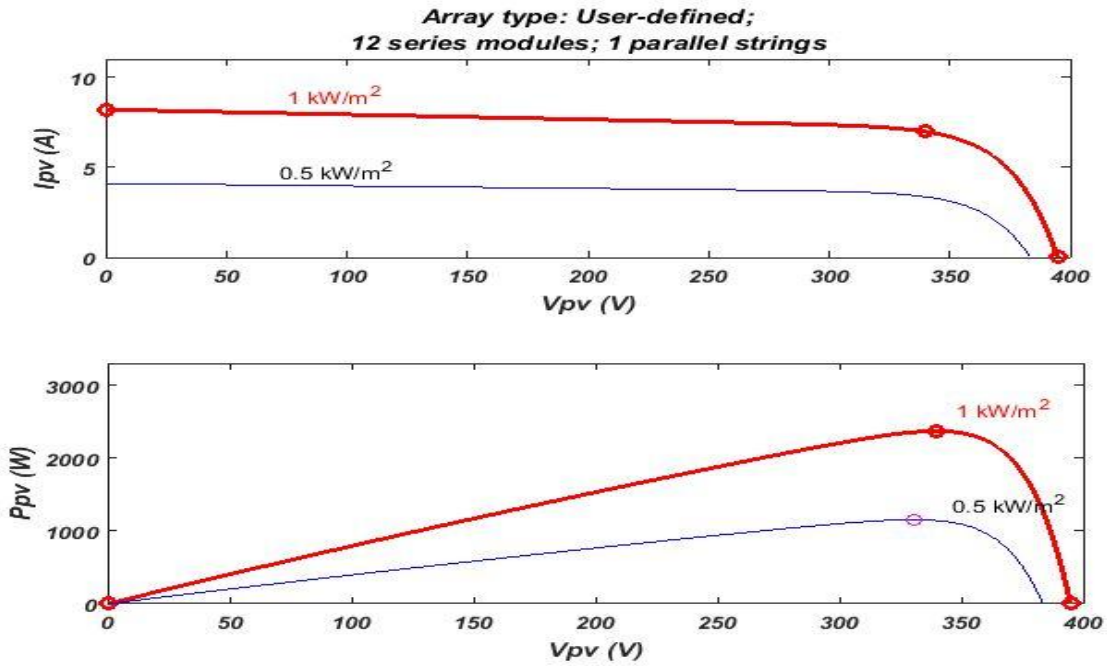

Fig.6.10 $I_{pv} - V_{pv}$ & $P_{pv} - V_{pv}$ Characteristics of Solar PV array

The 12 number of series module and 1 parallel module is used to build up SPV array. Fig.6.10. shows the PV characteristics at different irradiation level i.e. 1000W/m^2 & 500W/m^2.

b. DC-DC boost Converter design:

The design of boost converter is done by calculating the duty cycle value. $\frac{V_{dc}}{V_{pv}} = \frac{1}{1-d}$

Here, V_{dc} = 400V and V_{pv}=340V

The duty cycle comes out to be d= 0.15,

The value of the inductor (L_f) can be calculated by eq. (6.21)

$$Lf = \frac{Vs*d}{\Delta I_l * f_s} \tag{6.21}$$

Thus the value of inductor (L_f) value is selected as 2.3 mH

Where f_s are the switching frequency that is taken as 20 KHz, V_s is the input voltage across the boost converter and ΔI_l is the ripple current.

c. DC link Capacitor design:

The input voltage (dc link voltage) of a Voltage source inverter can be given as

$$V_{dc} = \frac{2\sqrt{2} * V_l}{\sqrt{3}} \tag{6.22}$$

$$=375.6V$$

Where V_l is the line to line voltage

The dc link voltage comes out to be 375.6V, therefore the DC link voltage is assumed as 400V

The DC link capacitor (C_{dc}) can be calculated by eq. (6.23) [40]

$$Cdc = \frac{6 * \propto * Vph * I * t}{V_{dcassumed}{}^2 - V_{dc}^2} \tag{6.23}$$

$$=1600\mu F$$

Where, α is the overloading factor for safety, t is the time to charge capacitor V_{ph} is the phase voltage and I is the motor current

d. Water Pump design:

In the water pump the load torque is proportional to the square of speed of motor and hence, the power of a water pump is proportional to the cube of speed of the motor, this is known as pump affinity law of water pump [41].

$$T \propto \omega_m^2 \tag{6.24}$$

$$T = K_l * \omega_m^2 \tag{6.25}$$

$$P \propto \omega_m^3 \tag{6.26}$$

$$P = K_l * \omega_m^3 \tag{6.27}$$

Where K_l is the proportionality pump constant and ω_m is the speed of the motor in rad/sec

When ω_m is 1430 rpm and torque is 14.70Nm the proportionality pump constant (K_l) comes out to be $6.5 * 10^{-4} \mathrm{Nm/(rps)^2}$.

6.5 SIMULATION RESULT AND DISCUSSION

A Solar Powered DTC controlled Water pump is developed in Matlab-Simulink, The system consists of solar PV array of 2.4 KW, INC based MPPT algorithm with a boost converter and the Direct torque control (DTC) technique is developed to give the switching to Voltage Source Inverter (VSI) to drive an Induction motor of 3hp, the motor parameters are given in Table X. The simulink model is shown in Appendix 5.

TABLE VII INDUCTION MOTOR PARAMETERS

Motor parameter	Value
Power Rating	3hp/2200 kW
Number of pole pairs(P)	2
Rated speed(N_r)	1430 rpm
Stator Self Inductance(L_{ss})	3.2 mH
Rotor Self Inductance(L_{rs})	2.93 mH
Mutual Inductance(L_m)	0.075 H
Stator Resistance(R_s)	0.603 Ω
Rotor Resistance(R_r)	0.7 Ω
Inertia constant (J)	0.0142 kgm^2

Solar Powered DTC controlled Water pump performance is analyzed from the result of model.

a. Starting Performance of the system

Solar PV array specification parameters such as Solar PV current I_{pv}(A), Solar PV voltage V_{pv}(V) and Solar PV power P_{pv}(W) is shown in fig.6.11. The parameter of SPV i.e. Voltage (V_{pv}), PV power (P_{pv}) increases at starting and the settles down at MPP within a portion of second by using INC algorithm. At the time of starting the irradiance is fixed to 1000W/m^2 and temperature is 25^0C, the reference speed components i.e. one component from pump affinity law by sensing PV power and another component by DC link voltage controller is successfully achieved corresponding simulink model is shown in Appendix 6. It is noticed that induction motor achieved soft starting by using direct torque control technique as shown in fig.6.13.

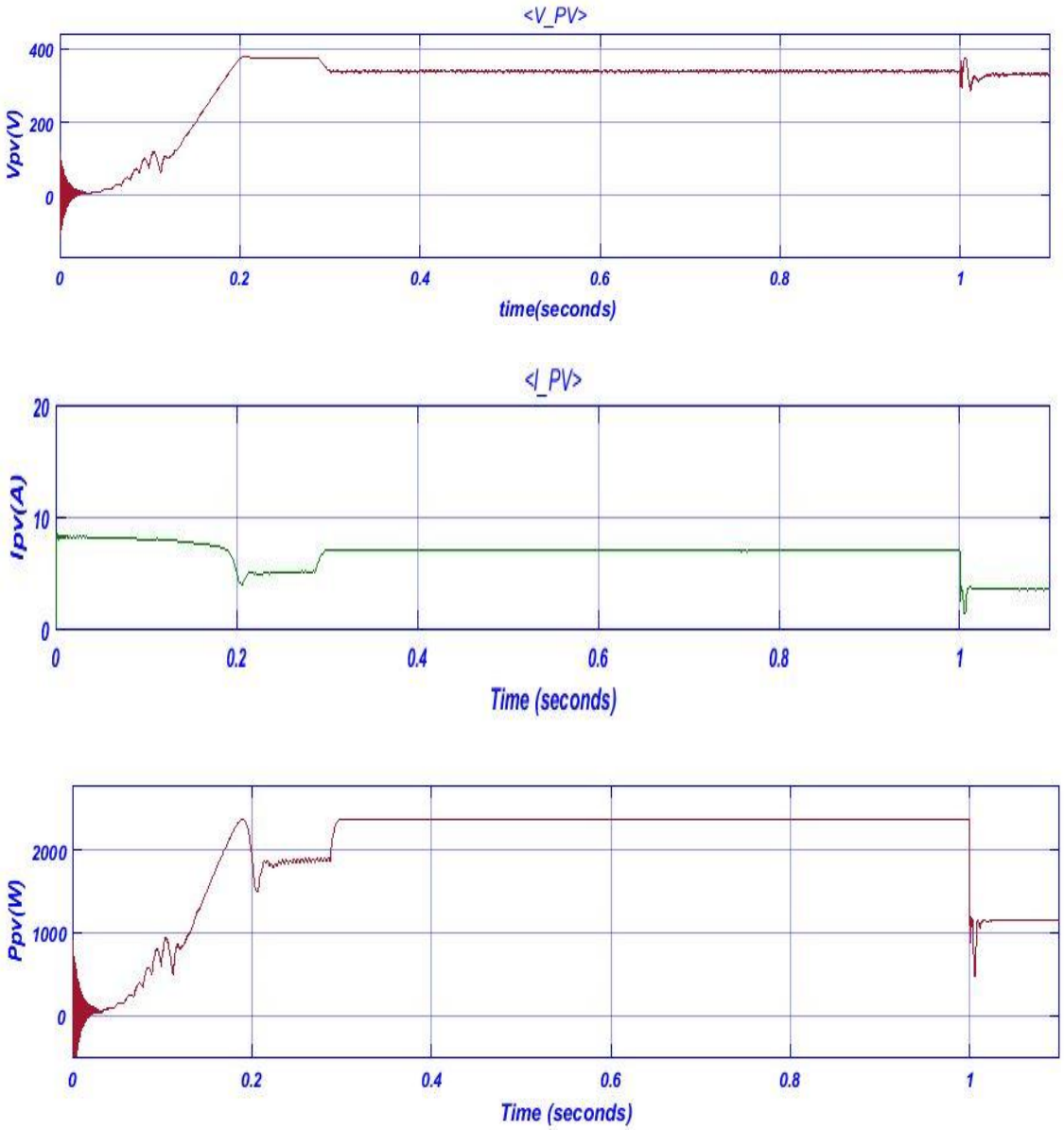

Fig.6.11 Starting, steady state and irradiation change performance of Solar PV Array

b. Steady State performance of the system

Fig.6.12. shows that after a fraction of second the speed (N_r) of the induction motor reached its rated value i.e. 1430rpm and also the torque (T_e), stator current(I_{abc}) & stator flux(Wb) of the motor is obtained at the irradiation level of 1000W/m^2, Solar PV parameters are operating on maximum point condition as shown in fig.6.11.

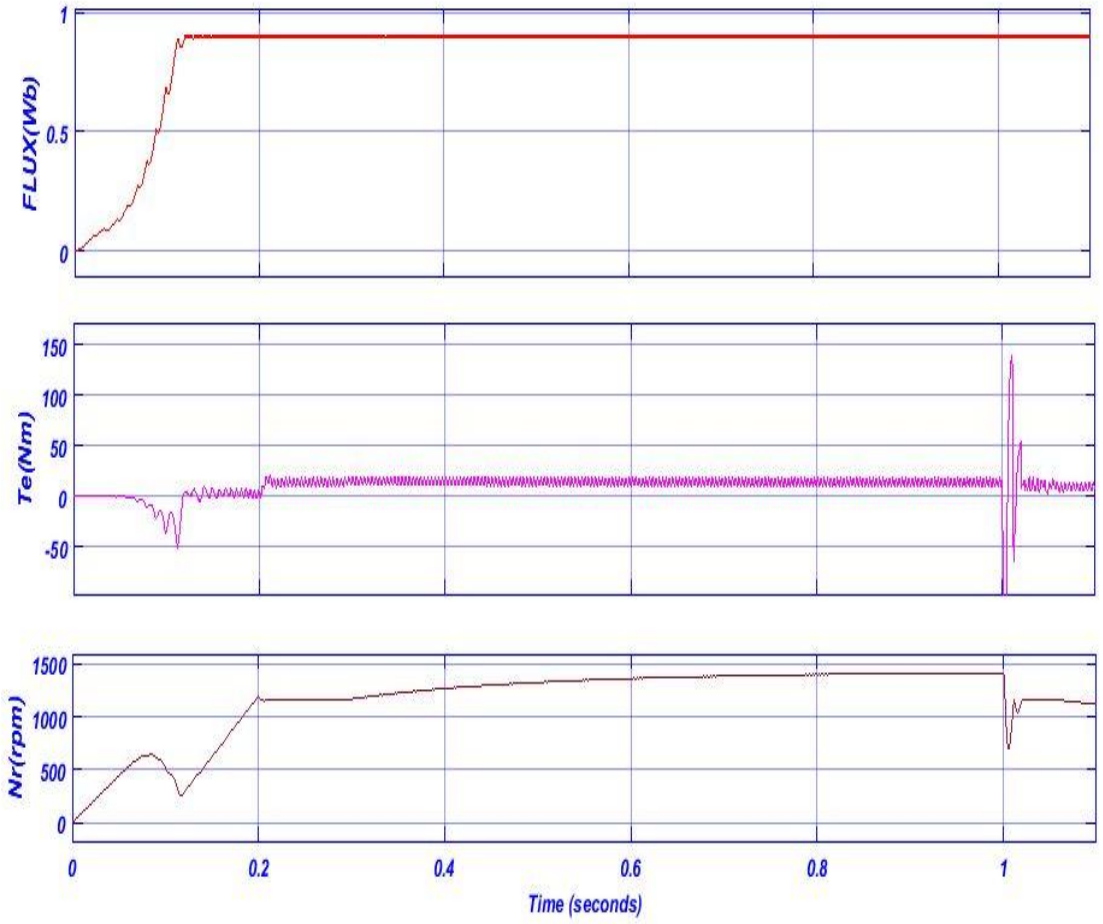

Fig.6.12 performance of Induction motor parameters under Starting, steady state and dynamic condition

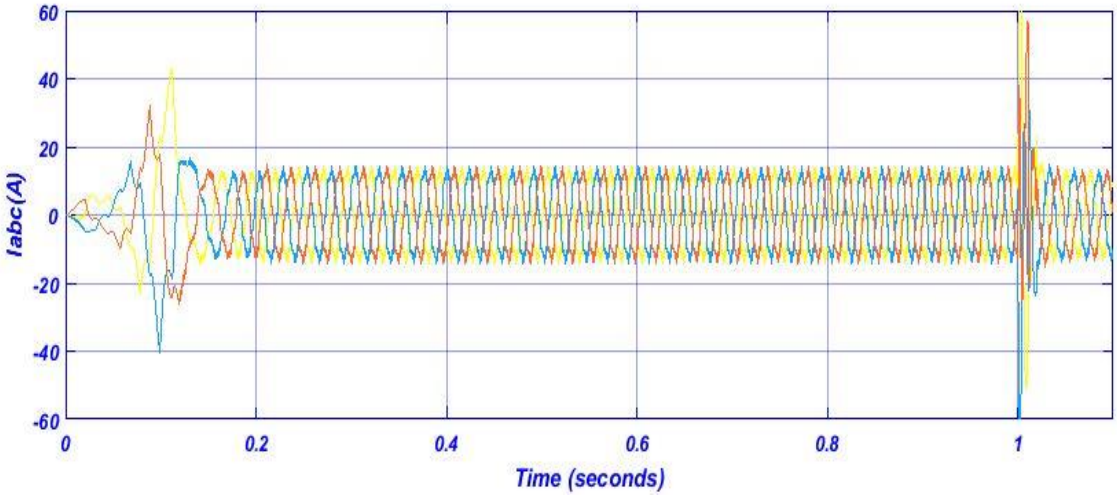

Fig.6.13 stator current of an Induction motor under Starting, steady state and dynamic condition

c. Performance Under the step change in Solar Irradiation

As the solar irradiation varies from 1000W/m^2 to 500W/m^2, the solar parameters also change as can seen from its I-V characteristics shown in fig.6.10 and the motor receive some transients that were end in few milliseconds as shown in fig.6.12. After the transient, the stator currents are maintained sinusoidal in nature, though a small decrease in the torque and motor speed as shown in fig.6.12 & 6.13.

6.6 CONCLUSION

The solar powered induction motor drive for water pumping system controlled by DTC vector control method has been operated at different condition and the starting, steady state, dynamic performance of induction motor is studied and has been found quite satisfactory. The PV power of the Solar PV array is maintained at maximum power point by using INC algorithm, when irradiation changes. The reference speed is obtained by pump affinity law and DC link voltage regulation.

CHAPTER 7

CONCLUSION & FUTURE SCOPE

7.1 CONCLUSION

Application of standalone PV system in Street lighting and Water Pumping System is successfully analysed in this thesis. Initially two MPPTs algorithm i.e. P&O and INC are studied for standalone PV system. Further most of the PV systems require energy storage elements for their efficient and reliable operation. In this work battery is used as a energy storage element and performance of the battery charging by both the MPPT algorithm is studied. It has been observed that INC gives better performance for standalone battery charging system.

Further the techno economic comparison of different lighting schemes is done which shows LED luminary is efficient. The driver circuits of LED are analysed which give low THD and high power factor. Then the two models of smart solar LED Street lighting viz. standalone PV LED streetlight with intensity control and PV Hybrid LED Street light are successfully designed and implemented. Based on the calculation and simulink results, it has been observed that intensity control of LED has benefits such as less energy consumption and battery can work more efficiently giving higher duration of backup than compare to the LED street light which is without intensity control. Further PV hybrid LED street lighting system is designed. It has advantage that it can work continuously under any weather conditions.

Another major application of standalone PV system is solar powered water pumping system using DTC controlled induction motor drive which is successfully implemented in different operating conditions such as variation in solar irradiation. The estimated reference speed regulator work satisfactory and the starting, dynamic performance of induction motor are also found quite satisfactory. The INC based algorithm used as an MPPT successfully track the maximum power under different irradiation conditions.

7.2 FUTURE SCOPE

In this thesis only one type of LED driver circuit is discussed but there no. of driver circuit which show efficient output like Zeta converter based LED drivers can also be analysed in future and more efficient algorithm for vitality control between battery unit, solar array and load can be developed so the charging of battery in solar street light can be performed efficiently.

In solar powered water pumping system the response of the system is not so much quick because of MPPT tracking is not so much fast. The system require some time to reach to maximum, so this can be minimised by optimisation the step size of the MPPT algorithm or using the Soft-Computing MPPT techniques.

APPENDICES

Appendix 1	Simulink model for comparison of algorithm in battery charging
Appendix 2	Simulink model of PFC buck converter based LED driver
Appendix 3	Simulink model Of Solar Streetlight
Appendix 4	Simulink Model Of PV Hybrid LED Street Lighting System
Appendix 5	Simulink model of Solar powered water pumping system
Appendix 6	Simulink model of reference speed generation

Appendix 1

Simulink model for comparison of algorithm in battery charging

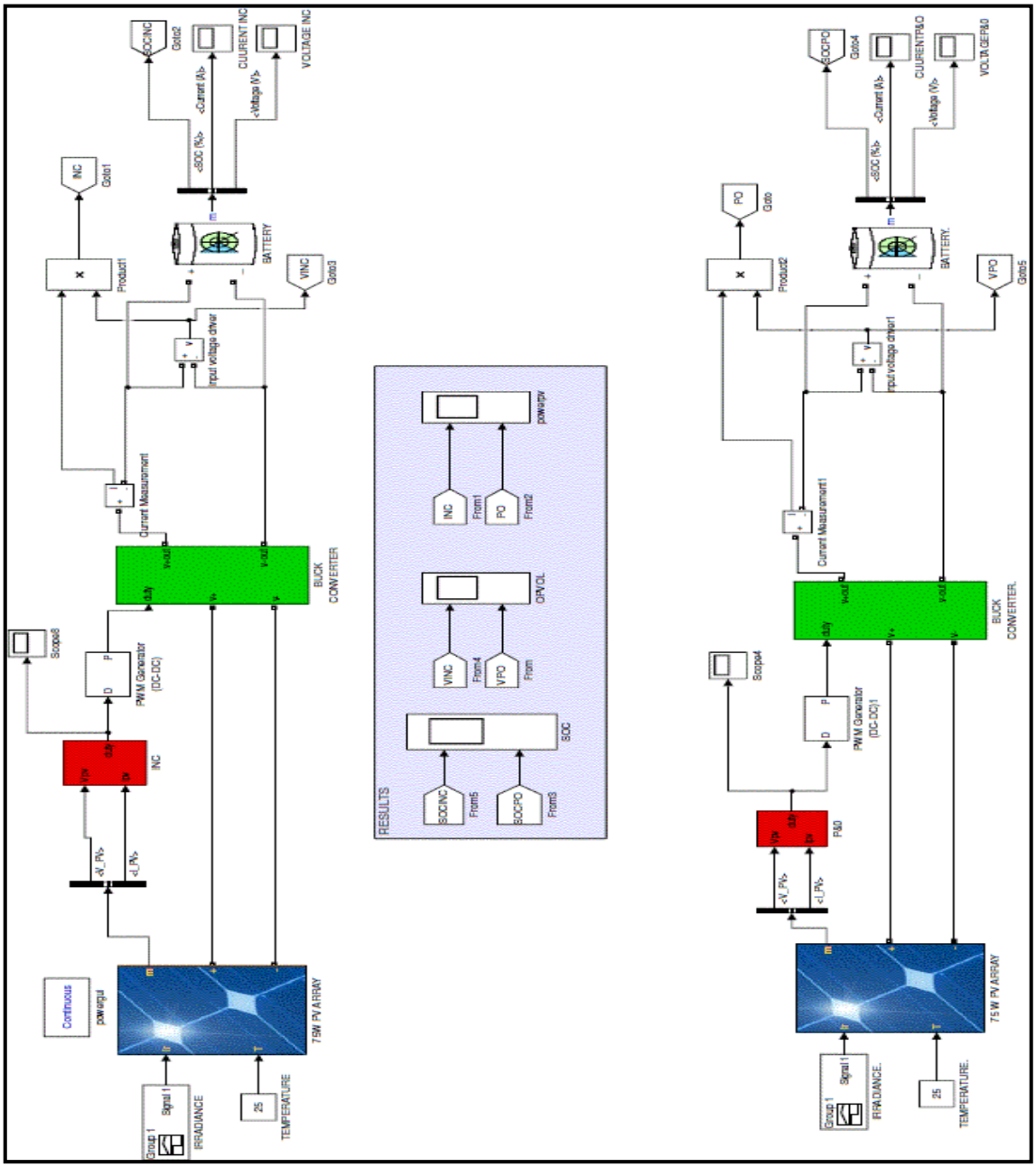

Appendix 2

Simulink model of PFC buck converter based LED driver

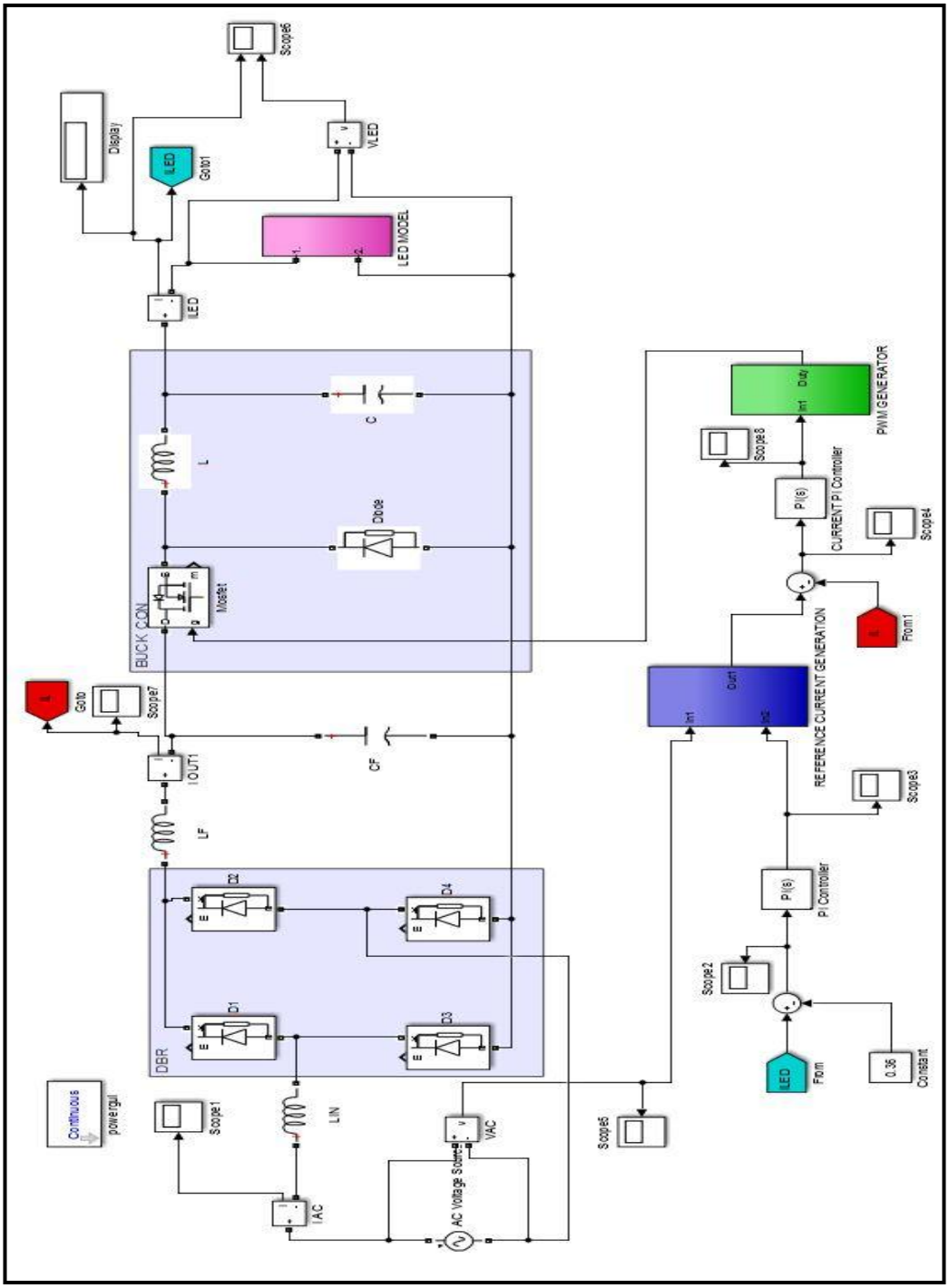

Appendix 3

Simulink model Of Solar Streetlight

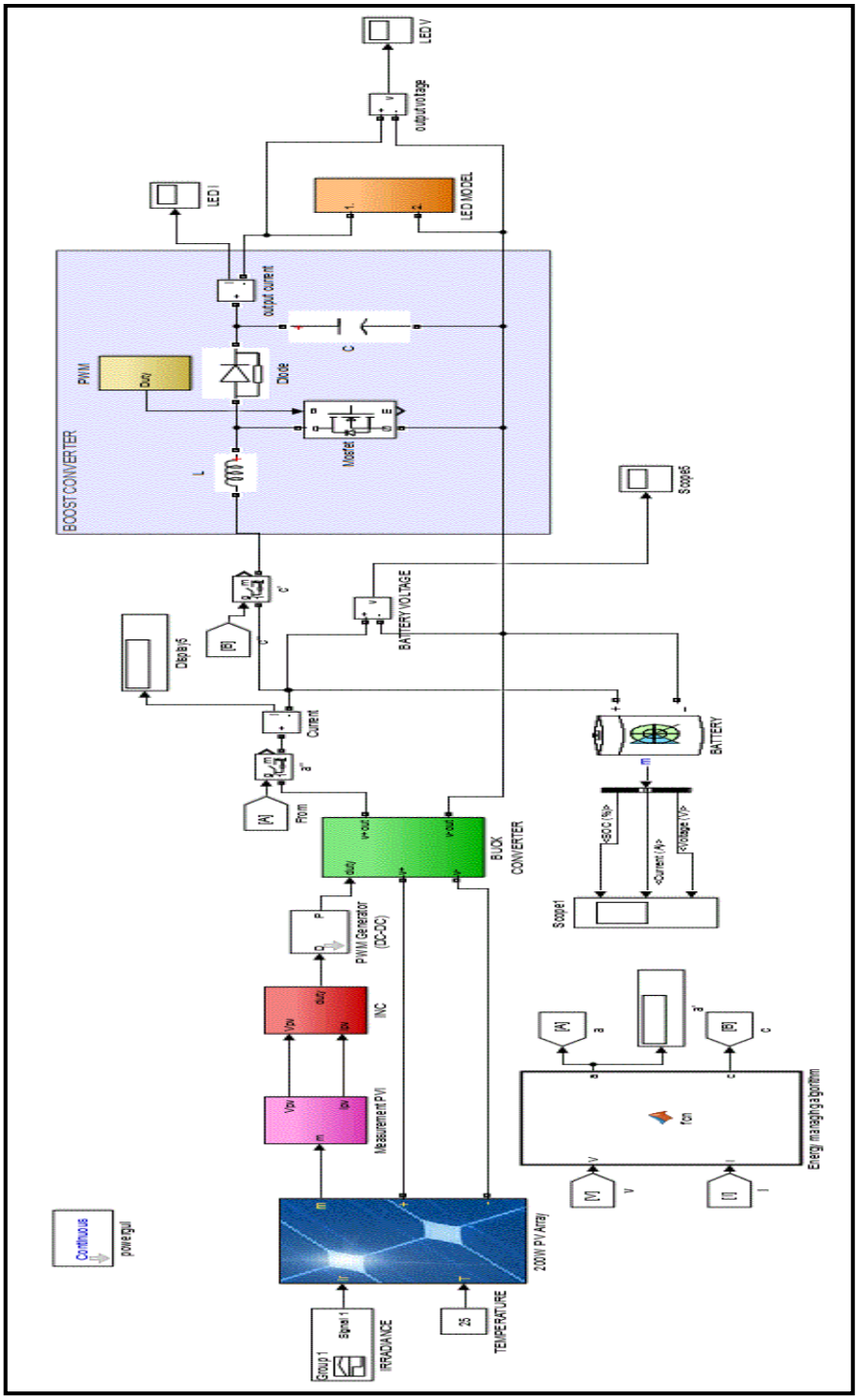

Appendix 4

Simulink Model of PV Hybrid LED Street Lighting System

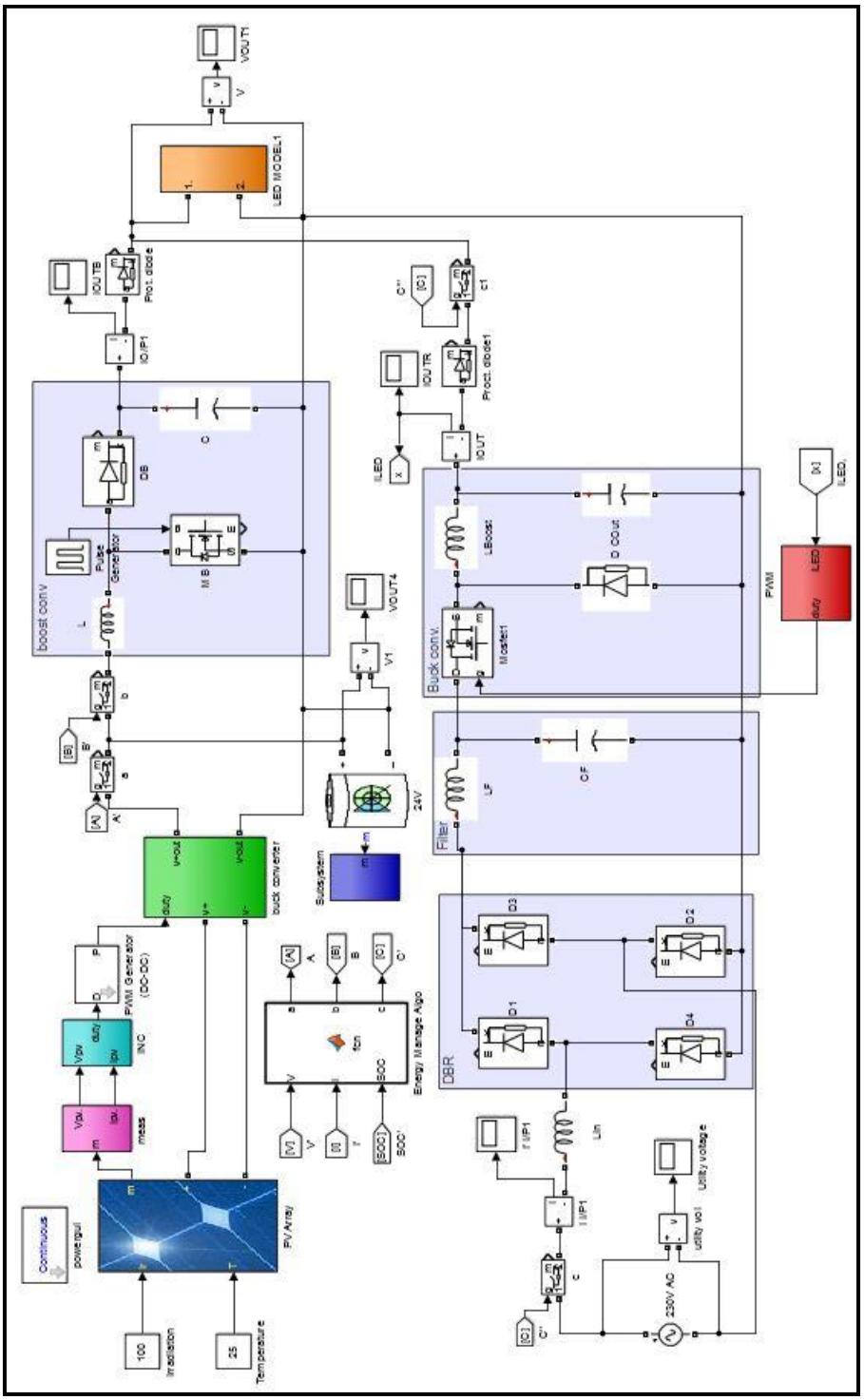

Appendix 5

Simulink model of Solar powered water pumping system

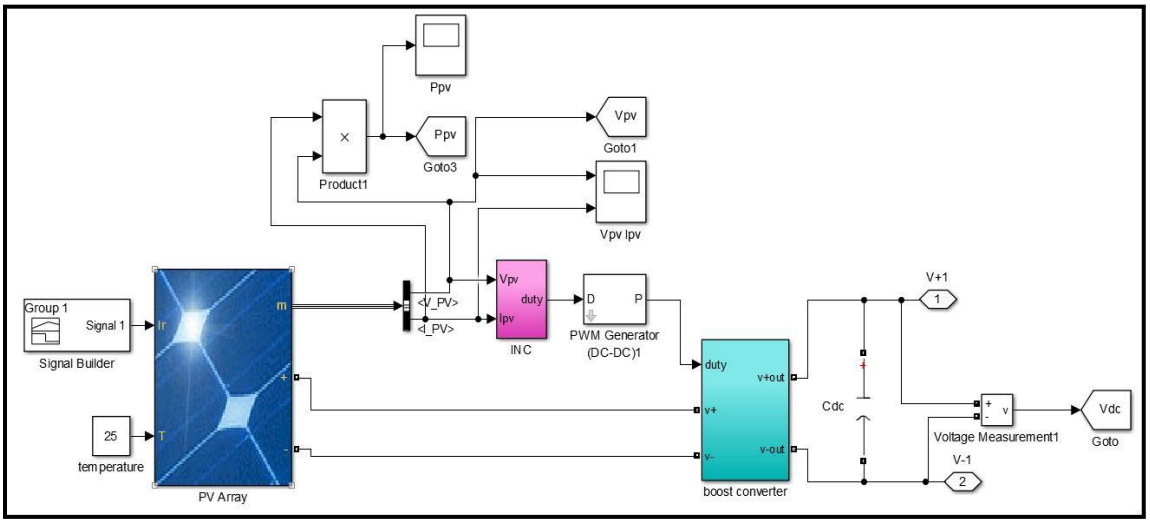

Subsystem of Solar PV system

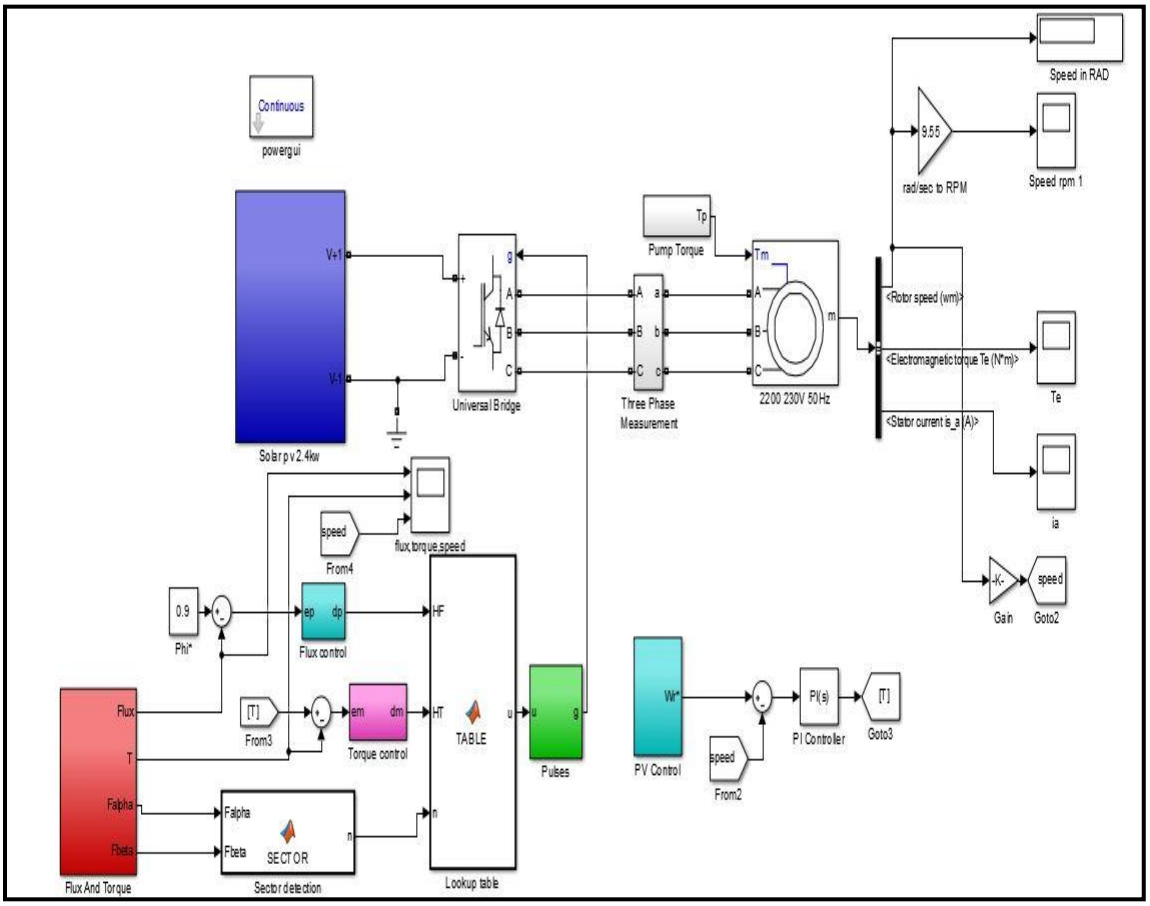

Appendix 6

Simulink model of Reference Speed Generation

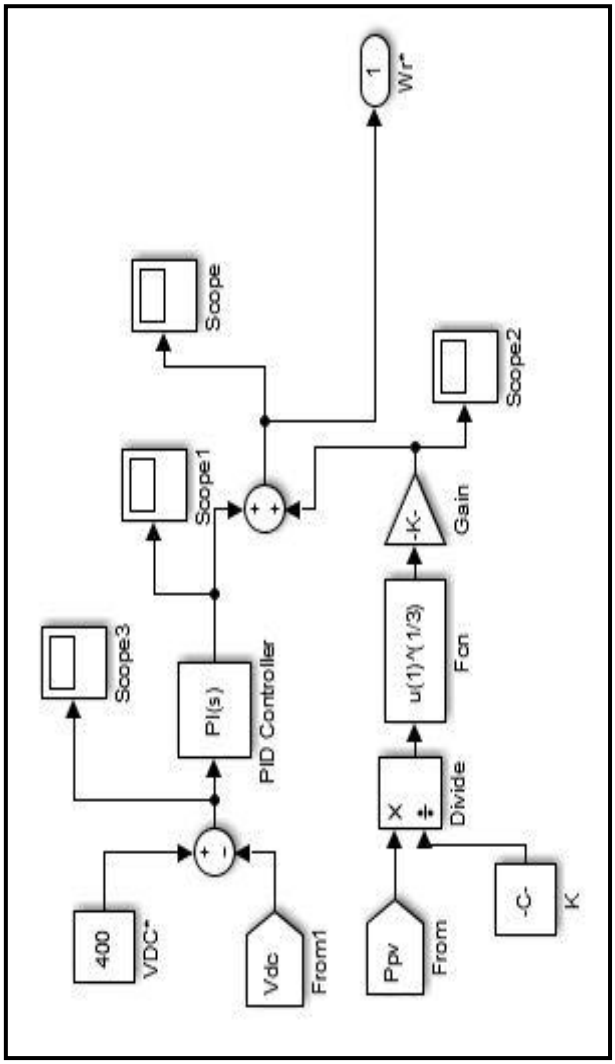

REFERENCES

[1] https://mnre.gov.in/file-manager/annual-report/2016-2017/EN/pdf/1.pdf

[2] Villalva, M. G., and Gazoli, J. R. "Comprehensive approach to modelling and simulation of photovoltaic arrays," *IEEE Trans. Power Electron.*, Vol. 24, No. 5, pp. 1198–1208, 2009.

[3] D. Sinha, A. B. Das,D, K. Dhak, P. K. Sadhu "Equivalent circuit configuration for solar PV cell" in 1*st International Conference on Non Conventional Energy (ICONCE),* 2014.

[4] Solanki, C.S. "Solar Photovoltaics Fundamentals, Technologies and Applications", 3rd ed. Delhi, India: PHI Learning Private Limited, 2016.

[5] Sharma, R.S. ,Katti, P.K., "Perturb & Observation MPPT algorithm for Solar Photovoltaic System," *International Conference on circuits Power and Computing Technologies,2017*

[6] Femia, G. Petrone, G. Spagnuolo and M. Vitelli, "Optimization of perturb and observe maximum power point tracking method," *IEEE Transactions on Power Electronics*, vol. 20, no. 4, pp. 963-973, July 2005.

[7] FR Islam, K Prakash, KA Mamun, A Lallu, R Mudliar "Design of an Optimum MPPT controller for Solar Energy System," *Indonesian Journal of Electrical Engineering and Computer Science Vol. 2, No. 3,* June 2016.

[8] R chafle, srushti & B vaidya, uttam. (2013) "Incremental Conductance MPPT Technique FOR PV System," *International Journal of Advanced Research in Electrical, Electronics and Instrumentation Engineering*, 2(6), 2719-2726.

[9] K. Zālītis and K. Bērziņa, "Effective and optimal simulation of light design in Riga Technical university's lighting laboratory from the point of view of energy efficiency," *2016 IEEE 4th Workshop on Advances in Information, Electronic and Electrical Engineering (AIEEE)*, Vilnius, 2016, pp. 1-9.

[10] K. Riad *et al.*, "A power flow control strategy for high energy efficient smart LED lighting system powered by PV and MPPT controlled DC grid," *IEEE Grenoble Conference*, Grenoble, 2013, pp. 1-6.

[11] The installer's guide to lighting design- *CIBSE*.[online].Available: https://www.cibse.org/getmedia/0276ac78-dc41-4694-9378-8f984ef924f2/GPG300-The-Installers-Guide- to-Lighting-Design.pdf.aspx. [Accessed: 20-Jan-2018].

[12] P. Sathya and R. Natarajan, "Energy estimation and photometric measurements of LED lighting in laboratory," *International Conference on Advances in Electrical Engineering (ICAEE)*, Vellore, 2014, pp. 1-5.

[13] A.F. C. Vizeu da Silva, A. O. Godinho, C. I. F. Agreira and M. M. T. Valdez, "An educational approach to a lighting design simulation using DIALux evo software," *51st International Universities Power Engineering Conference (UPEC)*, Coimbra, 2016, pp. 1-6.

[14] P. I. Domingues dos Santos, C. I. F. Agreira and M. S. Perdigão, "An educational approach to a cost-efficiency analysis between lighting solutions using DIALux," *Power Engineering Conference (UPEC), 2013 48th International Universities'*, Dublin, 2013, pp. 1-6.

[15] P. K. Soori and S. Alzubaidi, "Study on improving the energy efficiency of office building's lighting system design," *2011 IEEE GCC Conference and Exhibition (GCC)*, Dubai, 2011, pp. 585-588.

[16] *Tariff Schedule of BRPL, BYPL & TPDDL for FY 2015-16. DISCOM*. [online].Available: http://www.bsesdelhi.com/docs/pdf/DISCOM_Tariff_Schedule_FY_2015-16..pdf [Access:22-Jan-18].

[17] Alok Dixit, Gaurav Pathak and K. Sudhakar, "Comparative Study Of Life Cycle Cost Of Modern Light Sources Used In Domestic Lighting," *International Journal of Science, Environment and Technology, Vol. 4, No 2, 2015, 364 – 370*, 2015

[18] Ray-Lee Lin, Jhong-Yan Tsai,"Four-Parameter Taylor Series-Based Light-Emitting-Diode Model," *IEEE journal of emerging and selected topics in power electronics, VOL. 3, NO. 3*, SEPT 2015

[19] Ray-Lee Lin, Yi Fan Chen, "Equivalent Circuit Model of Light-Emitting-Diode for System Analyses of Lighting Drivers," *IEEE Industry Applications Society Annual Meeting*, Houston, Oct 2009

[20] Hwu, K.I., Yau, Y.T., Li-Ling, L.: 'Powering LED using high-efficiency SR flyback converter', *IEEE Trans. Ind. Appl.*, 2011, 47, (1),pp. 376–386

[21] Gacio, D., Alonso, J.M., Calleja, A.J., Garcia, J., Rico-Secades, M.:'A universal-input single-stage high power-factor power supply for HB-LEDs based on integrated buck-flyback converter', *IEEE Trans. Ind. Electron.*, 2011, 58, (2), pp. 589–599

[22] Yan-Cun, L., Chern-Lin, C.: 'A novel single-stage high-power-factor AC-to-DC LED driving circuit with leakage inductance energy recycling', *IEEE Trans. Ind. Electron*., 2012, 59, (2), pp. 793–802

[23] 'Limits for harmonic current emissions, International Electrotechnical Commission Standard 61000-3-2', ed, 2005

[24] Ramanjaneya Reddy U and Narasimharaju B. L, "Unity power factor buck-boost LED driver for wide range of input voltage application," *2015 Annual IEEE India Conference (INDICON)*, New Delhi, 2015, pp. 1-6

[25] Texas Instrumentation, "Basic Calculation of a Buck Converter's Power Stage," *SLVA477B*,December 2011–Revised August 2015

[26] B. Bryant and M. K. Kazimierczuk, "Modeling the closed-current loop of PWM boost dc–dc converters operating in CCM with peak current mode control", *IEEE Trans.Circuits Syst.I, Fundam. Theory Appl*., vol.52, pp.2404–2412, Nov. 2005.

[27] Deepu Vijay M., Kamlesh Shah, G.Bhuvaneswari and Bhim Singh, "LED Based Street Lighting with Automatic Intensity Control Using Solar PV," *IEEE IAS Joint Industrial And Commercial Power Systems / Petroleum And Chemical Industry Conference (ICPSPCIC*),2015

[28] http://www.cree.com/~/media/Files/Cree/LED%20Components%20and%20Modules/XLamp/Data%20and%20Binning/XLampXPE2.pdf. [Access - 5-March-2018]

[29] Liuyi Ling*, Xiaoliang Wu, Mengyuan Liu, Zhiqiang Zhu ,Van Li, Benben Shang, "Development of Photo voltaic Hybrid LED Street Lighting System," *IEEE Advanced Information Management, Communicates, Electronic and Automation Control Conference (IMCEC)*,China, 2016

[30] Vongmanee V, Monyakul V and Youngyuan U, "Vector control of induction motor drive system supplied by photovoltaic arrays," *IEEE International Conference on Communications, Circuits and Systems and West Sino Expositions*, vol.2, pp. 1753-1756, China 2002.

[31] S. Shukla and B. Singh, "Single Stage PV Array Fed Speed Sensorless Vector Control of Induction Motor Drive for Water Pumping," *IEEE transactions on industry applications*, Feb.2018

[32] U.Sharma,S.Kumar & B.Singh, "Standalone Photovoltaic Water Pumping System Using Induction Motor Drive with Reduced Sensors," *IEEE transactions on industry applications*, April 2018.

[33] R. Kumar and B. Singh, "BLDC Motor-Driven Solar PV Array-Fed Water Pumping System Employing Zeta Converter," *IEEE Transactions on Industry Applications*, vol. 52, no. 3, pp. 2315-2322, May-June 2016

[34] Takahashi and T. Noguchi, "A New Quick-Response and High-Efficiency Control Strategy of an Induction Motor," *IEEE Transactions on Industry Applications*, vol. IA-22, no. 5, pp. 820-827, Sept. 1986

[35] B. Bimal, "Power Electronics and Motor Drives: Advances and Trends," *Academic press*, 2011.

[36] Disha N. Patel, "Effect of change in stator sector region in direct torque control technique on induction motor," *International Conference on Energy, Communication, Data Analytics and Soft Computing (ICECDS,)* pp.2059-2062, Aug. 2017.

[37] Yasser G. Dessouky and Mona Moussa, "Vector Controlled-Induction Motor Drive: Operation And Analysis", unpublished

[38] Songbai Zhang, Zheng Xu, Youchun Li and Yixin Ni, "Optimization of MPPT step size in stand-alone solar pumping systems,"*IEEE Power Engineering Society General Meeting*, pp. 6, Montreal, Que., 2006

[39] Singh,S and Singh,B, "Solar PV water pumping system with DC-link voltage regulation" *Int J Power Electronics*, Vol. 7, No.1/2, 72-85, 2015.

[40] N. B. Yousuf, K. M. Salim, R. Haider, M. R. Alam and F. B. Zia, "Development of a three phase induction motor controller for solar powered water pump," *2nd International Conference on the Developments in Renewable Energy Technology (ICDRET)*, pp. 1-5, Dhaka, 2012.

[41] S. R. Bhat, A. Pittet and B. S. Sonde, "Performance Optimization of Induction Motor-Pump System Using Photovoltaic Energy Source," *IEEE Transactions on Industry Applications*, vol. IA-23, no. 6, pp. 995-1000, Nov. 1987

[42] B. P. Ganthia, P. K. Rana, S. A. Pattanaik, K. Rout and S. Mohanty, "Space vector pulse width modulation fed direct torque control of induction motor drive using Matlab-Simulink," *3rd International Conference on Electrical, Electronics, Engineering Trends, Communication, Optimization and Sciences (EEECOS)*, pp.1-5, Tadepalligudem, 2016.

LIST OF PUBLICATIONS

1. **"Techno Economic Analysis Of Different Lighting Schemes: A Case Study**" presented in *IEEE International Conference on Power Energy, Environment & Intellegent Control (PEEIC 2018)*, 2018, to be published on IEEE Xplorer.
2. **"Implementation of P&O Algorithm for MPPT in SPV System"** presented in *IEEE International Conference on Power Energy, Environment & Intellegent Control (PEEIC 2018)*, 2018, to be published on IEEE Xplorer.
3. "**Design & Implementation of Solar Fed Intensity Controlled Streetlight"** has been communicated in *IEEE international conference on ICPEICES-2018.*